Functional analysis of a heat shock inducible methyltransferase from *Escherichia coli*

Dissertation
zur Erlangung des akademischen Grades
des Doktors der Naturwissenschaften (Dr. rer. nat.)
an der Universität Konstanz,
Fachbereich Biologie

vorgelegt von
Jutta Hager

Tag der mündlichen Prüfung: 21. Juni 2005
Referent: Prof. Dr. Hans-Werner Hofer
Referentin: Prof. Dr. Ursula Jakob

Ich erkläre hiermit, dass ich die vorliegende Arbeit ohne unzulässige Hilfe Dritter und ohne Benutzung anderer als der angegebenen Hilfsmittel angefertigt habe. Die aus anderen Quellen direkt oder indirekt übernommenen Daten und Konzepte sind unter Angabe der Quelle gekennzeichnet. Weitere Personen, insbesondere Promotionsberater, waren an der inhaltlich materiellen Erstellung dieser Arbeit nicht beteiligt. Die Arbeit wurde bisher weder im In- noch im Ausland in gleicher oder ähnlicher Form einer anderen Prüfungsbehörde vorgelegt.

Ann Arbor, den _____ _____

(Unterschrift)

Zusammenfassung

RrmJ wurde in einer umfassenden Studie von Richmond et al. als hitzeinduzierbares *E. coli* Gen endeckt. In vorrausgegangenen Studien von uns und anderen wurde gezeigt, dass RrmJ als 2'-*O*-Methyltransferase das universell konservierte Nukleotid U_{2552} im A-loop der 23S rRNA methyliert. Der *rrmJ* Deletionsstamm zeigte stark verlangsamtes Wachstum und einen signifikanten Ribosomendefekt. Dies führte zu der Schlussfolgerung, dass die Um_{2552} Methylierung Einfluss auf die Assemblierung oder Stabilität des Ribosomes hat. Strukturelle Vergleiche von RrmJ mit anderen 2'-*O*-Methyltransferasen zeigte, dass vorallem VP39, ein bifunktionales Protein in *Vaccinia virus*, erstaunliche strukturelle Ähnlichkeiten mit RrmJ aufwies. Da VP39 in der Vergangenheit sehr eingehend untersucht wurde, war diese strukturelle Ähnlichkeit von grossem Vorteil für die funktionelle Charakterisierung von RrmJ.

Mit Hilfe einer umfassenden Mutagenese Studie konnte ich das katalytische Zentrum sowie die Substratbindestelle von RrmJ nachweisen. Unsere Ergebnisse zeigten, dass das katalytische Zentrum aus der Aminosäure Triade KDK besteht und erlaubten uns, einen S_N2 Mechanismus für die Methylierungsreaktion zu postulieren. Die Aminosäuren, die ich als wichtig für die Substratbindung identifizieren konnte, bilden eine positiv geladene Kante, die mit dem Ribose-Rückgrad des RNA Substrates interagieren kann. Modellierungsstudien, durchgeführt in Kollaboration mit Bart Staker, zeigten, dass der A-loop aus der eng gepackten 50S Struktur herausklappen muss, um von RrmJ methyliert werden zu können. Modellierungsstudien mit dem A-loop bestätigten ausserdem die zuvor postulierte Substratbindestelle und gaben zu erkennen, dass U_{2552} sich einem 'base flipping' Mechanismus unterziehen muss, um in das katalytische Zentrum von RrmJ zu passen.

Co-Fraktionierungsstudien mit RrmJ bildeten die Grundlage für die wichtige Entdeckung, dass RrmJ als Assemblierungshelferprotein eine Methyltransferase-unabhängige Funktion ausübt. Der N-terminus von RrmJ erwies sich dabei als absolut notwendig für die Bindung von RrmJ an die 50S ribosomale Untereinheit. Ich konnte zeigen, dass die Bindung von RrmJ an die 50S ribosomale Untereinheit die Assemblierung des 70S Ribosomes unterstüzt. Diese zweite Funktion von RrmJ und nicht, wie ursprünglich angenommen, die Um_{2552} Methylierung scheint für den Ribosomendefekt in der *rrmJ* Deletionsmutante

verantwortlich zu sein. Diese Schlussfolgerung wurde unterstüzt von Caroline Kumsta, die zeigen konnte, dass die Abwesenheit von U_{2552} keinen Ribosomendefekt verursacht.

Eingehende Analyse der N-terminalen verkürzten RrmJ Mutante zeigte, dass RrmJ vermutlich ein zweites Methylierungssubstrat besitzt, welches nicht die Bindung an die 50S ribosomale Untereinheit verlangt. Da eines der drei RrmJ Homologen in Hefe tRNA anstelle von rRNA methyliert und da in früheren Studien auch schon gezeigt wurde, dass RrmJ tRNA als Substrat erkennen kann, ist tRNA ein möglicher Kandidat. Die Methylierung des vermeintlichen zweiten Substrates könnte RrmJ's Hitzestress Funktion darstellen, da RrmJ unter diesen Bedingungen nicht an die 50S ribosomale Untereinheit gebunden zu sein scheint.

Mit der Beobachtung, dass RrmJ als Methyltransferase mit dualer Substratspezifität und als ribosomales Assemblierungshelferprotein unabhängig von der Methyltransferaseaktivität agiert, war es nun möglich, die vielen verschiedene Phänotypen und Effekte zu erklären, die durch die Deletion dieses hoch konservierten Proteins in einem *E. coli* Stamm verursacht werden.

Summary

RrmJ was originally discovered by Richmond and coworkers as a highly heat inducible *E. coli* gene. Previous studies by us and others have shown that RrmJ functions as a 2'-*O*-methyltransferase that methylates the universally conserved nucleotide U_{2552} in the A-loop of the 23S rRNA. Deletion studies revealed that a strain lacking RrmJ shows a severely impaired growth as well as a strong ribosomal defect. This led to the conclusion that the U_{2552} methylation is involved in either ribosome assembly or stability. Structural comparison of RrmJ with other 2'-*O*-methyltransferases revealed striking similarities with the bi-functional protein VP39 from *Vacchinia virus*. Because VP39 has been intensively investigated in the past this structural resemblance was extremely helpful for the functional characterization of RrmJ as it is presented in this work.

Using extensive site directed mutagenesis, I investigated the active site as well as substrate binding site of RrmJ. Our results revealed that RrmJ's active site is composed of a catalytic triad KDK, allowing us to propose a S_N2 reaction mechanism for the methylation reaction. The amino acids that I have identified to be involved in substrate binding were found to build a positively charged ridge, which should be able to interact with the sugar phosphate backbone of the RNA substrate. Modeling studies performed in collaboration with Bart Staker suggested that the A-loop has to loop out of the tightly packed structure of the 50S ribosomal subunit in order to be accessible for RrmJ. Furthermore, modeling of the A-loop onto the surface of RrmJ underlined the proposed substrate binding site and suggested a base flipping mechanism for U_{2552} in order to fit into the active site of RrmJ.

Co-fractionation studies of RrmJ built the foundation for the major observation that RrmJ has a methyltransferase independent function as a ribosome assembly helper protein. For the binding of RrmJ to 50S ribosomal subunits, the N-terminus of RrmJ appeared to be crucial. I showed that the binding of RrmJ to the 50S ribosomal subunits supports the assembly process of the 70S ribosome. This second function of RrmJ appears to be responsible for the ribosomal defect observed in the *rrmJ* deletion strain, which has originally been attributed to the Um_{2552} modification. This finding was supported by Caroline Kumsta, a diploma student in the lab, who showed that absence of U_{2552} does not lead to a ribosome assembly defect.

Lastly, analyzing the effects of the N-terminal truncated mutant of RrmJ revealed that RrmJ might have a second methylation target, which does not require RrmJ bound to the 50S ribosomal subunit. Because one of the three RrmJ homologues in yeast methylates tRNA instead of rRNA and because it has been shown in previous studies that RrmJ is able to recognize tRNA as methylation target as well, tRNA might be a possible candidate. The methylation of this putative second substrate might be RrmJ's heat shock function since RrmJ seems not to be bound to the ribosome upon heat shock induction.

With the observation that RrmJ acts as a methyltransferase with dual substrate specificities and as ribosome assembly helper protein independent of its methylation activity, it was now possible to understand and explain the many different phenotypes and effects that were observed in strains lacking this highly conserved protein.

Abbreviations

A	Absorption
Å	Ångström
AdoHCys	Adenosine-L-homocysteine
AdoMet	S-adenosine-L-methionine
ATP	Adenosine triphosphate
BSA	Bovine serum albumine
B. subtilis	*Bacillus subtilis*
ºC	Degree Celsius
COMT	catechol *O*-methyltransferase
ddH_2O	Double destilled water
Da	Dalton = g/mol
DMSO	dimethyl sulfoxide
DNA	Deoxyribonucleic acid
DTT	1,2-dithiothreitol
E. coli	*Escherichia coli*
EDTA	ethylenediamine tetra acetic acid
FPLC	fast pressure liquid chromatography
Fts	Filamentous and temperature sensitive
g	gravitation = 9.81 m/s^2
GA	Glutaraldehyde
Hsp	heat shock protein
IPTG	Isopropyl-b-D-thiolgalactopyranoside
kDa	kilo Dalton
M	Molar
min	Minutes
ml	milli liter
mM	milli molar
mRNA	messenger ribonucleic acid
mV	milli volt
µg	micro gram
µM	micro molar

Ng	nano gram
nM	nano molar
NMR	nuclear magnetic resonance spectroscopy
OD	Optical density
PAGE	Polyacrylamide gel electrophoresis
PCR	polymerase chain reaction
pI	isoelectric point
pmol	pico mol
Rrm	ribosomal RNA methyltransferase
RNA	ribonucleic acid
rRNA	ribosomal ribonucleic acid
SDS	Sodium dodecyl sulfate
Sec	Second
S_N	nucleophilic substitution
snRNA	small nuclear ribonucleic acid
TAE	tris-acetate electrophoresis
TBE	tris-borate electrophoresis
TBS-T	tris-borate saline-Tween
TCA	trichloracetic acid
tRNA	transport ribonucleic acid
U	enzymatical unit
UV	ultra-violet
V	Volt
v/v	volume/volume
W	Watt
w/v	Weight/volume

Contents

1 Introduction

1.1 RrmJ, a 23S rRNA methyltransferase in *E. coli*

RrmJ (FtsJ) is a highly conserved methyltransferase present in prokaryotes, archaea and eukaryotes (Bügl et al., 2000). RrmJ's protein sequence is to 43% identical to all three human homologues. In *E. coli*, the mRNA level of RrmJ increases up to 20-fold upon heat treatment (Richmond et al., 1999). The cellular concentration of RrmJ, which was found to be 1060 +/- 385 molecules/cell at 30ºC, increased by a factor of 1.76 +/- 0.25 within 10 min of heat shock treatment (Bügl, 2001). This increase at protein level upon heat treatment is comparable to other well known heat shock proteins (VanBogelen et al., 1997).

Functional studies revealed that RrmJ is responsible for the methylation of 23S rRNA at position U_{2552} in the aminoacyl (A)-site of the ribosome (Bügl et al., 2000; Caldas et al., 2000b). U_{2552} is one of the five universally conserved A-loop residues and is located adjacent to G2553, which base pairs with the A-site tRNA. U_{2552} has been shown to be methylated at the 2'-OH group of the ribose in the majority of organisms investigated so far (Hansen et al., 2002). This methylation is one of the only three modifications that have been identified in the minimally modified mitochondrial rRNA of yeast cells (Sirum-Connolly et al., 1995). This suggests that this modification might play an important role in the A-loop function.

Analysis of the *rrmJ* deletion mutant in *Escherichia coli* supports this view (Bügl et al., 2000; Caldas et al., 2000b). While deletion of most of the known *E. coli* 23S rRNA methyltransferases has been shown to not affect *E. coli* growth or ribosome assembly/stability (Lovgren and Wikstrom, 2001; Agarwalla et al., 2002; Madsen et al., 2003), deletion of RrmJ has been found to affect both (Bügl et al., 2000; Caldas et al., 2000a). Polysome profiles of *rrmJ* deletion strains prepared under non-stringent salt conditions reveal the accumulation of 30S and 50S ribosomal subunits at the expense of functional 70S ribosomes (Bügl et al., 2000; Caldas et al., 2000c). Moreover stringent salt conditions in the cell lysate of the *rrmJ* deletion strain cause the accumulation of ~40S ribosomal particles and a concomitant reduction in 50S ribosomal subunits (Bügl et al., 2000). This ribosomal defect is probably responsible for the decreased translational efficiency of S_{30} lysates prepared from the *rrmJ* deletion strain (Caldas et al., 2000c). Along with this severe ribosomal defect and a decreased peptidyltransferase activity, the *rrmJ*

deletion strain exerts a significant growth disadvantage (Bügl et al., 2000), especially at lower temperatures (unpublished data).

In vitro methylation assays revealed that only fully assembled 50S ribosomal subunits prepared from the *rrmJ* deletion strain serve as substrates for RrmJ, while ~40S ribosomal particles or naked 23S rRNA are not methylated by purified RrmJ (Bügl et al., 2000). This suggested that either the correct fold of the 23S rRNA or additional protein-protein interactions are necessary for the substrate recognition. The RrmJ-mediated methylation must, therefore, occur late in the maturation process of the ribosome (Bügl et al., 2000). This is in contrast to other known 23S rRNA modifications that occur in naked 23S rRNA (Bjoerk, 1996). Measurements of the initial velocity of RrmJ's methylation activity showed that the turnover number of RrmJ is rather slow with an apparent K_{cat} of 0.064 min^{-1}. The apparent K_m values for 50S ribosomal subunits and for the cofactor AdoMet have been determined to be 0.8 +/- 0.1 μM and 3.7 +/- 0.3 μM, respectively (Hager et al., 2002).

1.2 RrmJ's homologues in yeast

While *E. coli* cells only have one RrmJ homologue, eukaryotic cells usually have several. Yeast cells, for instance, have been found to harbor three RrmJ homologues; Trm7p in the cytosol (Pintard et al., 2002b), Mrm2p in mitochondria (Pintard et al., 2002a) and Spb1p in the nucleus (Pintard et al., 2000). Whereas the mitochondrial and nuclear RrmJ homologues function as rRNA methyltransferases, the cytosolic Trm7p has been shown to be responsible for two 2'-*O*-ribose methylations at position 32 (Cm32) and 34 (Gm34) in the anticodon loop of certain yeast tRNAs.

1.2.1 Spb1p – A rRNA methyltransferase in the yeast nucleolus

Spb1p has been shown by Pintard et al. to be located in the nucleolus of yeast cells, where it methylates 25S rRNA. Spb1p is almost three times the size of Mrm2p and Trm7p, which are 37.4 kDa and 34.7 kDa, respectively, and about ~100 amino acids longer than *E. coli* RrmJ (Pintard et al., 2000). The main methylation target of Spb1 appears to be the essential G_{2922}, whose equivalent nucleotide in *E. coli* 23S rRNA is G_{2553}. Methylation of the

U_{2552} equivalent nucleotide U_{2591} in yeast rRNA, on the other hand, is guided by the snoRNA snR52 (Lapeyre and Purushothaman, 2004). Although, Spb1p seems to have acquired a new specificity, it is still able to methylate U_{2591} when the snoRNA snR52 is deleted (Lapeyre and Purushothaman, 2004). G_{2922} in yeast and its counterpart in *E. coli*, G_{2553}, are the docking sites for aminoacyl tRNA and are critical for protein translation. In *E. coli* however, this highly conserved nucleotide G_{2553} is not modified.

Similar to the RrmJ mediated methylation of U_{2552}, the modification of G_{2922} occurs at a very late state of ribosome maturation (Lapeyre and Purushothaman, 2004). This late recruitment of the enzyme to the ribosome suggests that the protein itself rather than the methylation is important for ribosome processing (Lapeyre and Purushothaman, 2004). However, so far it was not possible to separate these potentially diverse functions of Spb1p. Deletion of Spb1p is lethal. A point mutation that disrupts AdoMet binding and leaves Spb1p methyltranferase inactive, however, shows a dramatic growth phenotype and ribosome defect. Impaired pre-rRNA processing leads to a decrease of the 60S peak and to a relative increase of the 40S peak (Lapeyre and Purushothaman, 2004).

1.2.2 Mrm2p – A rRNA methyltransferase in yeast mitochondria

The RrmJ homologue Mrm2p is located in the mitochondria and methylates U_{2791} in the 21S rRNA. This is the equivalent nucleotide to U_{2552}, the methylation target of *E. coli* RrmJ (Pintard et al., 2002a). Similar to RrmJ and Spb1p, this methylation occurs at a late stage of ribosome maturation. Unlike RrmJ, however, deletion of Mrm2p does not cause any ribosomal defect. However, a strain lacking the *mrm2* gene becomes unable to respire at 37°C and rapidly loses its mitochondrial DNA when grown in YPD at 30°C. Therefore, Mrm2p appears to have an important function, which might be involved in altering the mitochondrial translation ability. Noteworthy, Pintard and coworkers show that Mrm2p co-fractionates with its ribosomal substrate, the 60S ribosomal subunit, on sucrose gradients (Pintard et al., 2002a). This was a rather unexpected finding considering the fact that Mrm2p works as an enzyme where fast release of the substrate is usually necessary to provide efficient catalytic activity.

1.2.3 Trm7p – A tRNA methyltransferase in the yeast cytosol

Trm7p is localized in the cytoplasm of *S. cerevisiae* where it methylates tRNA instead of rRNA. Pintard et al. demonstrated that Trm7p methylates C32 and G34 in the anticodon loop of $tRNA^{Phe}$, $tRNA^{Trp}$ and possibly $tRNA^{Leu}$ (Pintard et al., 2002b). Both methylations occur at a late stage after the removal of the intron and are not dependent on other modifications in the respective tRNAs (Pintard et al., 2002b). Pintard et al. hypothesize that C32 is methylated in the conformational flexible, hypomodified anticodon hairpin, where its 2'hydroxyl can be presented to the active site of Trm7p. G34, on the other hand, is being methylated in a rigid, hypomodified loop. A *trm7* deletion mutant exerts a low rate of protein synthesis, which is reflected by a decrease in polysomes as well as a significant growth defect. A point mutation in the AdoMet binding region of Trm7p was unable to rescue this growth phenotype, indicating that the loss of methylation activity is responsible for the impaired growth of the *trm7* deletion strain.

The ability of yeast RrmJ homologues to recognize either rRNA or tRNA corroborates reports about a possible dual substrate specificity of *E. coli* RrmJ, which has been found to also be capable of methylating tRNAs *in vitro* in addition to 23S rRNA (Bügl et al., 2000).

1.2.4 Comparison of the RNA substrates

Structural comparison of the A-loop of the 23S rRNA, which harbors the target nucleotide of RrmJ, to the RNA substrates of RrmJ's homologues in yeast revealed significant similarities (Fig. 1). Only the tRNA anticodon loop, where the target nucleotides of Trm7p reside, seems to slightly differ from the three rRNA loops (Pintard et al., 2002b). However, although the tRNA anticodon loop is formed by seven nucleotides instead of five, the target nucleotide (C32) is in the same 5' position as U_{2552} in the A-loop of the 23S rRNA. Furthermore, the anticodon loop can be reduced to a five nucleotide-long loop due to a base pairing between positions 32 and 38. Therefore, all four proteins, RrmJ in *E. coli*, as well as Spb1p, Mrm2p and Trm7p in yeast, recognize a very similar loop structure suggesting that all three yeast proteins, which are present in distinct compartments have evolved from a common ancestor (Pintard et al., 2002b).

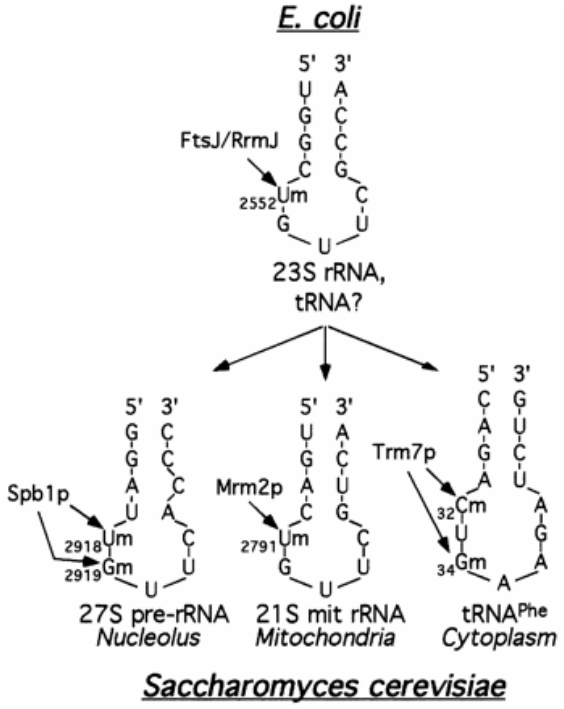

Figure 1: Comparison of the RNA substrates of *E. coli* RrmJ and its yeast homologues (Pintard et al., 2002b)
Schematic representation of the secondary structure of the target sites of *E. coli* RrmJ and each of the three enzymes in yeast that belong to the 2'-*O*-RNA methyltransferases (Pintard et al., 2002b).

1.3 Crystal structure of RrmJ

RrmJ has been co-crystallized in the presence of the cofactor AdoMet and its structure has been solved to a resolution of 1.5 Å (Bügl et al., 2000). The crystal structure of RrmJ does not contain the 29 N-terminal amino acids because this part had to be cleaved off in order for RrmJ to crystallize. The crystal structure of RrmJ revealed the classical methyltransferase fold. This common core structure consists of a seven stranded β-sheet, with the seventh β-strand being antiparallel to the other six and inserted into the sheet between strand 5 and 6. Six α-helices are associated with the β-strands, giving a α / β / α sandwich structure (Fauman, 1999). A special feature of RrmJ's structure is the extended α_4-helix which is seven turns longer than in the consensus structure, which is represented by the catechol-*O*-methyltransferase COMT (Bügl et al., 2000; Fauman, 1999).

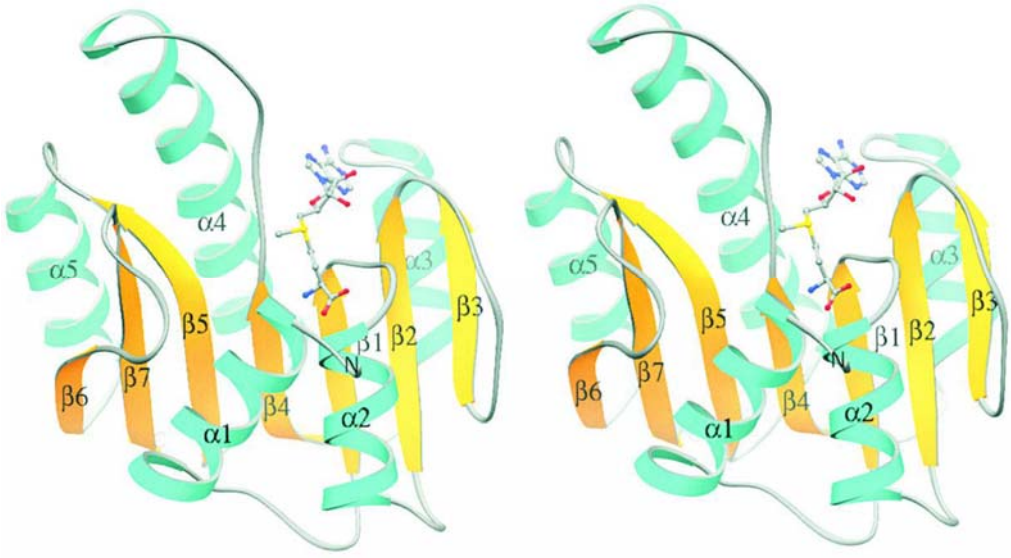

Figure 2: RrmJ has a methyltransferase fold (Bügl et al., 2000)
Stereo diagram of the RrmJ tertiary fold highlighting secondary structure element. Secondary structures were assigned and the figure was rendered by RIBBONS (Carson, 1997). The bound AdoMet is shown in ball and stick representation.

1.3.1 Structurally related methyltransferases

Structure analysis and comparison of RrmJ with other methyltransferase structures (Dali 2.0; Holm and Sander, 1997) revealed five highly similar proteins: catechol-*O*-methyltransferase (COMT) (Vidgren et al., 1994), Taq I polymerase (Schluckebier et al., 1997), *Vaccinia virus* mRNA 2'-*O*-methyltransferase VP39 (Hodel et al., 1996), rRNA methyltransferase ErmC (Bussiere et al., 1998) and 1FBN, the fibrillarin homologue from *Methanococcus jannaschii* (Wang et al., 2000). Both, COMT and VP39 are single domain structures like RrmJ. VP39 contains a homologous core domain and a substrate binding groove, which is highly similar to the surface of RrmJ (Bügl et al., 2000).

1.3.1.1 VP39

VP39 is a bifunctional protein in *Vacchinia virus,* which participates in the maturation of both mRNA ends. At the 5' end, VP39 acts as an AdoMet-dependent cap specific mRNA 2'-*O*-methyltransferase, catalyzing the ribose methylation of the first transcribed nucleotide.

At the 3'end of the mRNA, the protein acts as a smaller subunit of the heterodimeric *Vacchinia virus* poly (A) polymerase (Hodel et al., 1996).

VP39 has been co-crystallized in the presence of an mRNA substrate analog, a m7(5')Gppp-capped single stranded RNA hexamer and the competitor Adenosine-L-homocysteine (AdoHCys). It comprises a compact single core domain with the typical α/β/α fold (Hodel et al., 1996). Surface comparison between VP39 and RrmJ revealed striking similarities (Fig. 2) (Staker, 2000). A significant feature in both RrmJ and VP39 is the extended α_4-helix located next to the AdoMet binding site and above the substrate binding site of VP39. The VP39 mRNA binding groove strongly resembles a highly conserved surface area of RrmJ in both size and distribution of positively charged residues (Staker, 2000). A structure based sequence alignment showed 18 identical amino acids in VP39 and RrmJ (Staker, 2000). Modeling studies revealed that VP39's mRNA substrate fits nicely into the putative substrate binding site of RrmJ (Staker, 2000). Four of the six amino acid residues in VP39, which have direct contact to the mRNA substrate, are structural identical in RrmJ. All four are highly conserved amino acids and are *Lys41* (Lys38), *Lys175* (Lys164), *Ser205* (Ser197) and *Glu207* (Glu199) (VP39 residues are in italics). In VP39, they form a hydrogen bond network that coordinates the phosphate atoms on each side of the methylated nucleoside (Bügl et al., 2000).

Enzymatic characterizations of purified VP39 revealed that this enzyme has a K_{cat} of 0.13 min^{-1} and therefore, a similarly low turnover rate than RrmJ (Hu et al., 2002). In addition, the K_m value for the cofactor AdoMet (2 μM) was similar to the K_m value that was observed for RrmJ (3.7 +/- 0.3 μM) (Barbosa and Moss, 1978; Hager et al., 2002). VP39's K_m value determined for the mRNA substrate (5 nM) was found to be significantly lower compared to RrmJ's K_m value for 23S rRNA (0.8 +/- 0.1 μM) (Barbosa and Moss, 1978; Hager et al., 2002). This, however, might simply reflect the abundance of the respective substrates in the cell, where only 5-10% of total RNA is mRNA, but 75-80% of total RNA is rRNA (Knippers, 1995).

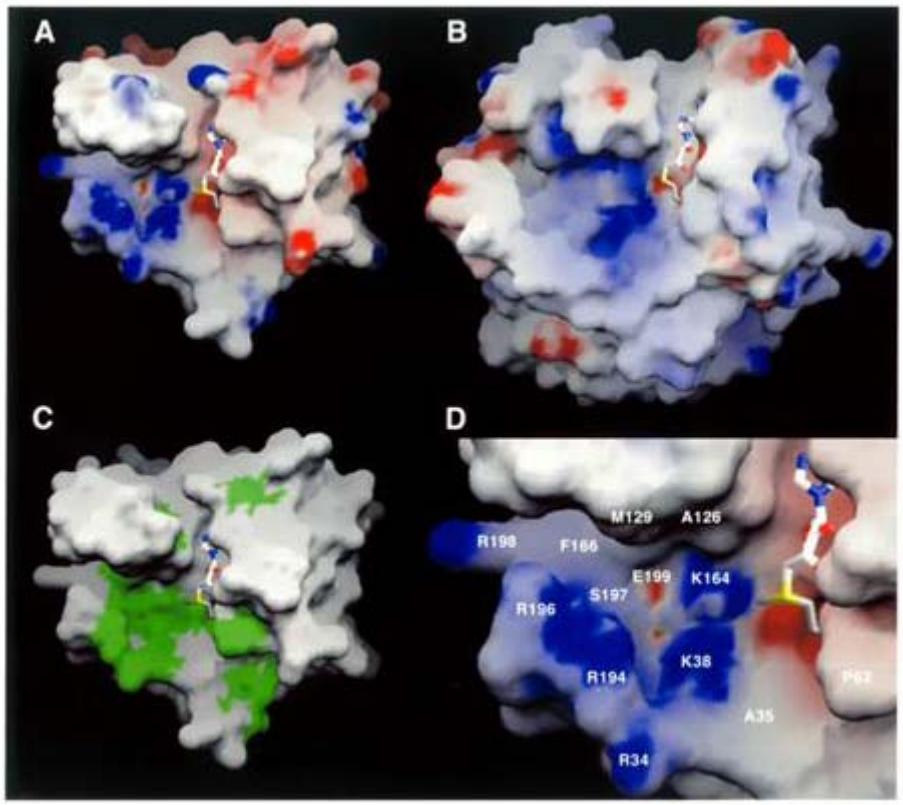

Figure 3: Comparison of RrmJ and VP39 Surfaces (Bügl et al., 2000)
(A) Solvent contact surface of RrmJ. The electrostatic potential is shown by the color code: -15 (blue), 0 (white) and +15 K_bT (red). The bound AdoMet is shown in stick presentation. (B) Solvent contact surface of VP39 and its electrostatic potential. The bound AdoHCys is shown. It is identical in orientation, scale and coloring to RrmJ in (A). (C) The 27 most conserved RrmJ residues are colored green. (D) The putative substrate binding groove of RrmJ is shown. The amino acids that might be important for substrate binding are indicated.

1.3.1.2 Fibrillarin

A second structurally similar enzyme of RrmJ is the *Methanococcus jannaschii* fibrillarin 1FBN, whose structure has been solved to a resolution of 1.6 Å (Wang et al., 2000). Comparison of the two proteins revealed that RrmJ and fibrillarin share 19% sequence identity and 154 amino acids between RrmJ and fibrillarin superposed with an rmsd of 2.6 $Å^3$ (Staker, 2000). In contrast to RrmJ, however, fibrillarin consists of a globular two-domain structure, built of a smaller N-terminal domain and a larger C-terminal domain. While the N-terminal domain represents a novel fold, the core of the connected C–terminal domain shows the classical methyltransferase fold (Wang et al., 2000). The crystal structure

revealed that the two N-terminal domains of fibrillarin join together to form a homodimer. Because fibrillarin was crystallized without bound AdoMet, the exact position of the cofactor is not known. Also methyltransferase activity has not yet been detected *in vitro* and a complete biochemical characterization of fibrillarin remains to be performed (Wang et al., 2000). However, based on the structural analysis and the association of fibrillarin with box C/D snoRNAs, it has been suggested that fibrillarin functions as rRNA 2'O-methyltransferase. The homology to RrmJ furthermore supports this hypothesis.

In yeast, several temperature sensitive mutants of the fibrillarin homologue Nop1p have been isolated (Tollervey et al., 1991; Tollervey et al., 1993). Nop1p functions in all three major posttranscriptional activities; i) it takes part in the cleavage of the large pre- ribosomal RNA into the mature 18S, 5.8S and 25S RNAs, ii) it is involved in 25S modification by methylating and pseudouridylation of the rRNA sequences and iii) it takes part in the assembly of the ribosomes (Tollervey et al., 1993). Some of these Nop1p mutants show severe ribosome assembly defects as well as significantly impaired growth. In order to understand the effects of the Nop1 mutants better, the mutations were localized in the structure of fibrillarin and compared to the structure of RrmJ (Staker, 2000). In this way residues in Nop1 could be identified which might be involved in AdoMet binding and therefore, the effect of four of the Nop1 mutations could be attributed to impaired AdoMet binding (Staker, 2000).

1.4 Catalytic mechanism of AdoMet-dependent methyltransferases

Very little is known about the mechanism of the methyltransfer reaction of 2'-*O*-ribose methyltransferases such as VP39 and RrmJ. One of the few extensively characterized methyltransferases, however, has been the catechol-*O*-methyltransferase (COMT). COMT is a single domain protein that catalyzes the methylation of a hydroxyl group on catechols and requires Mg^{2+} for its activity (Vidgren et al., 1994). It has been shown that the cofactor AdoMet binds first. This is followed by the binding of a magnesium ion, which has no contact to the bound AdoMet. Finally, the substrate catechol associates (Lotta et al., 1995). Schowen et al. showed that the methyl transfer catalyzed by COMT proceeds via a tight and symmetrical S_N2-transition state and that the methyl transfer is the rate determining step

(Hegazi et al., 1976). The COMT structure reveals that the Mg^{2+} ion functions by bringing one of the hydroxyl groups of the catechol very close to the active methyl group of AdoMet (Vidgren et al., 1994). The magnesium ion as well as two basic protein side chains next to it are proposed to induce the deprotonation of the target hydroxyl by lowering its pK_a (Hodel et al., 1998) and, therefore, to facilitate the catalysis. In this reaction, Lys144 in COMT has been proposed to act as a general base due to its close proximity to the methyl acceptor hydroxyl group and increases the nucleophilicity of the hydroxyl group of the bound substrate (Ovaska and Yliniemela, 1998).

COMT reveals some resemblances to VP39. Both COMT and VP39 have similar methylation targets and the active sites of COMT and VP39 reveal a number of similarities. One major difference between the two enzymes is, however, that VP39 does not require Mg^{2+} ions for its activity (Hodel et al., 1998).

1.5 Substrate binding site of 2'-*O*-methyltransferases

Unlike the catalytic domain, which is structurally conserved among methyltransferases, the substrate binding region is featured through high variability. Studies on various rRNA methyltransferases revealed that some enzymes including RrmJ prefer a partly or fully assembled ribosomal subunit as substrate (Poldermans et al., 1979; Tscherne et al., 1999; Weitzmann et al., 1991; Bügl et al., 2000; Caldas et al., 2000b), whereas others are only able to recognize their methylation target in free rRNA since the contact sites would be hidden in the fully assembled subunit (Gu et al., 1999; Hansen et al., 2001; Skinner et al., 1983; Liu et al., 2000). So far, for only a very small number of methyltransferases, the substrate recognition and binding sites have been investigated.

VP39 is the only 2'-*O*-methyltransferase that has been crystallized in complex with its cofactor and a substrate analogue (Hodel et al., 1996). The recognition of VP39's capped mRNA substrate is achieved by stacking the methylated base between two aromatic side chains (Hu et al., 1999). VP39 shows a novel mechanism for sequence-nonspecific recognition of single-stranded RNA. It recognizes only the backbone conformation of a helical trimer of stacked bases because it has been shown that the RNA bases interact exclusively with each other in a three base stack (Hodel et al., 1998). Therefore, VP39

interacts primarily with the sugar-phosphate backbone of the first RNA trimer and not with the bases. Comparison with RrmJ revealed, however, that RrmJ and VP39 ought to differ in substrate binding and recognition due to the different nature of their RNA substrates. VP39 has to recognize the methylated 5' end of mRNA while RrmJ recognizes the A-loop of the 23S rRNA and, therefore, lacks those aromatic side chains in this position.

1.6 The importance of posttranscriptional modifications in rRNA

Protein synthesis is a fundamentally important process for cells and organisms and depends on the accurate functioning of the translational apparatus. Protein translation is dependent on modified nucleosides (Curran, 1998). Almost one hundred posttranscriptional modifications have been characterized in different RNAs, of which about one third are found in rRNAs (Rozenski et al., 1999). The nucleotide modifications in rRNA are of three main types: (1) conversion of uridine to pseudouridine (Ψ); (2) methylation of 2' hydroxyls (Nm) and (3) alterations of bases, most of which involve methylation at different positions (mN) (Decatur and Fournier, 2002). Most of these modifications cluster in conserved regions of functionally important rRNA domains and are critically important for the survival of the cells (Brimacombe et al., 1993). In the large ribosomal subunit in *E. coli,* almost all modifications are found to be in the domains II, IV and V and, therefore, occur near the center and front of the subunit (Decatur and Fournier, 2002). The modifications have been suggested to be crucial for the structure and function of the ribosome and have been shown to be important for the interaction of rRNA with ribosomal proteins in subunit assembly as well as for the association of the subunits to form translationally active ribosomes (Green and Noller, 1996; Hansen et al., 2001). Specific rRNA modifications have been shown to confer antibiotic resistance by interfering with the binding of the antibiotic (Hansen et al., 2002). The importance of rRNA modification for the activity of the ribosomes has also been demonstrated with *in vitro* assembly studies. It has been shown to be impossible to assemble catalytical active 50S ribosomal subunits with *in vitro* transcribed, unmodified 23S rRNA. In contrast, when *in vivo* modified rRNA was used instead, the *in vitro* assembled 50S ribosomal subunits displayed full activity (Green and Noller, 1996).

1.6.1 The A-loop - The rRNA substrate of RrmJ

The peptidyltransferase center of the ribosome is predominantly composed of domain V, which comprises the A- and P-loop of the 23S rRNA. The precise alignment of the A-site and P-site tRNA's to the A- and P-loop, respectively, is essential for ribosome function. All five A-loop residues are highly conserved and the base pairing between tRNA and rRNA occurs via highly conserved nucleotides. In the A-loop, G_{2553} basepairs with C75 of the A-site tRNA (Blanchard and Puglisi, 2001). Mutagenesis studies showed that the nucleotides of the A-loop are functionally very important. Mutations in G_{2550}, G_{2553} and G_{2557} are likely to affect the accommodation of the A-site tRNA and reduce the efficiency of the peptidyltransferase activity *in vitro* (Kim and Green, 1999; Porse and Garrett, 1995; Liu and Horowitz, 1994; Green and Noller, 1996). Substitution of U_{2555} with an adenosine increases frameshift errors and miscoding by the ribosome (O'Connor and Dahlberg, 1995).

Due to the high conservation of the Um_{2552} modification in the A-loop and the Gm_{2251} modification in the P-loop it has been suggested that 2'-*O*-methylations play an important role in tRNA selection and accommodation (Sirum-Connolly and Mason, 1993; Sirum-Connolly et al., 1995). Moreover, these two modifications belong to the only three modifications found in the minimally modified mitochondrial 21S rRNA. Yeast mitochondrial 21S rRNA harbors the three modifications Gm_{2251}, Um_{2552} and Ψ_{2580} (*E. coli* numbering) (Sirum-Connolly et al., 1995).

In 23S rRNA, mutations in either G_{2251} or G_{2252} are lethal (Gregory and Dahlberg, 1999). Substitutions of U_{2552} in 23S rRNA with adenosine or cytosine due to random mutagenesis led to a slow growth phenotype as well as to a decrease in peptidyltransferase activity (Kim and Green, 1999; Porse and Garrett, 1995). This suggested that the Um_{2552} modification is important for the correct functioning of the ribosomes. Furthermore, Richarme and coworkers were able to show that a *rrmJ* deletion strain, which is lacking the Um_{2552} modification increases its translational accuracy supporting the idea that translational accuracy in wild type strains is rather optimal than maximal (Widerak et al., 2005). NMR studies performed by Puglisi and coworkers revealed that U_{2552} forms an unusual pyrimidine-pyrimidine basepair with G_{2556} (Blanchard and Puglisi, 2001). Therefore, the Um_{2552} modification has been found to have an impact on local conformational features of the critical nucleotides U_{2555} and U_{2556} that mediate tertiary interactions of the A-loop in the ribosome.

However, the lack of the U_{2552} methylation has only little effect on the overall structural fold of the A-loop (Blanchard and Puglisi, 2001).

1.6.2 23S rRNA methyltransferases in *E. coli*

One of the most widespread RNA modifications is nucleoside methylation on either the base or the 2'-*O*-ribose of the respective nucleotide. Although the chemical nature of the individual rRNA modifications has been known now for some years, most of the enzymes, that are responsible for these modifications, have not yet been identified. In the case of *E. coli* 23S rRNA, which has at least 14 different methylated nucleotides, only five modifying enzymes have been identified so far. These are the three base modifying methyltransferases $RlmA^I$ (m^1G_{745}) (Gustafsson and Persson, 1998), RumA (m^5U_{1939}) (Agarwalla et al., 2002) and RumB (m^5U_{747}) (Madsen et al., 2003), as well as the two unrelated 2'-*O*-ribose methyltransferases RlmB (Gm_{2251}) (Lovgren and Wikstrom, 2001) and RrmJ (Um_{2552}) (Bügl et al., 2000; Caldas et al., 2000a).

In vitro characterization showed that RrmJ is the only 23S rRNA methyltransferase identified that methylates its target nucleotide late in the maturation process of the ribosome. $RlmA^I$, RumA and the yeast homologue of RlmB, Pet56p, have been shown to methylate only naked 23S rRNA (Sirum-Connolly and Mason, 1993). RlmB has not yet been characterized *in vitro* and purified RumB protein showed no activity. *In vivo*, only $RlmA^I$ shows a phenotype that is comparable to RrmJ. The deletion strain of $RlmA^I$ revealed a growth defect. Lysates of the *rlmA^I* deletion strain showed an increased amount of free ribosomal subunits and a decreased translation rate (Gustafsson and Persson, 1998). Deletion of RlmB (Lovgren and Wikstrom, 2001) and RumB (Madsen et al., 2003), on the other hand, did not cause any growth disadvantage or ribosomal defect.

Except for RumB, the crystal structures of all of these 23S rRNA methyltransferases have been solved (Lee et al., 2004; Das et al., 2004; Michel et al., 2002). The crystal structures reported for RumA, $RlmA^I$, and RlmB display quite unique features. RumA can be divided into three functional domains: the N-terminal domain, which contains sequence homology to the conserved TRAM motif and displays characteristics of an oligosccharide/oligonucleotide binding fold (Lee et al., 2004), the central domain, which

contains a [Fe_4S_4] cluster coordinated by four conserved cysteine residues and the C-terminal domain, which shows the classical methyltransferase fold. An [Fe_4S_4] cluster is highly unexpected since methylation reactions usually do not involve a redox step. However, it has been suggested that oxidation of the cluster could be a mechanism for regulating RumA's activity under oxidative stress conditions (Agarwalla et al., 2004). The crystal structure of $RlmA^I$ revealed that $RlmA^I$ acts as a dimer (Das et al., 2004). Each $RlmA^I$ molecule has a Zn binding domain, which is involved in substrate recognition and binding, and a methyltransferase domain. The RNA binding cleft in the assymetric dimer is shown to be W-shaped. Two AdoMet cofactor molecules are located at the two valleys of this cleft. The crystal structure of RlmB consists of an N-terminal domain, which is connected by a flexible extended linker domain to a catalytic C-terminal domain (Michel et al., 2002). In solution, RlmB also forms a dimer. The C-terminal domain contains the methyltransferase active site, which does not display the classical AdoMet binding site but a divergent methyltransferase fold with a unique knot.

1.6.3 RrmJ's homologues in human – link between methyltransferases, cancer development and mental retardation

In analogy to yeast, humans have three RrmJ homologues called FtsJ1, FtsJ2 and FtsJ3, which show 34% sequence identity to RrmJ (Bügl et al., 2000; Ching et al., 2002; Ramser et al., 2004).

FtsJ1, which is 330 amino acids long and is therefore comparable in size to Trm7p and Mrm2p from yeast, has been detected in all fetal and adult tissues tested so far. Freude et al. associated human FtsJ1 with the Trm7 subfamily in yeast, suggesting that it may be involved in posttranscriptional modification of tRNA (Freude et al., 2004). However, Ramser et al. published that Spb1 is the yeast homologue to FtsJ1 suggesting a function as rRNA methyltransferase (Ramser et al., 2004). Experimental evidence for FtsJ1's function is still lacking. Mutations in human FtsJ1, which is the most abundant in fetal brain tissues, cause X-linked mental retardation (XLMR), whose prevalence has been estimated to be 1 in 500 males (Freude et al., 2004). Furthermore, a splice site mutation was described, which also appears to be associated with non-syndromic mental retardation (MRX) (Ramser et al.,

2004). This splice site mutation results in skipping of exon 4 and is predicted to cause a truncated FtsJ1 protein of 82 amino acids, which is assumed to severely affect a highly conserved domain of FtsJ1.

For FtsJ2 it has been reported that in addition to the residues that are identical 52% of the amino acids are similar to RrmJ (Ching et al., 2002). With a predicted molecular size of 27.4 kDa, FtsJ2 is slightly larger than RrmJ. FtsJ2 is a nucleolar protein, which is mainly detected in muscle, placenta and heart tissues (Ching et al., 2002). Noteworthy, FtsJ2 transcripts were 8.9 fold more abundant in lung carcinoma cells than in normal lung tissue and have been detected in all cancer cell lines tested (Ching et al., 2002). No further studies have been published for FtsJ2 so far, but due to its conserved methyltransferase domain, the homology to RrmJ and its nucleolar location, it is assumed to be involved in rRNA methylation and processing. No data are available at this point for FtsJ3.

2 Results

2.1 The Substrate of RrmJ

RrmJ is able to methylate 23S rRNA in isolated 50S ribosomal subunits, as well as in 70S ribosomes (Bügl et al., 2000; Caldas et al., 2000b), but is unable to methylate naked 23S rRNA or 23S rRNA that is present in ~40S ribosomal particles that have been shown to accumulate in cell lysates of the *rrmJ* deletion strain under dissociating salt conditions (Bügl et al., 2000). To analyze the substrate requirements of RrmJ in more detail, Hans Bügl, a former member of our lab, had performed 2D gel analysis to compare the protein composition of the 50S ribosomal subunits of the *rrmJ* deletion strain with that of wild type strains. As shown in Fig. 4, all 33 ribosomal proteins of the large 50S ribosomal subunit were detectable at similar levels in the two strains (Fig. 4, *A* and *B*). These data revealed that the absence of methylation of the highly conserved U_{2552} does not affect the folding of the 23S rRNA to an extent that impairs the correct assembly of the 50S ribosomal subunit. To get an idea how accessible U_{2552} is in the intact 50S ribosomal subunit, modeling studies in collaboration with Bart Staker were performed using the crystal structure of the *Deinococcus radiodurans* 50S ribosomal subunit (Harms et al., 2001) and RrmJ. Although solvent-accessible, U_{2552} (*E. coli* nomenclature) is positioned at the bottom of a deep cleft. Assuming that this conserved residue has the same position in the *E. coli* 50S ribosomal subunits, this would make it rather inaccessible for RrmJ methylation and would require the 23S rRNA to loop out for RrmJ to gain access.

The ~40S ribosomal particles that accumulate under dissociating salt conditions in lysates prepared from the *rrmJ* deletion strain HB23 are not *in vitro* substrates of RrmJ (Bügl et al., 2000). 2D gel analysis of the ~40S peak revealed that at least seven different ribosomal proteins (L5, L16, L18, L25, L27, L28, L30) are present in significantly diminished amounts compared to 50S ribosomal subunits from the *rrmJ* wild type or deletion strain (Fig. 4, C). All of these proteins belong to the group of late assembly proteins (Nierhaus, 1991). Therefore, RrmJ seems to be involved in either the assembly or stability of the 50S ribosomal subunit.

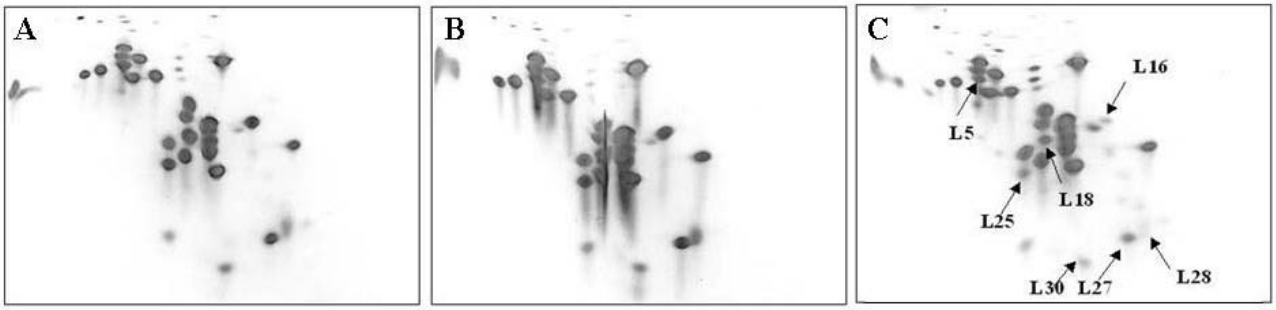

Figure 4: 2D-Gel analysis of 50S ribosomal subunits and 40S particles prepared from WT and *rrmJ* deletion strains (Hager et al., 2002).
Protein composition of (A) 50S ribosomal subunits from HB24 (WT), (B) 50S ribosomal subunits from HB23 (*rrmJ*Δ567) and (C) ~40S ribosomal particles from HB23. 2D gel analysis revealed identical protein composition and concentration in 50S ribosomes of wild type and *rrmJ* deletion strain. The ~40S ribosomal particles showed substantially decreased amounts of the late assembly proteins L5, L16, L18, L25, L27, L28 and L30, as indicated by the arrows.

2.2 RrmJ Is a Thermostable Heat Shock Protein

Richmond et al. reported that the mRNA level of RrmJ increases by more than 20-fold upon heat shock treatment of the cells (Richmond et al., 1999). This would make RrmJ the first methyltransferase under heat shock control. As a first approach, in order to cast light on RrmJ's unknown heat shock function, it was considered that one possible reason for the heat shock induction of RrmJ could be a temperature lability of the enzyme. This would require the overexpression of RrmJ at heat shock temperatures to compensate for the potential loss of function. For this reason, the activity of RrmJ was measured under saturating substrate concentrations over a variety of temperatures (Fig. 5). The temperature optimum of the methyltransferase activity of RrmJ was found to be at 55°C. The decreased activity at temperatures beyond 55°C is either because of instability of the 50S ribosomal subunits or because of thermal inactivation of RrmJ. In either case, these results excluded the possibility that the heat shock regulation of RrmJ is based on thermal lability of the enzyme.

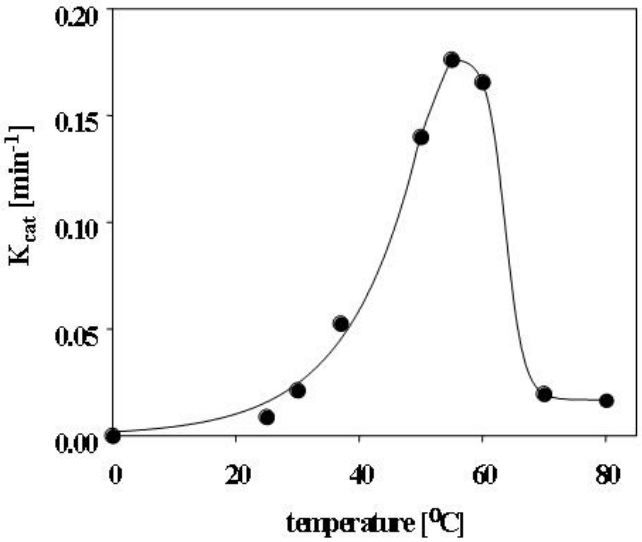

Figure 5: Temperature optimum of RrmJ's methyltransfer reaction (Hager et al., 2002).
Wild type RrmJ (100 nM) was incubated with 5 µM 50S ribosomal subunits and 50 µM AdoMet (200 µC/ml) at temperatures ranging from 25ºC to 80ºC. The initial rate of the methyl incorporation was determined as described in "Materials and Methods" and was plotted against the temperature. The temperature optimum under these conditions was found to be 55ºC.

2.3 The Active Site of RrmJ

2.3.1 Rational RrmJ mutant design

Surprisingly little is known about the catalytic mechanism of any 2'-*O*-ribose methyltransferase. Although a reaction mechanism has been postulated for VP39 on the basis of its crystal structure (Hodel, 1999), experimental data have not been obtained to support this hypothesis. We have therefore decided to combine structural analysis and site-specific mutagenesis to investigate the methyltransfer reaction of RrmJ. The first step in this analysis was to determine which residues are essential for catalysis.

Of all the methyltransferases that have been crystallized so far, VP39 and fibrillarin are the two enzymes whose structures resemble that of RrmJ the most (Bügl et al., 2000). VP39 methylates the first transcribed nucleotide in mRNA following the m^7(5')Gppp-cap (Schnierle et al., 1992). The structure of VP39, which was solved in complex with an mRNA substrate analog m^7(5')Gppp-capped RNA hexamer and the inhibitor *S*-adenosyl homocysteine, showed that the mRNA binds to a groove on the surface of VP39 (Hodel et al., 1998). Structural analysis of the RrmJ·AdoMet complex revealed that RrmJ has a very similar groove adjacent to the AdoMet binding site (Bügl et al., 2000). In collaboration with Bart Staker, the mRNA substrate analog of VP39 was modeled onto the RrmJ structure and the ssRNA was found to fit well into this putative substrate binding site of RrmJ. In this

model, the 2'-hydroxyl group of the ribose to be methylated is positioned next to the reactive Cα group of AdoMet.

Lys-38, Asp-124, Lys-164, and Glu-199 of RrmJ are the most highly conserved amino acids among RrmJ homologues. A comparison of the crystal structures of RrmJ and VP39 indicated that these residues are located almost at the identical position as the homologous Lys-41, Asp-138, Lys-175 and Glu-207 residues in VP39 (Fig. 6, *A* and *B*). These residues, which form a hydrogen bond network that coordinates the phosphate atoms on each side of the methylated nucleoside, have been suggested by us and others (Bügl et al., 2000; Bujnicki and Rychlewski, 2001; Pintard et al., 2002a) to play a critical role in the catalytic mechanism of RrmJ. In addition, Tyr-201 is highly conserved among RrmJ homologues and is located exactly underneath the putative active site, suggesting that it could also play a catalytic role in RrmJ.

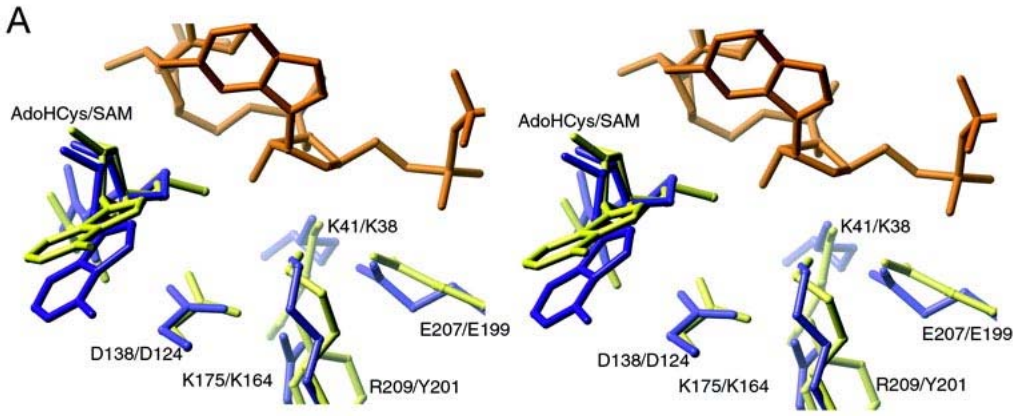

Figure 6: Structural comparison between RrmJ and VP39 (Hager et al., 2002)
A, Stereo view of the proposed active site in RrmJ and VP39. The active site residues of RrmJ (yellow) (Bügl et al., 2000) and VP39 (blue) (Schnierle et al., 1992) were overlayed using a structural alignment calculated as described in figure legend 3B. The m^7G capped RNA hexamer from the structure of VP39 (Hodel et al., 1998) is diagrammed in orange. The close structural alignment of the active site regions of VP39 and RrmJ suggests a similar mechanism of binding RNA substrate in the active site of RrmJ. This comparison was performed by Bart Staker.

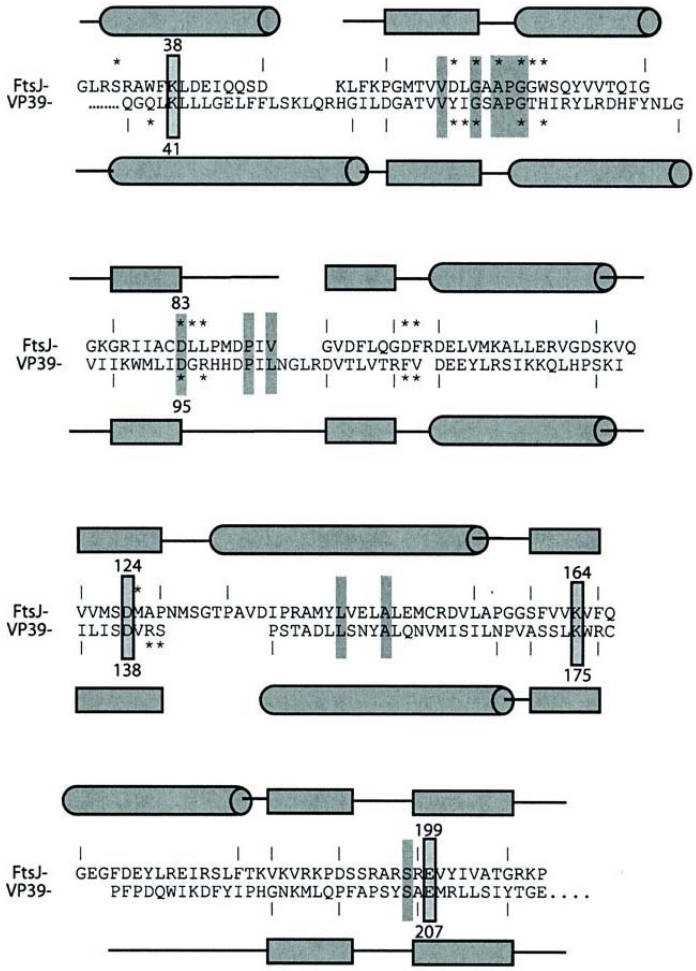

B, Structure based sequence alignment of RrmJ and VP39. Amino acid sequence alignment is based on a 3D structural alignment of RrmJ and VP39. Structural alignments were calculated using least squares difference between alpha carbons of the beta strand portions of the methyltransferase core domains using the program Xtalview (McRee, 1993). Tick marks indicate beginning and end of secondary structure elements, alpha-helix (rectangle) and beta-strand (cylinder). Gray shaded residues represent those residues that are conserved within homologues of the RrmJ (Bügl et al., 2000) and VP39 related gene families, as well as structurally conserved in the methyltransferase fold of both proteins. Boxed residues are implicated in the catalytic mechanism. The residues that have been shown to make AdoMet contacts in the crystal structure (Bügl et al., 2000) are labeled with an asterix. This alignment was performed by Bart Staker.

To analyze whether these residues are important for catalysis of the methyltransfer reaction, site-specific mutagenesis was performed to replace these five amino acids in RrmJ (Lys38, Asp-124, Lys-164, Glu-199, and Tyr-201) individually with alanine residues. Also the highly conserved amino acid Asp-83 was substituted with an alanine. This residue, which interacts with AdoMet via two hydrogen bonds, has been predicted to play a crucial role in AdoMet binding (Bügl et al., 2000).

2.3.2 Growth analysis of the RrmJ mutants on McConkey plates

After introducing the individual mutations into wild type *rrmJ* using site-specific mutagenesis, the *rrmJ* mutant plasmids were transformed into HB23 (*rrmJ*Δ*567*) to investigate their *in vivo* function. All the mutant and wild type *rrmJ* genes were cloned into the pET11a expression system. Fortunately, the expression level of all of the mutated RrmJ proteins in the absence of induced T7 polymerase was found to be very similar to the level of RrmJ seen from a chromosomal copy (data not shown). This allowed us to be confident that any phenotype observed for the mutant proteins was not because of massive over or underexpression of the protein. As a first step in the *in vivo* characterization of the RrmJ mutants, the inability of *rrmJ*Δ*567* cells to grow on McConkey plates at 37°C were utilized (Bügl et al., 2000). In contrast, wild type strains harboring a chromosomal copy of *rrmJ* (HB24) or the *rrmJ* deletion strains that expresses RrmJ from the pET11a *rrmJ* plasmid (HB25) form large colonies. As shown in Fig. 7, expression of the RrmJ-D83A mutant as well as the two lysine mutants, RrmJ-K38A and RrmJ-K164A, are unable to rescue the growth defect of the *rrmJ* deletion strain, indicating that all three mutations cause the inactivation of RrmJ *in vivo*. These results served as a first indication that the two lysine residues might be involved in the catalytic mechanism of RrmJ. Almost as severe was the phenotype of cells expressing the D124A mutant, suggesting that this amino acid also plays a crucial role in the function of RrmJ. *rrmJ* deletion strains expressing the E199A or Y201A variant protein showed only slight growth defects, suggesting that these two residues are not as important in the catalytic mechanism.

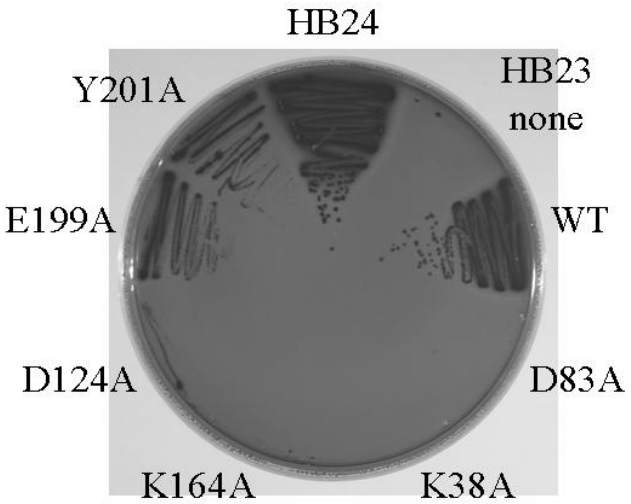

Figure 7: Phenotype of the active site mutants in RrmJ (Hager et al., 2002)
Growth of HB24 (WT) and HB23 (*rrmJ*Δ567) strains harboring either no plasmid or pHB1 derived plasmids encoding wild type *rrmJ* (WT) or the mutant *rrmJ* genes as indicated. The growth was analyzed on McConkey plates at 37°C.

The growth defect of the *rrmJ* deletion strain HB23 is not only apparent on McConkey plates but can also be observed in liquid LB medium (Bügl et al., 2000). Therefore, the growth rate of the mutant strains was also analyzed in liquid medium. *rrmJ* deletion strains expressing no RrmJ or one of the D83A, K38A, D124A, or K164A active site mutants revealed a 2.5–3-fold slower growth rate than cells expressing wild type RrmJ (data not shown). RrmJ deletion strains expressing the E199A or the Y201A variant protein grew almost as well as wild type cells. Therefore, both phenotypes were consistent and gave the first indication on how the amino acid substitutions affect the function of RrmJ.

2.3.3 Analysis of Polysome Profiles

The *RrmJ* deletion strain HB23 shows a significantly altered polysome profile as compared to polysome profiles analyzed from wild type strains (Bügl et al., 2000; Caldas et al., 2000c). In the absence of functional RrmJ, cell lysates prepared under dissociating salt conditions (200 mM NH_4Cl, 1 mM $MgCl_2$) accumulate a large ~40S intermediate peak at the expense of intact 50S ribosomal subunits (see (Bügl et al., 2000) and Fig. 8). To further investigate to what extent the amino acid substitutions in RrmJ's potential active site affect the *in vivo* function of RrmJ, the polysome profile of the *rrmJ* deletion strain expressing wild type RrmJ (HB25) or the mutant RrmJ variants from a plasmid were analyzed. The *rrmJ* rescue strain HB25 accumulates slightly higher levels of 30S, ~40S and 50S ribosomal subunits than a wild type *E. coli* strain that expresses RrmJ from its chromosomal copy (Bügl et al., 2000). Because all of the tested RrmJ variants are expressed in this background strain, we decided to use this rescue strain HB25 as the appropriate "wild type" control in all of the *in vivo* experiments described throughout this thesis. As shown in Fig. 8, HB23 expressing the mutant proteins D83A, K38A, and K164A exhibited a ribosome profile that was very similar to the profile of the *rrmJ* deletion strain. This agreed very well with the growth defects that were observed with these mutants and suggested that the ribosome defect is responsible for the observed growth disadvantage of the *rrmJ* deletion strain.

Polysome profiles prepared from the *rrmJ* deletion strain expressing the D124A variant revealed a slightly larger proportion of stable 50S ribosomal subunits than *rrmJ* deletion strains that express the K38A or K164A variant. Comparison of the polysome profiles of these three mutant strains prepared under associating salt conditions, however, showed very similar ribosome defects (data not shown), suggesting that all three residues Lys-38, Lys-164, and Asp-124 are important for the *in vivo* function of RrmJ. The ribosome profile of cells expressing the E199A and Y201A RrmJ variants, on the other hand, showed only a slight accumulation of ~40S ribosomal subunits, suggesting that mutation of these two residues does not cause a severe defect in RrmJ function.

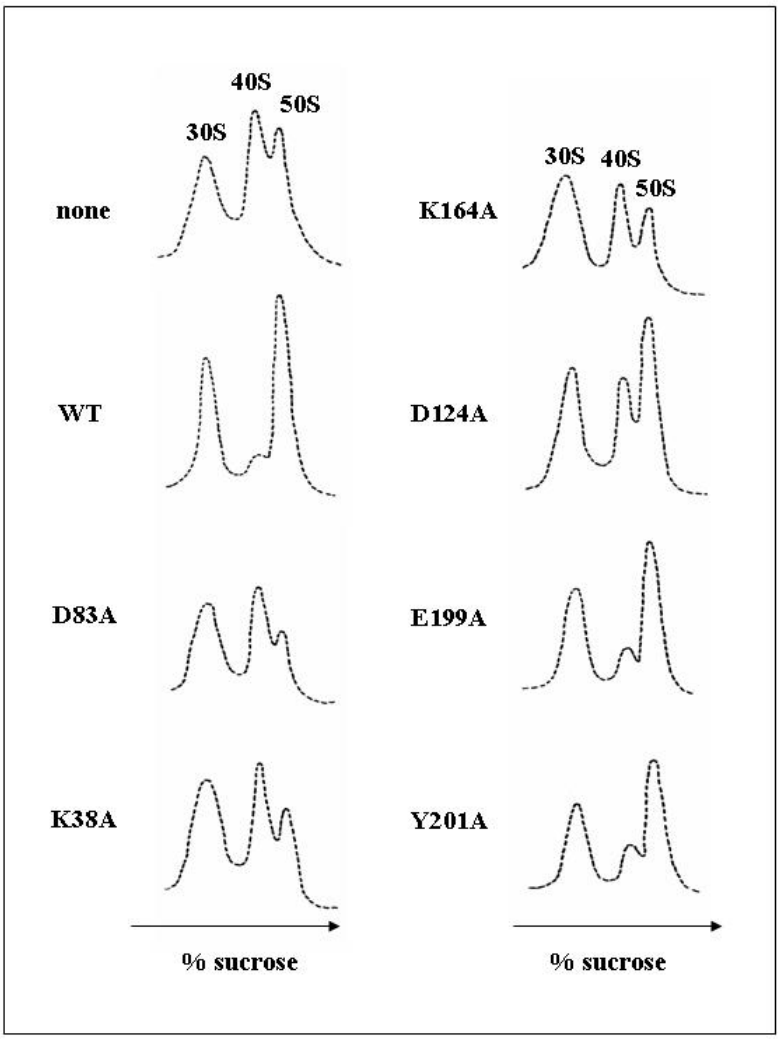

Figure 8: Polysome profiles of the active site mutants in RrmJ (Hager et al., 2002)
Polysome profiles of the *rrmJ* deletion strain HB23 expressing no plasmid or pHB1 derived plasmids encoding wild type RrmJ (WT) or the active site mutants, under dissociating conditions (1 mM $MgCl_2$, 200 mM NH_4Cl) in 10% - 50% sucrose gradients. In the absence of functional RrmJ, ~40S ribosomal particles accumulate at the expense of intact 50S ribosomal subunits.

2.3.4 AdoMet binding affinity of purified RrmJ mutants

To analyze the structural integrity and *in vitro* activity of the RrmJ mutants, the plasmids overexpressing the mutant *rrmJ* genes were transformed into BL21 *rrmJ*Δ*567* strains, and the respective mutant proteins were overexpressed. All but one of the proteins were soluble and could be purified according to the protocol established for wild type RrmJ. The D124A mutant protein was present in inclusion bodies, a fact that prevented me from purifying this RrmJ variant.

Wild type RrmJ contains bound AdoMet cofactor when purified, as demonstrated by mass spectrometry (Bügl et al., 2000). The amount of bound AdoMet can be quantified from the absorption ratio at 280 and 260 nm ($A_{280/260}$ ratio), because AdoMet absorbs at 260 nm. Wild type RrmJ has an $A_{280/260}$ ratio of 0.9 (Bügl et al., 2000), whereas nucleotide-free proteins typically show $A_{280/260}$ ratios of 1.8 – 1.9. As a first measure of the structural integrity of the mutant proteins, the ability of each of the mutant proteins to retain AdoMet during the purification process was assessed. As predicted from the structure of the RrmJ-AdoMet complex, the D83A mutant which should no longer bind AdoMet showed an $A_{280/260}$ ratio equivalent to that of nucleotide-free proteins ($A_{280/260}$ = 1.8), demonstrating that D83 is indeed crucial for AdoMet binding. All other mutant proteins, however, revealed $A_{280/260}$ ratios smaller than 1.8, indicating that various amounts of AdoMet were still associated with the proteins after the purification. To determine the approximate amount of bound AdoMet for wild type RrmJ and the mutants, an AdoMet-titration curve was established using the AdoMet free D83A mutant as standard protein (Fig. 9, *inset*). This standard curve was generated by titrating defined amounts of AdoMet to a RrmJ-D83A mutant protein solution and determine the $A_{280/260}$ ratio after each titration step. The $A_{280/260}$ ratios were then plotted against the amount of titrated AdoMet. Using this curve, the amounts of bound AdoMet were calculated for wild type and each mutant protein using their respective $A_{280/260}$ ratios. As shown in Fig. 9, preparations of wild type RrmJ and of the active site mutants of RrmJ contained between 70 and 80% bound AdoMet. The ability of all mutants to bind and retain the cofactor AdoMet to a similar extent than wild type RrmJ during the purification suggested that the introduced mutations did not cause substantial structural changes in the respective proteins that would lead to significantly altered AdoMet binding affinities.

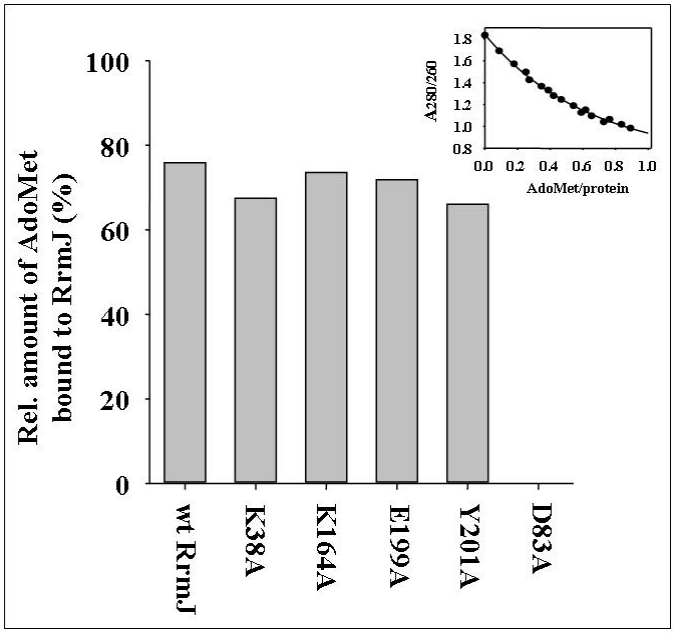

Figure 9: AdoMet binding of the active site mutants (Hager et al., 2002).
The amount of AdoMet bound to wild type RrmJ and the mutant proteins after the purification was calculated according to the AdoMet standard curve (see insert). All of the mutant proteins except D83A contained approximately the same amount of AdoMet after the purification process.
Insert: AdoMet was titrated in 1 µM steps to a 24 µM solution of the AdoMet free RrmJ mutant D83A. The absorption spectra were measured after each AdoMet addition and the respective $A_{280/260}$ ratios were plotted against the corresponding amount of AdoMet/ protein.

2.3.5 *In Vitro* Activity of the RrmJ Mutants

To analyze the influence of the amino acid substitutions on the methyltransfer activity of RrmJ, we first needed to characterize the enzymatic properties of wild type RrmJ (Hager et al., 2002). The apparent V_{max} of the methyltransfer reaction, as well as the apparent K_m values for 50S ribosomal subunits and AdoMet, were determined by *in vitro* methylation assays using purified RrmJ and radioactively labeled AdoMet. 50S ribosomal subunits were prepared from the *rrmJ* deletion strain HB23, because their 23S rRNA lacks the U_{2552} methylation catalyzed by RrmJ. The assay conditions have been established (see "Materials and Methods") in which the rate of [^{3}H]methyl incorporation from [^{3}H]AdoMet into 23S rRNA was proportional to the RrmJ concentration and linear over more than 150 min (data not shown). Thus, the initial rate measurements represented true initial velocities, and the dependence of the rate on substrate concentration could be measured. The apparent K_m value for 23S rRNA within 50S ribosomal subunits was determined to be 0.8 $\pm$ 0.1 µM with an apparent K_{cat} of 0.064 min^{-1} at 37ºC. The apparent K_m for AdoMet was determined to be 3.7 $\pm$ 0.3 µM (Hager et al., 2002).

To characterize the *in vitro* methylation activity of the mutant proteins, the specific activity of the purified RrmJ mutant proteins was determined under conditions in which the two substrates, 50S ribosomes and AdoMet, are present in saturating concentrations (see Fig. 10 and Table 1). Both lysine mutants, K38A and K164A, showed an at least a 50-fold decrease in their *in vitro* methylation activity. The very small amount of methyl incorporation observed was within the limits of the background incorporation, and an increase in enzyme concentration did not cause any increase in methyl incorporation (data not shown). This showed that these two lysine residues play a critical role in the methyltransfer reaction and corroborated the *in vivo* data that suggested that both residues are important for the overall function of RrmJ. Substitution of E199 caused a 16-fold reduction in K_{cat} without changing the K_m for 50S ribosomal subunits. This suggested a less important role for this residue in the catalytic mechanism, an assumption that agreed well with the phenotype of *rrmJ* deletion strains expressing this E199A mutant protein. These cells showed only slightly affected polysome profiles and minor growth disadvantages on McConkey plates suggesting that the activity of this mutant protein is sufficient *in vivo* to partly rescue the *rrmJ* deletion.

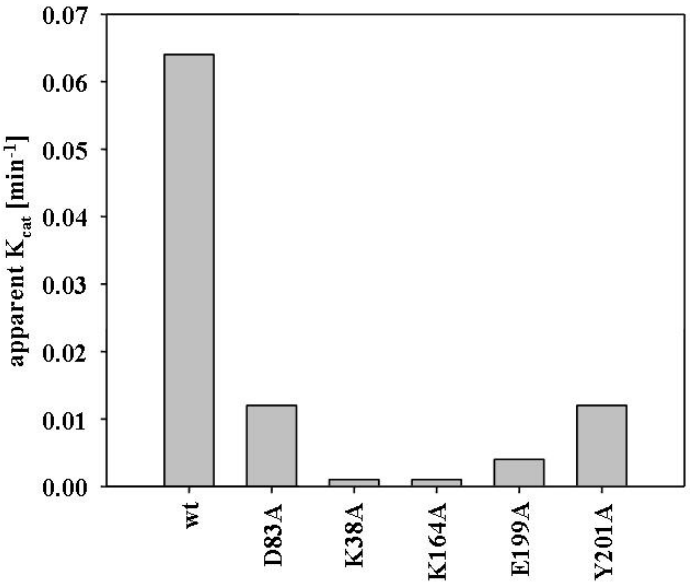

Figure 10: Apparent K_{cat} values of the inactive mutants in RrmJ (Hager et al., 2002)
100 nM purified enzyme was incubated with 50 µM ^{3}H-AdoMet (200 µC/ml) in methylation buffer (50 mM HEPES•KOH, pH 7.5, 100 mM NH_4Cl, 3 mM $MgCl_2$, 2 mM β-mercaptoethanol; 40 U RNasIn) at 37°C. The methylation reaction was started by the addition of 5 µM 50S ribosomal subunits prepared from the *rrmJ* deletion strain HB23. At defined time points, aliquots were taken and the ^{3}H-methyl incorporation was determined as described.

To ascertain that the E199A mutant protein shows indeed sufficient *in vivo* methylation activity to account for the rescued phenotype, the extent of 23S rRNA modification in 50S ribosomal subunits prepared from this mutant strain was analyzed, by

testing them as substrates in the *in vitro* methylation assay (Fig. 11). If the E199A mutant was fully active *in vivo*, most of the 50S ribosomal subunits should be already methylated, and the *in vitro* methyl incorporation should be as low as the methyl incorporation observed with 50S ribosomal subunits prepared from the wild type strain HB24. If the E199A mutant was inactive *in vivo*, on the other hand, the *in vitro* methylation should be as substantial as the *in vitro* methylation of 50S ribosomal subunits prepared from the *rrmJ* deletion strain HB23. More than 60% of 50S ribosomal subunits prepared from HB23 strains expressing the E199A mutant were methylated and no longer served as *in vitro* substrate for RrmJ. These results confirmed the *in vivo* data that revealed the presence of a substantial amount of stable 50S ribosomal subunits and suggested a considerable methylation activity of the E199A mutant *in vivo*.

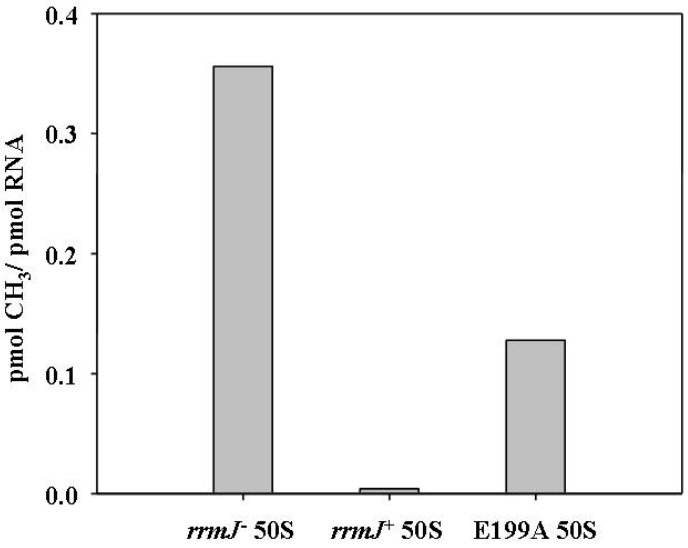

Figure 11: *In vitro* methylation of 50S prepared from the E199A mutant strain
300 nM purified enzyme was incubated with 50 µM ^{3}H-AdoMet (200 µC/ml) in methylation buffer (50 mM HEPES•KOH, pH 7.5, 100 mM NH_4Cl, 3 mM $MgCl_2$, 2 mM β-mercaptoethanol; 40 U RNasIn) at 37°C. The methylation reaction was started by the addition of 2 µM 50S ribosomal subunits prepared from the *rrmJ* deletion strain HB23, the *rrmJ* wild type strain HB24 and the *rrmJ* deletion strain expressing the RrmJ-E199A mutant from a plasmid (JuH 26). After 14 hours the total ^{3}H-methyl incorporation was measured.

The specific activity of the Y201A mutant protein was not as severely impaired as the activity of the K38A and K138A mutant proteins, suggesting that this residue does not take a direct part in the methyltransfer reaction (Fig. 10). Surprisingly, the D83A mutant protein that showed no activity *in vivo* showed about 20% of wild type activity *in vitro*, which has been determined to be 0.064 min^{-1}. This may reflect the fact that this mutant shows an increase in K_m for both substrates. While the apparent K_m values of wild type RrmJ for 50S ribosomal subunits and for AdoMet were determined to be 0.8 $\pm$ 0.1 µM and 3.7 $\pm$ 0.3 µM,

respectively (Hager et al., 2002), the D83A mutant revealed an apparent K_m of 7.0 µM for 50S ribosomal subunits and an apparent K_m of 1.4 µM for AdoMet, leading to a more significant decrease in catalytic activity at lower substrate concentrations, that might be present in the cell.

Table 1: Summary of the *in vivo* and *in vitro* characterization of RrmJ's active site mutants (Hager et al., 2002)

Mutation	Growth 37°C	Polysome profile	AdoMet bound [%]	app. K_{cat} [min^{-1}]	app. K_m (50S) [µM]
wild type	+++	+++	76	0.064	0.8
D83A	-	-	0	0.012	1.4[a]
K38A	-	-	68	< 0.001	n.d.
D124A	(+)	(+)	n.d.[b]	n.d.[b]	n.d.[b]
K164A	-	-	74	< 0.001	n.d.
E199A	++	++	72	0.004	0.7
Y201A	++	++	66	0.012	0.5

[a] The apparent K_m for AdoMet was determined to be 7.0 µM.
[b] D124A mutant aggregated upon overexpression in BL21*rrmJΔ567* cells and could not be purified. This mutant protein was soluble in the strains that were used to investigate the *in vivo* activity of the protein.

The *in vivo* data presented for wild type RrmJ were obtained with the *rrmJ* deletion strain HB23 expressing wild type *rrmJ* from a pET 11a plasmid (HB25). Growth of this strain is very similar to that of the corresponding wild type *E. coli* strain (MG1655) but it accumulates slightly higher levels of 30S and 50S ribosomal subunits in lysates prepared under associating conditions and 40S ribosomal subunits in lysates prepared under dissociating salt conditions. Western blot analysis revealed that all mutant variants were soluble and expressed in similar amounts as the single copy of wild type RrmJ from its normal chromosomal location in MG1655. ND, not determined; -, (+), ++ or +++, ribosome profiles are severely, moderately, slightly, or not impaired in lysates prepared under the indicated salt conditions.

2.3.6 The effect of magnesium on the methylation activity of RrmJ

The small catechol *O*-methyltransferase (COMT) whose methyltransfer reaction has been analyzed and that we used to propose a reaction mechanism for RrmJ (see chapter 3) binds the cofactor AdoMet only in the presence of bound Mg^{2+} (Vidgren et al., 1994) and

requires Mg^{2+} for its activity. The crystal structure of COMT showed that its catalytic site includes a Mg^{2+} ion (Jeffery and Roth, 1987; Vidgren et al., 1994).

Our lab has previously shown that the *in vitro* methylation activity of RrmJ is also dependent on the presence of magnesium ions (Bügl et al., 2000). However, the crystal structure of RrmJ in complex with AdoMet did not reveal any bound Mg^{2+} ions. Furthermore, the active site of RrmJ superimposed very well with the active site of the methyltransferase VP39 (Fig. 6A, (Hager et al., 2002)) which was found to act Mg^{2+} independently (Hodel et al., 1998). Therefore, it appeared less likely that the methyltransferase activity of RrmJ itself required Mg^{2+} but suggested that the observed Mg^{2+} dependence of the RrmJ mediated reaction might be due to the stability requirements of RrmJ's substrate, the 50S ribosomal subunits. A decrease in the Mg^{2+} concentration to 1 mM causes the 50S ribosomal subunits in a lysate of the *rrmJ* deletion strain to dissociate into ~40S particles (see section 2.3.3; Fig. 8), which do no longer serve as substrate for RrmJ (Bügl et al., 2000). To determine the optimal magnesium concentration for the *in vitro* methylation reaction of RrmJ, the assays was conducted in the presence of increasing concentrations of Mg^{2+}. Surprisingly, high concentrations of Mg^{2+} showed an inhibitory effect on the methylation activity of RrmJ and decreased the apparent K_{cat} of RrmJ by ~2 fold. However, contradictory with our previous consideration, concentrations of as low as 0.9 mM Mg^{2+} RrmJ showed a significant increase in methylation activity instead of the expected decrease due to the assumed instability of the 50S ribosomal subunits (Fig. 12).

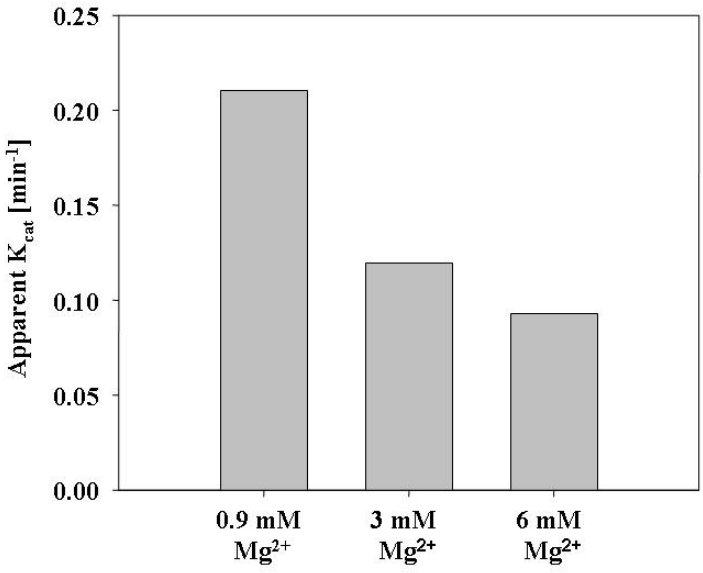

Figure 12: Mg^{2+} dependence for wild type RrmJ.
The initial rate for methylation was measured in the presence of 100 nM purified RrmJ, 50 µM AdoMet (200 µC/ml), 5 µM 50S ribosomal subunits prepared from the *rrmJ* deletion strain HB23 and increasing concentrations of $MgCl_2$ in methylation buffer (50 mM HEPES·KOH, pH 7.5, 100 mM NH_4Cl, 2 mM β-mercaptoethanol). At defined time points of the incubation reaction at 37°C, aliquots were taken and the incorporation of radioactivity due to methylation of 23S rRNA of the 50S subunit was determined (see Materials and Methods). The highest

methylation activity was received at 0.9 mM $MgCl_2$.

2.3.7 The stability of the ribosomal subunits in the rrmJ deletion strain HB23

Lysates prepared from the *rrmJ* deletion strain accumulate ~40S ribosomal particles when the magnesium concentration is decreased to 1 mM. Therefore, it was surprising that the methylation activity of RrmJ increased at these low magnesium concentrations as shown in section 2.3.6. If the 50S ribosomal subunits dissociate into ~40S particles which do not serve as a substrate for RrmJ (Bügl et al., 2000) the methylation activity should decrease rather than increase due to a loss of suitable substrate. In order to investigate the stability of isolated 50S ribosomal subunits from the *rrmJ* deletion strain, 50S ribosomal subunits were prepared under associating (10 mM $MgCl_2$ and 100 mM NH_4Cl) as well as dissociating (1 mM $MgCl_2$ and 200 mM NH_4CL) salt conditions. These 50S preparations were then applied onto a dissociating gradient to monitor the occurrence of the ~40S peak. As shown in Fig. 13 only 50S ribosomal subunits prepared from the *rrmJ* deletion strain under associating conditions fall apart into ~40S particles. The 50S ribosomal subunits prepared from the *rrmJ* deletion strain under dissociating conditions, however, remained stable when subjected to low magnesium concentrations. This shows that in the *rrmJ* deletion strain ~40S and 50S ribosomal subunits occur as two distinct populations that are not in an equilibrium with each other. This finding also explains why the methylation activity of RrmJ does not decrease at low magnesium concentrations. The 50S ribosomal subunits that are used in the *in vitro* methylation assay were prepared under dissociating condition and therefore do not dissociate into ~40S particles but remain stable 50S ribosomal subunits even at a magnesium concentrations lower than 1 mM. This observation now raised the question, which population of 50S ribosomal subunits is present in the 70S ribosomes of the *rrmJ* deletion strain. To address this question, 70S ribosomes prepared under associating conditions were applied onto a dissociating gradient. As shown in Fig. 13 these 70S ribosomes dissociate into 30S, ~40S and 50S ribosomal subunits. Therefore, both the ~40S particles and 50S ribosomal subunits are able to assemble with the small 30S ribosomal subunit to form the 70S ribosome.

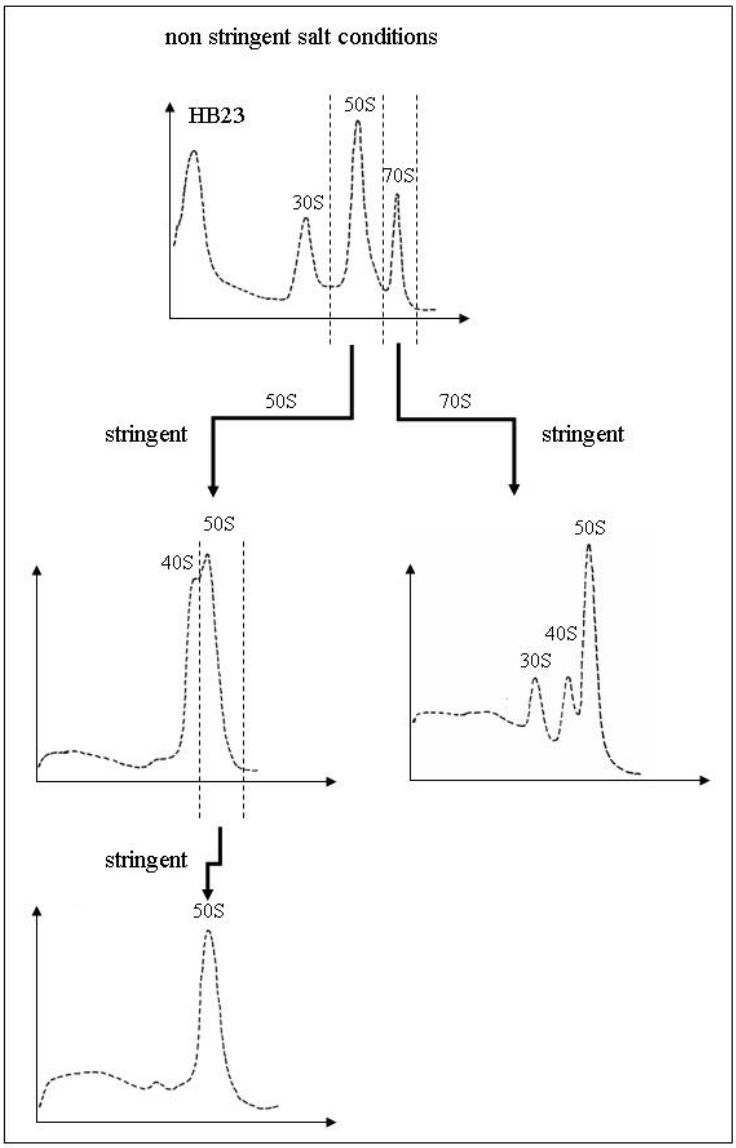

Figure 13: Stability of ribosomal subunits prepared from the *rrmJ* deletion strain.
50S ribosomal subunits prepared from the *rrmJ* deletion strain under non stringent salt conditions dissociate partly into ~40S ribosomal particles under stringent salt conditions. 50S ribosomal subunits taken from these stringent salt conditions and subjected again to a gradient under stringent salt conditions remain stable. Therefore, ~40S and 50S ribosomal subunits of the *rrmJ* deletion strain represent two stable subunit populations that appear in an equilibrium. Applying 70S ribosomes prepared from the *rrmJ* deletion strain onto a dissociating gradient reveals that both ~40S and 50S populations are present in completely assembled ribosomes of the *rrmJ* deletion strain.

2.4 Substrate Binding Analysis

2.4.1 Rational RrmJ mutant design

The conservation of an amino acid residue in a protein is a strong indicator of its importance in the structure and/or function of the protein. Residues that are exposed to the surface of a protein are usually highly variable unless they are involved in the catalytic mechanism of the protein, its structural integrity or in substrate and/or cofactor binding. Therefore, to investigate the potential substrate binding site of the 23S rRNA methyltransferase RrmJ, the site directed mutagenesis has been extended, substituting the majority of highly conserved residues in RrmJ. Only those residues were spared that have been shown to be involved in S-adenosylmethionine (AdoMet) binding and/or the catalytic site of RrmJ (see section 2.3) (Hager et al., 2002) as well as those that were predicted to play a structural role in the protein fold (Fig. 14).

From the 27 most highly conserved amino acids in RrmJ (Bügl et al., 2000), 11 aa either directly contact the cofactor AdoMet or are active site residues (see section 2.3) (Bügl et al., 2000; Hager et al., 2002). Analysis of the crystal structure of RrmJ allowed us to predict, furthermore, that the highly conserved residues P127, F161, F182, P190 and S193 are likely to perform structural functions in the methyltransferase, either by forming the AdoMet binding pocket (e.g. P127), or by building the hydrophobic core of the α/β protein (e.g. F161, F182). Q119 and G159 were also excluded from the mutagenesis studies because both amino acids are located on the opposite site of the RrmJ molecule and appeared, therefore, rather unlikely to be involved in substrate binding. These considerations left us with nine highly conserved residues (D20, Y22, R32, R34, Q67, D136, F166, R194, S197), eight of which were individually or pair-wise substituted with alanine residues. D136 was substituted with an asparagine residue to maintain the size of this residue but change its biophysical character.

To expand the mutagenesis scheme advantage was also taken of the fact that the structures of the 2'-*O*-methyltransferases VP39 and RrmJ are so closely related. Therefore, a structure based sequence alignment between these two enzymes and modeling studies of the mRNA substrate analogue of VP39 onto the RrmJ structure by our collaborator Bart Staker, revealed four additional, somewhat less conserved residues in RrmJ, that were also

suggestive of being involved in the substrate association. These considerations led us to make additional alanine substitutions of the residues F37, L39, Y68 and K189 in RrmJ.

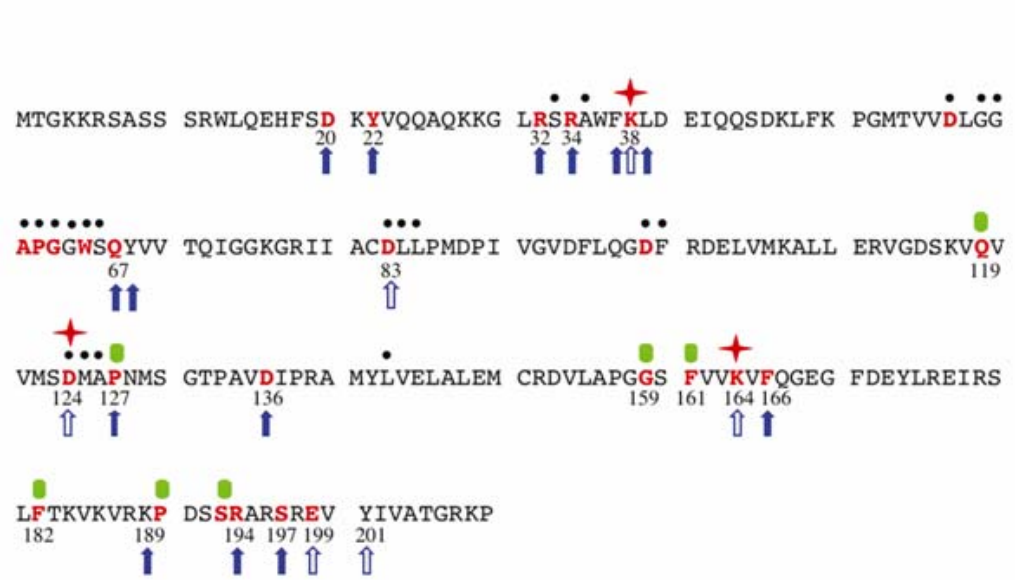

Figure 14: Rational mutant design (Hager et al., 2004)
The 27 most highly conserved residues in RrmJ are shown in bold red. These amino acids have been identified as highly conserved by aligning a set of 1112 non redundant paralog sequences to a set of 29 likely RrmJ orthologs (Bügl et al., 2000). The black dots above the RrmJ sequence indicate the residues that have been identified to be involved in AdoMet binding (Bügl et al., 2000). Red stars mark the three amino acids that have been shown to built the active site in RrmJ (see section 3.2) (Hager et al., 2002). The closed green cylinders above the sequence depict the amino acids, which are either predicted to play a structural role in RrmJ, or reside on the opposite site of the RrmJ molecule. The open blue arrows mark all highly conserved residues that have been mutated in order to investigate the active site of RrmJ (see section 3.2; Table 1) (Hager et al., 2002). The closed blue arrows depict the residues that were now mutated for analyzing the substrate binding site.

2.4.2 *In vivo* phenotype of the RrmJ mutants

To first analyze how the individual mutations affect the *in vivo* function of RrmJ, the plasmids encoding the respective RrmJ mutants were transformed into the *rrmJ* deletion strain HB23. Quantitative western blot analysis was used to determine the expression level of the various mutant proteins and the mutant proteins were found to be all soluble and expressed in similar amounts as compared to a single copy of wild type RrmJ expressed from its normal chromosomal location (data not shown). This excluded the possibility that any observed *in vivo* phenotype was due to inappropriately low or high RrmJ mutant protein levels. This wild type like expression level of the RrmJ mutant proteins has been already described before (see section 2.3.2) and is due to their leaky expression from the un-induced pET11a vector (Hager et al., 2002).

To evaluate the *in vivo* function of the RrmJ mutant proteins, first their growth phenotype was analyzed in liquid LB medium at 37^{o}C. As summarized in Table 2, wild type *E. coli* strains show a doubling time of 25 min at 37^{o}C, while the *rrmJ* deletion strain grows significantly slower with a doubling time of more than 50 min. This severe growth defect is clearly due to a defect in the methyltransferase activity of RrmJ because expression of the active site mutant RrmJ-K38A in the *rrmJ* deletion strain did not rescue the growth defect (Table 2). Analysis of the growth of the putative substrate binding mutants revealed that three of these mutant proteins show a significantly compromised *in vivo* activity. The doubling times for these *rrmJ* deletion strains expressing the RrmJ-F166A mutant were 40 min, for the RrmJ-R32A/R34A mutant 43 min and for the RrmJ-D136N mutant 45 min. These were clearly all much longer than the doubling time of 25 min that was determined for the *rrmJ* deletion strain expressing wild type RrmJ. Noteworthy, all other mutant strains showed also slightly longer doubling times than the wild type strain, ranging from 32 min to 38 min per doubling. This suggested that substitution of any of the conserved amino acids might impair the *in vivo* function of RrmJ to some extent.

2.4.3 Ribosome profiles of the RrmJ mutant strains

The growth defect of strains lacking functional RrmJ was proposed to be due to the absence of the highly conserved Um_{2552} modification in the A-loop of the 23S rRNA, which was thought to cause either assembly or stability problems of the 70S ribosome and leads to an impaired translational efficiency (Caldas et al., 2000c). To investigate to what extent the growth defect of the mutant strains correlated with the ribosome profile in these strains, lysates of the individual *rrmJ* mutant strains were prepared and the ribosome profiles under non-stringent and stringent salt conditions were compared to the lysate of the *rrmJ* deletion strain expressing wild type RrmJ from a plasmid (HB25). As mentioned before, the ribosome defect of an *rrmJ* deletion strain is revealed by the accumulation of large amounts of 30S and 50S ribosomal subunits in lysates prepared under non-stringent salt conditions (Fig. 15 left panel), and by the population of ~40S ribosomal particles in lysates prepared under stringent salt conditions (Fig. 15, right panel) (Bügl et al., 2000).

The degree of ribosome defects observed in the individual mutant strains corresponded only to a certain extent to the degree of growth of the respective mutant strains in liquid culture. The three mutant strains that showed the slowest growth in liquid LB media (R32A/R34A, D136N, F166A) had indeed the strongest ribosome defect. R32A/R34A and D136N mutant strains accumulated larger amounts of 30S and 50S ribosomal subunits as compared to wild type strains under non- stringent salt conditions, and had a significant amount of ~40S ribosomal particles under stringent salt conditions. The F166A mutant protein accumulated more ribosomal subunits without populating the ~40S particles. All other mutant strains, however, showed ribosome profiles that were either slightly altered or identical to the ribosome profiles prepared from wild type strains (Table 2). This was in contrast to the growth disadvantages that was observed in all of these strains and suggested that the growth defects observed in the *rrmJ* deletion strain might not be directly connected to defects in ribosome assembly and/or stability.

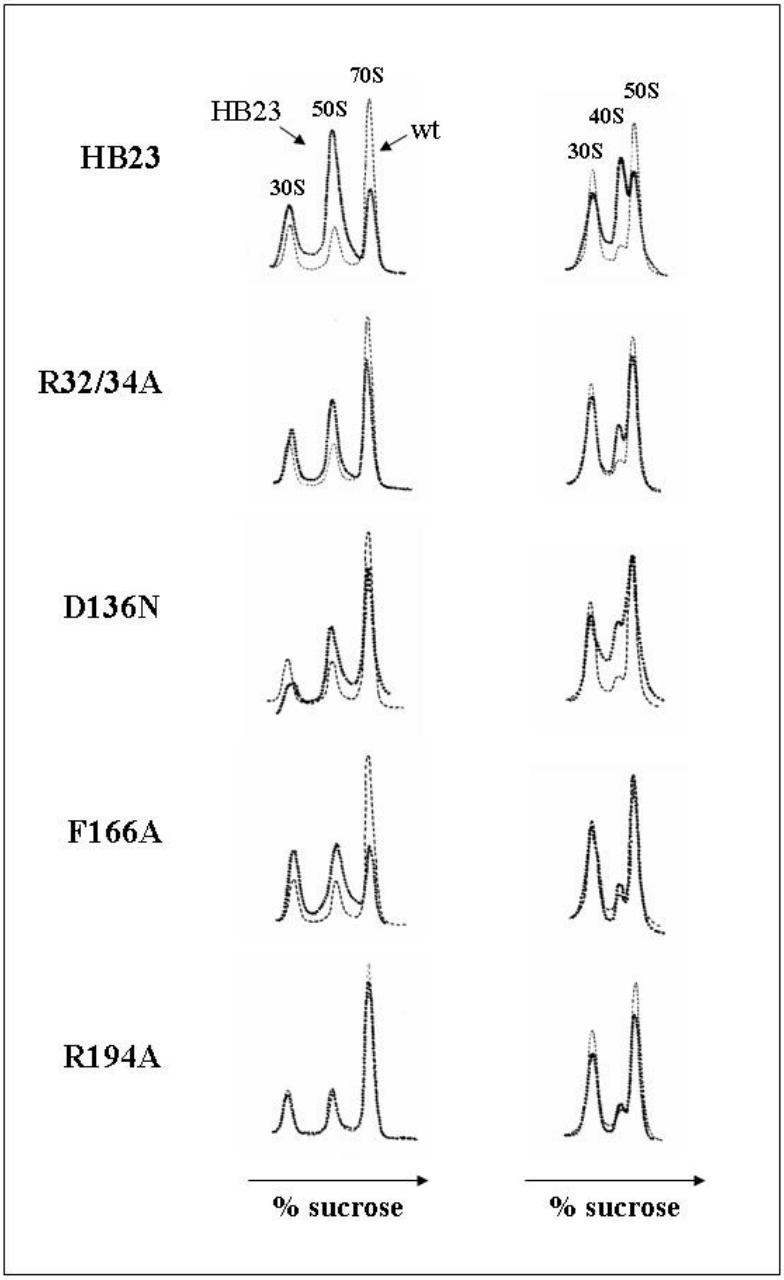

Figure 15: *In vivo* activity of the RrmJ mutants (Hager et al., 2004)
Polysome profiles of *rrmJ* deletion strain HB23 expressing no RrmJ or expressing wild type RrmJ or the mutant proteins from a plasmid to wild type protein levels. The ribosome profiles were either analyzed under (left panel) associating, non-stringent salt conditions (10 mM $MgCl_2$, 100 mM NH_4Cl) or (right panel) under dissociating, stringent salt conditions (1 mM $MgCl_2$, 200 mM NH_4Cl). The ribosome profiles of lysates prepared from the individual strains are represented by dotted lines and compared to the polysome profile of an *rrmJ* deletion strain expressing wild type RrmJ (dashed line).

2.4.4 Kinetic characterization of the RrmJ mutant proteins

Biochemical characterization of the mutated RrmJ proteins was necessary to further elucidate which residues might be involved in substrate binding. Therefore, all mutant proteins were purified excluding only those two RrmJ variants that had substitutions in less-conserved amino acids (F37A/L39A, Q67A/Y68A) and showed ribosome profiles that were indistinguishable from wild type ribosome profiles (Table 2). All mutant proteins were expressed as soluble proteins to near wild type protein level in the transformed *rrmJ* deletion strain, indicating that the mutations did not significantly alter the stability of the proteins. Again, to obtain additional evidence that the respective mutations did not cause a major change in the conformation of the mutant proteins, the amount of AdoMet that remained associated with each of the eight mutant RrmJ proteins after their purification was determined as described before in section 2.3.4 (Hager et al., 2002). As shown in Table 2, all but one RrmJ mutant protein had at least 59% and up to 81% AdoMet associated after their purification, confirming that the overall structural integrity of the mutant proteins has probably been maintained. Only the RrmJ-F166A mutant protein, which showed one of the most severe growth and ribosome defects when expressed in the *rrmJ* deletion strain *in vivo*, was associated with significantly less AdoMet after purification. This either suggested a decrease in AdoMet binding affinity and/or the presence of a certain amount of inactive yet stably folded RrmJ mutant species in the preparation that is no longer able to bind AdoMet. Therefore this mutant protein has not been used for the further *in vitro* studies.

To test the enzymatic activity of the various RrmJ mutant proteins *in vitro*, their ability to methylate 50S ribosomal subunits prepared from the *rrmJ* deletion strain (HB23) was investigated. By using 100 nM enzyme and keeping both substrates, AdoMet and 50S ribosomal subunits in large excess, the apparent K_{cat} values for each of the purified mutant proteins were determined at 37˚C. As shown in Fig. 16 and summarized in Table 2, four of the mutant proteins revealed an at least 50% decrease in their apparent K_{cat} values, with the RrmJ variants harboring a mutation in R32/R34 and K189 showing the most significant decrease in enzymatic activity. Mutations in D20 and D136 also led to slight decrease in apparent K_{cat} while mutations in Y22, R194 and S197 did not dramatically alter the turnover number of RrmJ under the conditions tested.

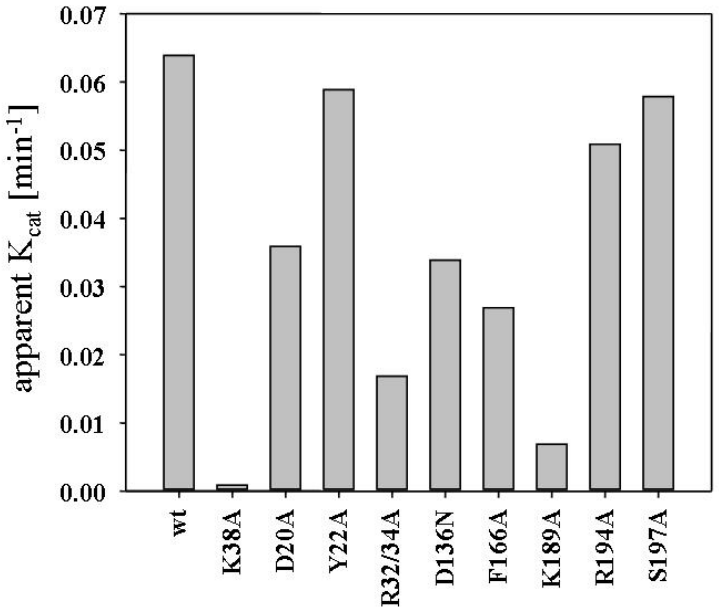

Figure 16: *In vitro* activity of the various RrmJ mutants (Hager et al., 2004)
100 nM purified enzyme was incubated with 50 µM ^{3}H-AdoMet (200 µC/ml) in methylation buffer (50 mM HEPES•KOH, pH 7.5, 100 mM NH_4Cl, 3 mM $MgCl_2$, 2 mM β-mercaptoethanol; 40 U RNasIn) at 37°C. The methylation reaction was started by the addition of either 5 µM or 8 µM 50S subunits prepared from the *rrmJ* deletion strain HB23. At defined time points, aliquots were taken and the ^{3}H-methyl incorporation was determined as described.

Next, the apparent K_m values of 50S ribosomal subunits for each of the purified RrmJ mutants were determined. For these experiments, the AdoMet concentration was kept constant at 50 µM, and the concentration of 50S ribosomal subunits was varied from 0.2 µM to 10 µM. As shown in Table 2, an increased apparent K_m value for 50S ribosomal subunits was found for four of the RrmJ variants. These RrmJ mutants harbored substitutions in the surface exposed amino acids D20, R32/R34, R194 or S197, implicating these amino acids as potentially involved in the binding of the 23S rRNA. The observed changes in apparent K_m values for 50S subunit binding in RrmJ mutant proteins were very similar to the changes in K_d and K_m values that have been determined for substrate binding mutants of the 23S rRNA dimethyltransferase ErmC' (Maravic et al., 2003). In ErmC' mutant proteins, K_d and K_m values increased by about 1.6 to 5-fold. This indicated that RNA binding is a highly cooperative, multivalent process, in which the mutation of single amino acids in the substrate binding site might not alter the substrate binding affinity as dramatically as do amino acid substitutions in the substrate binding site of other non-nucleic acid binding proteins.

Table 2: Summary of the *in vivo* and *in vitro* activities of RrmJ and the mutants (Hager et al., 2004)

mutation	*doubling time (37°C) [min]*	*ribosome profiles*		*AdoMet/ protein [%]*	*app. K_{cat} [b] [min^{-1}]*	*app. K_m [b] [μM]*	*K_{cat}/ K_m [$\mu M^{-1} min^{-1}$]*
		associating conditions	*dissociating conditions*				
wild type	25	+++	+++	76	0.064	0.7 ± 0.05	0.080
rrmJ -	53	*rrmJ* -	*rrmJ* -				
K38A[a]	58	*rrmJ* -	*rrmJ* -	68	<0.001		
D20A	36	+++	+++	81	0.036 ± 0.007	1.5 ± 0.40	0.024
Y22A	32	+++	++	78	0.059 ± 0.004	0.7	0.084
R32A/34A	43	+	+	72	0.017 ± 0.013	2.7 ± 0.60	0.006
F27A/L39A	38	+++	+++	n.d.	n.d.	n.d.	n.d.
Q67A/Y68A	38	+++	+++	n.d.	n.d.	n.d.	n.d.
D136N	45	+	+	71	0.034 ± 0.007	0.5 ± 0.20	0.068
F166A	40	+	+++	40 ± 4	n.d.	n.d.	n.d.
K189A	32	++	+++	65	0.007 ± 0.002	0.5	0.014
R194A	33	+++	++	59	0.051 ± 0.010	1.5 ± 0.40	0.034
S197A	34	+++	++	74	0.058 ± 0.004	1.4 ± 0.01	0.041

[a] See reference (Hager et al., 2002).
[b] The apparent K_{cat} and K_m values are the means and standard deviations of results from at least three independent experiments.

The *in vivo* data presented for wild type RrmJ were obtained with the *rrmJ* deletion strain HB23 expressing wild type *rrmJ* from a pET 11a plasmid (HB25). Western blot analysis revealed that all mutant variants were soluble and expressed in similar amounts as the single copy of wild type RrmJ from its normal chromosomal location in MG1655. ND, not determined; +, ++ or +++, ribosome profiles are moderately, slightly, or not impaired in lysates prepared under the indicated salt conditions.

2.4.5 *In vitro* enzymatic activity and *in vivo* ribosome profile - A good but not absolute correlation

Comparison of the *in vitro* and *in vivo* activity of RrmJ and the mutants indicated a good but not absolute correlation between changes in the apparent K_{cat} and K_m values of the purified RrmJ variants and alterations in the ribosome profiles of the corresponding mutant strains. The two most obvious outliers in this correlation were the RrmJ-K189A and the RrmJ-D136N mutant protein. The RrmJ-K189A mutant strain revealed no apparent ribosome defect *in vivo* and no significant change in K_m for 23S rRNA but had an almost 10-fold decreased apparent K_{cat} value (Table 2). This result could be explained by the possibility that analysis of the ribosome profiles under steady state conditions might not be sufficiently sensitive to detect these changes in the catalytic activity of RrmJ. The RrmJ-D136N mutant protein, on the other hand, showed a very severe growth disadvantage and ribosome defect *in vivo* but had wild type apparent K_{cat} and K_m values *in vitro*. To investigate whether the D136N mutant protein was indeed inactive *in vivo*, the methylation status of 23S rRNA prepared from RrmJ-D136N expressing mutant strains was analyzed. The rationale was, that if the D136N mutant protein was inactive *in vivo*, the 50S ribosomal subunits would be un-methylated and would serve as *in vitro* substrates for wild type RrmJ, much like 50S ribosomal subunits prepared from the *rrmJ* deletion strain. If, on the other hand, the D136N mutant protein was active *in vivo*, the ribosomal subunits would be methylated and would, like 50S ribosomal subunits prepared from wild type strains, no longer serve as *in vitro* substrates. 50S ribosomal subunits from the *rrmJ* deletion strain expressing the RrmJ-D136N mutant protein were prepared and the ability of wild type RrmJ to methylate these ribosomal subunits *in vitro* was tested. As shown in Fig. 19, 50S ribosomal subunits prepared from the *rrmJ* deletion strain expressing the D136N mutant showed the same incorporation of methyl groups upon incubation at 37^{o}C as subunits prepared from the strain that lacked RrmJ altogether (Fig. 19, compare closed squares and triangles). This clearly showed that D136N mutant is indeed unable to methylate 23S rRNA of 50S ribosomal subunits *in vivo*, which agreed well with the observed ribosome defect of D136N expressing *rrmJ* deletion strain.

2.5 The A-loop as Minimal Substrate for RrmJ

2.5.1 Modeling of the A-loop structure onto the surface of RrmJ

U_{2552}, the methylation target of RrmJ, is one of the five residues that constitute the A-loop in the peptidyltransferase center of the ribosome. Both the crystal structure (Ban et al., 2000) and the solution structure (nucleotides 2548-2560) (Blanchard and Puglisi, 2001) of the A-loop have been solved. To model the solution structure of the A-loop into RrmJ, our collaborator Bart Staker positioned the A-loop initially manually into RrmJ. He used the crystal structure of the mRNA 2'-*O*-methyltransferase VP39 from *Vaccinia virus* bound with the reaction product S-adenosylhomocysteine and 5' m^7G-capped single stranded RNA hexamer as a guide (Hodel et al., 1998). The RNA was positioned by first overlaying the ribose and phosphate atoms of the reactive nucleotides into the active site of RrmJ (Fig. 17A, red model). This positioning gave close agreements between the individual atom positions in the active site between U_{2552} of the A-loop RNA model and the 5' m^7G -capped RNA of VP39. However, the rest of the A-loop clashed with protein residues. Most noteworthy, the double-helical stalk of the A-loop clashed severely with the protruded helix 4 of RrmJ (Fig. 17A, red model).

To accommodate the A-loop, he then kept the phosphodiesters of the reactive U_{2552} in position and rotated the A-loop by approximately 85 degrees. This prevented all clashes between the A-loop and RrmJ protein (Fig. 17A, blue model). The phosphodiesters of the double-helix now fit snuggly into a deep cleft of RrmJ. Importantly, RNA-protein interactions involved exactly those residues (R34, R194, S197) in RrmJ that when mutated to alanine residues exerted an increased K_m for 23S rRNA binding (Fig. 17C). This suggested that these amino acids are indeed involved in the binding and positioning of 23S rRNA in RrmJ. In this model, the phosphodiesters occupy now the same location as the phosphodiesters of the 5' m^7G-capped RNA hexamer in the VP39 structure. Additionally, the minor groove of the A-loop RNA is now positioned to sit nicely atop helix 4 of RrmJ, rather than clashing with the protein.

Interestingly, however, once the A-loop was turned to fit into the protein, the 2'-hydroxyl group of U_{2552} was no longer accessible to the active site of RrmJ (Fig. 17B, yellow nucleotide). These observations suggested a base-flipping mechanism for U_{2552} methylation in which the A-loop RNA first binds into the RrmJ binding site, then undergoes a base-

flipping rotation of U_{2552} by 85 degrees, thereby placing the 2'-hydroxyl in position for the methylation.

The base-flipped model of the A-loop RNA was constructed and positioned into the putative binding site of RrmJ (Fig. 17B, red nucleotide). Both base-flipped U_{2552} and "unflipped" models were then energy minimized by positional and simulated annealing using the program CNX (Brunger et al., 1998). During these refinements the protein atoms were allowed to adjust to the RNA model. Only two residues were found to move slightly. The side chains of Arg194 and Arg196 both located on the surface of RrmJ, are required to change conformation in order for the A-loop RNA model to position into the substrate binding cleft optimally. These residues are then closely positioned next to the phosphate backbone of the model A-loop.

Very similar results were obtained when he modeled the crystal structure of the A-loop into RrmJ. This was due to the fact that the major differences between the A-loop conformation in the crystal structure and in the solution structure involve parts of the A-loop that do not contact RrmJ. The phosphate backbone of the A-loop, however, which makes most of the contacts with RrmJ are not significantly different in the two structures.

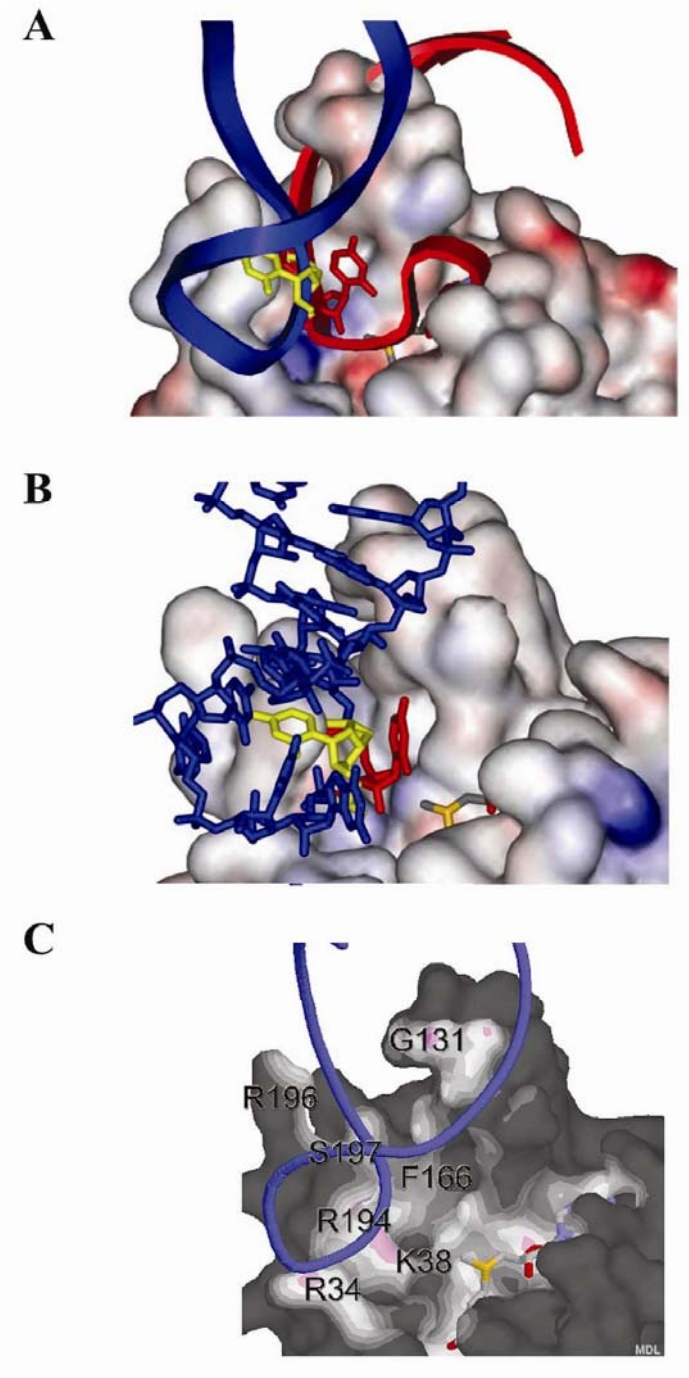

Figure 17: Modeling of the A-loop onto the surface of RrmJ (Hager et al., 2004)

A. *In situ* modeling of the A-loop structure (nucleotides 2548-2560) as solved by NMR (Blanchard and Puglisi, 2001) onto the surface of RrmJ. Modeling is based on overlaying the U_{2552} reactive nucleotide into RrmJ's active site with the 5' m^7G-capped reactive nucleotide in the VP39 structure. Without turning the A-loop, the double helical stalk of the A-loop clashes severely into the extended α_4 helix of RrmJ (red model). To avoid this clashing, the A-loop is turned by 85 degrees (blue model). Now, phosphodiesters occupy the same location in the model of RrmJ as do phosphodiesters of the 5' m^7G-capped RNA hexamer in the VP39 structure.

B. Base flipping of U_{2552}. The model shows U_{2552} in the closed position (colored in yellow), where the 2' hydroxyl group of the ribose is not accessible to the methyl donor AdoMet and in the flipped out configuration (colored in red), where the 2' hydroxyl group is in the optimal position to be methylated.

C. Solvent accessible surface of RrmJ colored by distance to ligand atoms from U_{2552}-flipped A-loop RNA (shown as blue ribbon) and AdoMet (shown as stick). The surface is colored by distance from nearby atoms. Dark areas are too far away from any atoms outside the surface to be bonded. White or light areas are close enough for hydrophobic van der Waals interactions. Pink areas are close enough for hydrogen bonds. Figure made with Protein Explorer (Martz, 2002).

2.5.2 The unmodified A-loop - The minimal substrate of RrmJ

Modeling studies revealed that the A-loop can be modeled into the identified substrate binding site of RrmJ. This suggested that the A-loop might serve as an *in vitro* substrate for RrmJ. Therefore, *in vitro* methylation assays were performed using the same unmodified A-loop that was used in the NMR (Blanchard and Puglisi, 2001) and our modeling studies (Fig. 17). The Um_{2552} methylated A-loop was used as control (Blanchard and Puglisi, 2001). As shown in Fig. 18, a significant RrmJ-mediated methyl incorporation into the non-modified A-loop was observed (Fig. 18, circles). The methylated A-loop, on the other hand, did not serve as an *in vitro* substrate for purified RrmJ (Fig. 18, triangles), strongly suggesting that the methylation of the A-loop by RrmJ was indeed a specific process. Because the methyl incorporation into the A-loop was slow compared to the methyl incorporation into 50S ribosomal subunits, we wanted to exclude the possibility that the observed A-loop methylation is due to small amounts of a different methyltransferase that might contaminate the wild type RrmJ preparation. Therefore, the active site mutant RrmJ-K38A was tested, and found to be completely unable to methylate the unmodified A-loop *in vitro* (data not shown). Together, these results showed that RrmJ can specifically recognize, bind and methylate the A-loop when it adopts its solution structure. The slow methyl incorporation, however, might be due to missing contact sites that are present in the 50S ribosomal subunit and, as suggested by later experiments, due to the missing association of the 30S ribosomal subunit during ribosome assembly which triggers RrmJ's substrate release (section 2.6.6).

Analysis of the ribosome structure suggested that RrmJ is unable to access the A-loop unless it is looped out of the ribosome. Such reversible undocking of the A-loop has been proposed before and was suggested to occur as a regular step in tRNA selection and accommodation (Blanchard and Puglisi, 2001). My findings confirmed these considerations and suggested that the A-loop adopts its solution structure when looped out of the ribosome, where it can be methylated by RrmJ. This provides an excellent explanation as to how RrmJ is able to methylate a buried 23S rRNA residue so late in the maturation process of the ribosome.

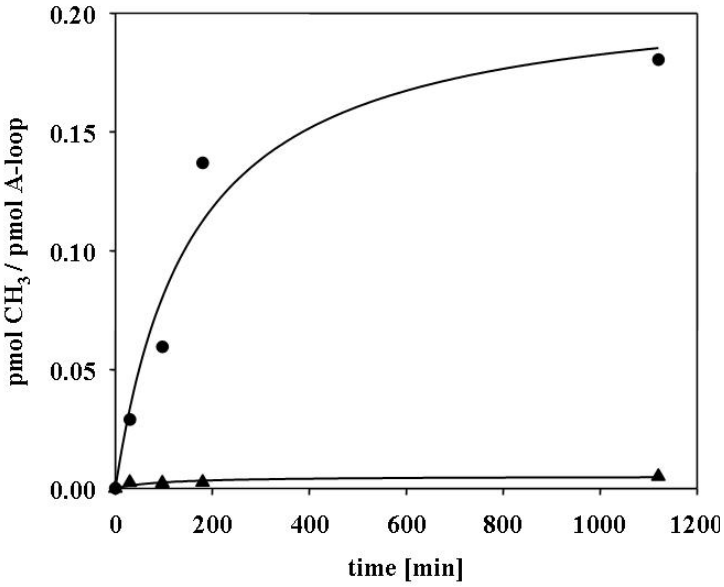

Figure 18: Non methylated, isolated A-loop - A minimal substrate for RrmJ *in vitro* (Hager et al., 2004)
5 µM wild type RrmJ was incubated with either (circles) 1 µM non-modified or (triangles) 1 µM methylated A-loop (nucleotides 2545-2563) and 50 µM ^{3}H-AdoMet (200 µC/ml) in methylation buffer (50 mM HEPES•KOH, pH 7.5, 50 mM NaCl, 10 mM EDTA, 1 mM DTT; 40 U RNasIn; 0.1 mg/ml BSA) at 37°C. Aliquots were taken at defined time points and the ^{3}H-methyl incorporation was measured as described.

2.6 RrmJ Associates with its Ribosomal Substrate

2.6.1 RrmJ binds to 50S ribosomal subunits *in vivo*

Analysis of the *in vitro* methyl incorporation into ribosomal subunits of D136N mutant cells was only in part dependent on the presence of exogenous wild type RrmJ. Incubation of the D136N-50S ribosomal subunits at 37°C in the presence of ^{3}H-AdoMet but in the absence of purified RrmJ led to a substantial methylation of the 23S rRNA (Fig. 19, open squares). This was in contrast to 50S ribosomal subunits prepared from the *rrmJ* deletion strain, whose methylation was absolutely dependent on the presence of exogenous RrmJ (Fig. 19, compare closed and open triangles) and to the results obtained with 50S ribosomal subunits prepared from the wild type strain, which did not show any methyl incorporation independently of the presence of purified RrmJ (Fig. 19, compare closed and open circles). These results suggested that a methyltransferase activity was present in the 50S ribosomal subunits prepared from the *rrmJ* deletion strain expressing the RrmJ-D136N protein, which only became active under the chosen *in vitro* methylation conditions. The purified D136N mutant protein showed near wild type activity *in vitro* when tested on unmethylated 50S ribosomal subunits prepared from the *rrmJ* deletion strain. This finding, together with the observation that the yeast RrmJ homologue Mrm2p co-fractionates with mitochondrial 21S rRNA (Pintard et al., 2002a), led us to investigate whether the observed

methyltransferase activity was indeed the RrmJ-D136N mutant protein bound to its 50S ribosomal subunits, which might become active under our chosen *in vitro* conditions. As shown in insert to Fig. 19, western blot analysis of 50S ribosomal subunits from *rrmJ* wild type strain and the *rrmJ* deletion strain expressing the D136N mutant protein showed that *E. coli* RrmJ stays associated with the 50S ribosomal subunit during their preparation under stringent, high salt conditions (1 mM $MgCl_2$, 200 mM NH_4Cl). No RrmJ was detected in 30S subunits or in the intact 70S ribosome (data not shown). The amount of bound D136N mutant protein, in combination with the observed slightly lower *in vitro* activity of purified D136N mutant (Fig. 16), explained very well the methylation activity that was observed with isolated 50S ribosomal subunits prepared from the D136N expressing *rrmJ* deletion strain. This suggested that there might be a lack of efficient substrate release of D136N from 50S subunits *in vivo*, which could cause the apparent inactivity of the D136N mutant protein *in vivo* but might be less apparent under the chosen *in vitro* conditions.

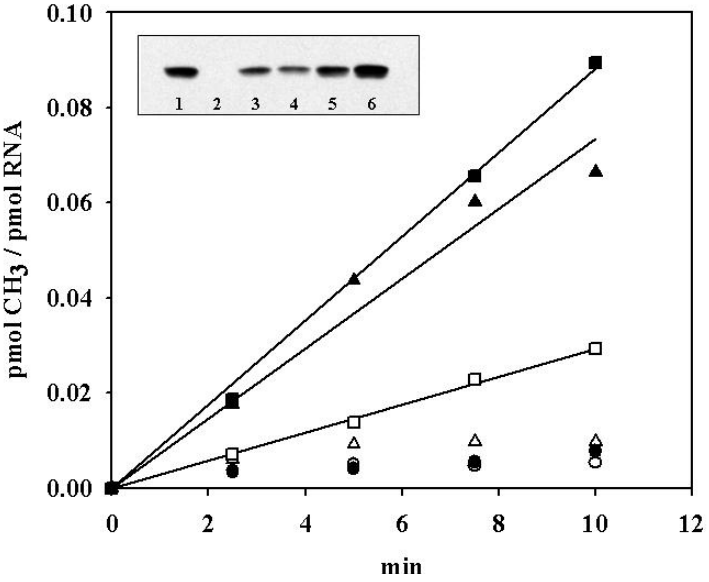

Figure 19: RrmJ is associated with 50S ribosomal subunits *in vivo* (Hager et al., 2004)
Methyl incorporation into 2 µM 50S ribosomal subunits prepared from (circles) wild type strain HB24, (triangles) *rrmJ* deletion strain HB23 or (squares) *rrmJ* deletion strain HB23 expressing the D136N mutant protein, either in the absence (open symbols) or in the presence (closed symbols) of 300 nM purified wild type RrmJ. At defined time points, aliquots were taken and the ^{3}H-methyl incorporation was determined as described.

Insert: RrmJ is bound to 50S ribosomal subunits. Analysis of the RrmJ content in 2 µM 50S ribosomal subunits prepared from (lane 1) wild type strain (HB24), (lane 2) *rrmJ* deletion strain (HB23) or (lane 3) *rrmJ* deletion strain expressing the D136N mutant from a plasmid. To evaluate how much RrmJ is bound to the ribosomal subunits, 50S ribosomal subunits prepared from the *rrmJ* deletion strain (HB23) were supplemented with (lane 4) 50 nM, (lane 5) 100 nM or (lane 6) 200 nM purified RrmJ. Aliquots of the ribosomal subunits were loaded onto a 14% SDS-PAGE and western blot analysis was performed using antibodies against RrmJ.

2.6.2 RrmJ binds specifically to free 50S ribosomal subunits in stoichiometric amounts

The methyltransferase RrmJ co-fractionated with free 50S ribosomal subunits on sucrose gradients (Hager et al., 2002). This finding was in excellent agreement with reports about the closely related mitochondrial RrmJ homologue Mrm2p, which has also been demonstrated to stay associated with the large ribosomal subunit (Pintard et al., 2002a). These were quite surprising findings, given that RrmJ functions as an enzyme and is, therefore, not expected to stay bound to its substrate. In order to test what proportion of RrmJ associates with 50S *in vivo* and to investigate the stoichiometry of the binding, co-fractionation studies in wild type *E. coli* lysate were performed. Lysates of the *rrmJ* wild type strain HB24 were prepared and analyzed on sucrose gradients. As shown in Fig. 20A, under high salt conditions (1 mM $MgCl_2$, 200 mM NH_4Cl), where 70S ribosomes dissociate into 30S and 50S subunits, all of the endogenous wild type RrmJ co-fractionated with the 50S ribosomal subunits. Not even the precipitation of the complete "top of the gradient" fraction revealed the presence of any unbound RrmJ, indicating that all of the wild type RrmJ stayed associated with the 50S ribosomal subunits under ribosome dissociating salt conditions (Fig. 20A). In lysates prepared under salt conditions that stabilize the 70S ribosome (low salt conditions), the majority of endogenous RrmJ was detected in the top of the gradient. This was apparently not due to the chosen salt conditions but based on the presence of only a small amount of 50S subunits. The few 50S ribosomal subunits that were detected under these conditions appeared to still be associated with RrmJ (Fig. 20B). These results showed that RrmJ interacts specifically with free 50S ribosomal subunits and suggested that binding of RrmJ to the 50S ribosomal subunits can occur upon dissociation of the 70S ribosomes. The fact that not even traces of RrmJ were found to be associated with the 30S subunits indicated that this is a very specific interaction between RrmJ and the 50S ribosomal subunit and is not merely due to non specific interactions of a positively charged protein and nucleic acids. The same specific association of RrmJ with 50S ribosomal subunits was observed when purified RrmJ was incubated with isolated 30S and 50S ribosomal subunits prepared from the *rrmJ* deletion strain HB23, where RrmJ also co-fractionated exclusively with the 50S ribosomal subunit (20C, data not shown). To investigate the stoichiometry of RrmJ binding, increasing amounts of purified RrmJ were titrated to 50S ribosomal subunits prepared from the *rrmJ* deletion strain. As shown in Fig. 20C, in a 0.5:1 ratio of RrmJ to 50S ribosomal subunits, all of the added RrmJ was bound to the ribosomal subunits and no free

RrmJ was detected in the top of the gradient fraction. Similar results were obtained upon incubation of RrmJ and 50S ribosomal subunits in a 1:1 ratio. In the presence of a 2:1 ratio of RrmJ to 50S ribosomal subunits, however, nearly equal amounts of RrmJ were now detected in the top of the gradient fraction. This suggested that wild type RrmJ associates with the 50S ribosomal subunit in a close to 1:1 stoichiometry.

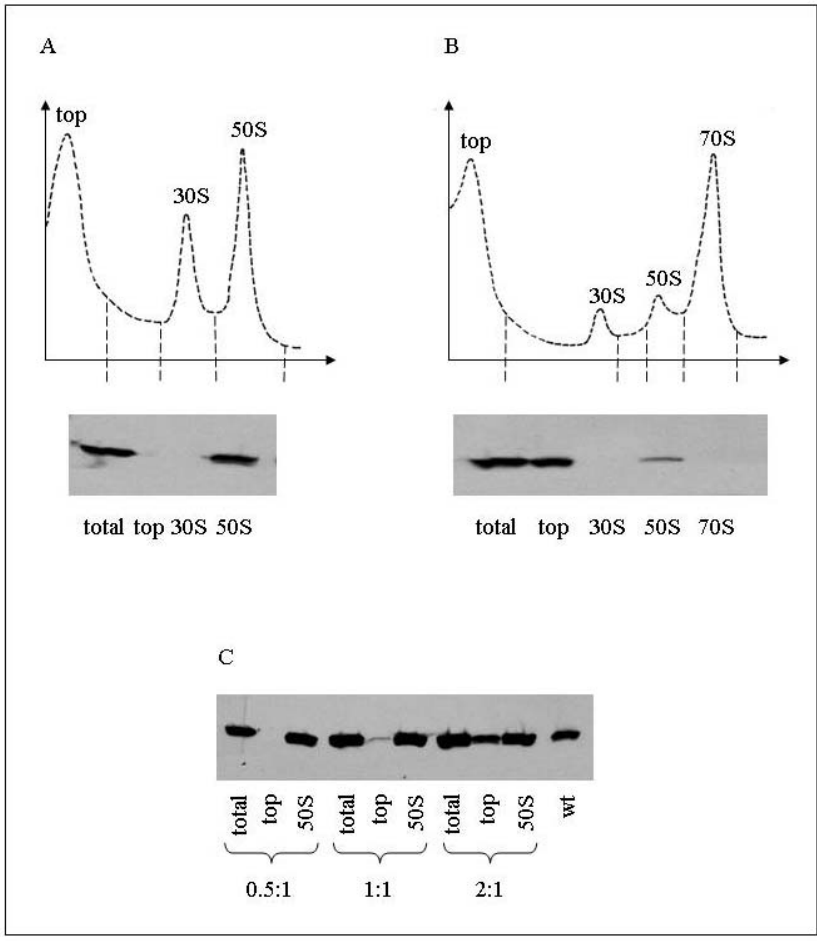

Figure 20: RrmJ co-fractionates specifically with 50S
A and B, Ribosome profile of the *rrmJ* wild type strain HB24 under stringent (A) and non stringent salt conditions (B). Marked peaks were collected and the proteins of each peak were precipitated with 5% v/v TCA. The presence of RrmJ in the respective peaks was then analyzed by western blots. C, Wild type RrmJ was titrated to 50S ribosomal subunits prepared from the *rrmJ* deletion strain HB23 in the ratios 0.5:1, 1:1 and 2:1. After 10 min incubation at 37°C, the samples were applied onto sucrose gradients under non-stringent salt conditions. Western blot analysis of the collected fractions was performed and showed that RrmJ binds to 50S ribosomal subunits in stoichiometric amounts.

2.6.3 Binding of RrmJ to 50S ribosomal subunits is methyltransferase independent

In order to investigate whether the ability of RrmJ to stay associated with the 50S ribosomal subunit depends on its methyltransferase activity and/or AdoMet binding, the binding of two methyltransferase deficient RrmJ mutants was tested (Hager et al., 2004). The RrmJ-K38A mutant protein harbors a mutation in the active site of RrmJ rendering RrmJ methyltransferase inactive, while the RrmJ-D83A mutant protein has a mutation in the AdoMet binding site, which makes the enzyme unable to bind the cofactor. The two inactive RrmJ mutant proteins were incubated with 50S ribosomal subunits prepared from the *rrmJ* deletion strain HB23 in a 2:1 ratio for 10 min at 37°C and the binding of RrmJ was analyzed on sucrose gradients. As shown in Fig. 21, both mutants were able to bind to the 50S ribosomal subunit with the same apparent affinity than wild type RrmJ. These results clearly emphasized the fact that the binding ability of RrmJ to the 50S ribosomal subunit is not dependent on its methyltransferase activity. Furthermore, since the 50S ribosomal subunits used in this experiment were prepared from the *rrmJ* deletion strain and, therefore, do not harbor the methylated U_{2552}, it also shows that RrmJ's binding does not depend on any conformational A-loop rearrangements that might be caused by the Um_{2552} modification (Blanchard and Puglisi, 2001).

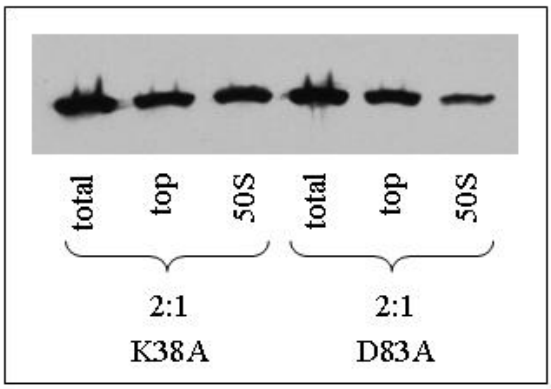

Figure 21: RrmJ's binding is methyltransferase activity independent
50S ribosomal subunits prepared from an *rrmJ* deletion strain were incubated with the inactive mutant K38A and the AdoMet binding deficient mutant D83A in a 1:2 ratio. After applying onto 10-50% sucrose gradients, fractions were collected and analyzed by western blot.

2.6.4 Determination of RrmJ's binding site

RrmJ was found to stay associated with the 50S ribosomal subunit. Therefore it was interesting to investigate where the binding site for RrmJ is located on the surface of the 50S ribosomal subunit. Due to its methylation target, the A-loop of the 23S rRNA, RrmJ presumably binds on the intersubunit face of the 50S ribosomal subunit close to the peptidyltransferase center. In order to pinpoint its exact location crosslinking studies were performed to identify interactions between RrmJ and ribosomal proteins. The attempt was to crosslink RrmJ to proteins of the 50S ribosomal subunits prepared from the *rrmJ* deletion strain using the chemical crosslinker glutaraldehyde (GA). In the presence increasing of concentrations of glutaraldehyde RrmJ was incubated with 50S ribosomal subunits at 37 ºC for 2 min. Then, SDS-PAGE and western blot analysis was used to detect RrmJ. In the crosslinking experiment two additional bands appeared that were not visible when RrmJ was incubated with GA in the absence of 50S ribosomal subunits (Fig. 22). This suggested that these two bands represent complexes between RrmJ and a ribosomal protein. Since both bands became only apparent when GA was used in a concentration of 600 µM or higher, this GA concentration was used for further optimization attempts. The same two bands became visible when 50S ribosomal subunits from the *rrmJ* wild type strain were supplemented with exogenous RrmJ and used for crosslinking studies. In order to see the crosslinked complexes on a colloidal coomassie blue stained SDS-PAGE, which would enable us to analyze the protein complexes by mass-spectrometry, various attempts were made to upscale the incubation reaction. Unfortunately, I was never able to see any cross-linked bands in quantities that were large enough to identify by mass-spectrometry.

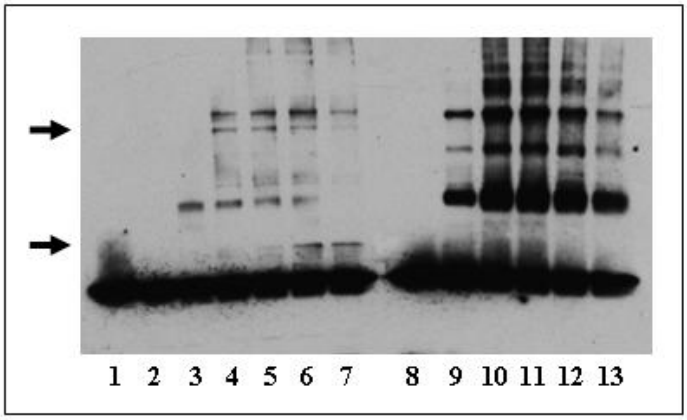

Figure 22: Crosslinking of RrmJ to the 50S ribosomal subunit
200 nM RrmJ was incubated with or without 200 nM 50S ribosomal subunits prepared from the *rrmJ* deletion strain in the presence of increasing concentrations of glutaraldehyde (GA) at 37ºC for 2 min. The reaction was stopped by adding Tris, pH 8.0, to a final concentration of 20 mM. The samples were loaded onto a 14% SDS PAGE and western blot analysis was performed with polyclonal antibodies against RrmJ.
Lane 1 shows purified wild type RrmJ as standard. Lanes 2-7 show RrmJ crosslinked to 50S ribosomal subunits using 20, 100, 250, 400, 600 and 800 µM GA, respectively. Lanes 8 – 13 show RrmJ alone crosslinked with 20, 100, 250, 400, 600 and 800 µM GA, respectively. The arrows point to the bands that appeared only when RrmJ is cross-linked to 50S ribosomal subunit reactions, but not in the crosslinking reactions with RrmJ alone, therefore showing protein complexes consisting of RrmJ and ribosomal protein. 600 µM GA appears to be the optimal concentration for obtaining both crosslinked complexes.

2.6.5 30S ribosomal subunits displace RrmJ during ribosome assembly

Under destabilizing "dissociating" salt conditions, where 70S ribosomes rapidly dissociate into their ribosomal subunits, all of the endogenous RrmJ was found to be stably associated with the 50S ribosomal subunits. In contrast, however, under associating salt conditions where the 70S ribosomes stay intact, most of RrmJ was found free in the "top of the gradient" (compare Fig. 20A and B). This suggested that assembly of the 70S ribosome might cause the displacement of RrmJ from the 50S ribosomal subunit. Considering the fact that RrmJ's methylation target is the A-loop of the 23S rRNA, which is located directly at the inter-subunit space, it appeared plausible that the displacement of RrmJ was caused by the assembly of 30S and 50S. To investigate this in more detail, *in vitro* ribosome reconstitution experiments were performed according to Nierhaus et al. (Blaha et al., 2002). 50S ribosomal subunits prepared from the *rrmJ* wild type strain were supplemented with additional purified RrmJ and the RrmJ-50S ribosomal subunit complexes were incubated with 30S ribosomal subunits in a 1:2 ratio. Then, the ribosome reconstitution was analyzed on sucrose gradients

and the localization of RrmJ was monitored. To avoid nonspecific interaction of RrmJ with the 30S subunits, salt concentrations had to be used that were slightly higher (100 mM KCl) than the reported salt conditions (30 mM KCl) that allow the reconstitution of 30S and 50S into 70S (Blaha et al., 2002). Under these chosen salt concentrations, association of 30S and 50S ribosomal subunits do not produce 70S particles but generate a ~ 55S ribosomal particle instead (Blaha et al., 2002). As shown in Fig. 23 (dashed line), incubation of isolated 30S and 50S ribosomal subunits under conditions that do not support ribosome assembly, did not cause the dissociation of 50S associated RrmJ. In contrast, however, incubation at 40°C, which triggers ribosome assembly *in vitro*, quickly led to the formation of the ~55S particle and the almost complete dissociation of RrmJ (Fig. 23, dotted line). This finding clearly indicated that RrmJ is released from the 50S ribosomal subunit in the course of ribosome assembly.

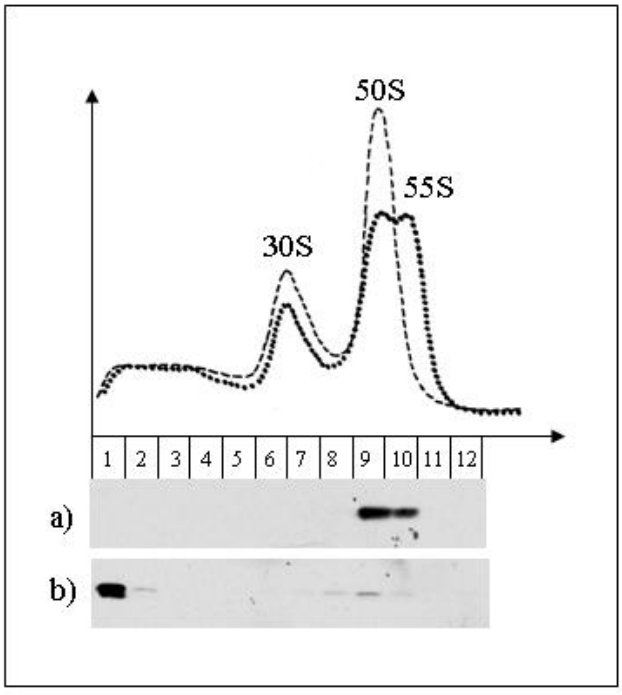

Figure 23: 30S ribosomal subunits replace RrmJ during ribosome assembly
30S and 50S prepared from the *rrmJ* wild type strain (HB24) were incubated in reconstitution buffer (20mM Hepes-KOH, pH 7.5, 20 mM $MgCl_2$, 100 mM KCl, 4 mM β-mercaptoethanol, 40 U of RNasIn) in the presence of 50µM AdoMet and exogenous wild type RrmJ in stoichiometric amounts to 50S at 40ºC for 10 min (dotted line) or left on ice (dashed line). Subsequently, the samples were analyzed on 10-50 % sucrose gradients. Continuous fractions were collected and western blot analysis was performed.

2.6.6 Addition of 30S ribosomal subunits stimulate RrmJ's turnover number

RrmJ's binding to the 50S ribosomal subunit was found to be independent of the methylation status of U_{2552} in the A-loop of the 23S rRNA suggesting that RrmJ forms a stable complex with both the modified and the unmodified A-loop. In this case, however, release of RrmJ from the 23S rRNA would become a rate-limiting step in catalysis, which could explain the fairly low turnover numbers that have been observed with RrmJ *in vitro* (K_{cat} =0.064 min^{-1}) (Hager et al., 2004). Because interaction between the 50S subunit and the 30S subunit under ribosome associating conditions causes the release of RrmJ (Fig. 23), it has been investigated to what extent addition of 30S subunits to the RrmJ catalyzed methylation reaction of 50S ribosomal subunits might increase the turnover number of this reaction. The addition of the 30S subunits was reasoned to cause the dissociation of the enzyme-substrate complex and, therefore, to make RrmJ available for another round of catalysis. As shown in Fig. 24, addition of 30S ribosomal subunits to the methylation reaction significantly increased the turnover number of RrmJ. Addition of a 2-fold excess of 30S to 50S accelerated the initial rate of methylation by more than 2.5-fold. 30S ribosomal subunits prepared from HB23 appeared not to serve as *in vitro* substrates for RrmJ, and the total methyl incorporation into 50S ribosomal subunits after 16 h of incubation was very similar, and independent of the presence of additional 30S ribosomal subunits. This clearly showed that the release of RrmJ from the 23S rRNA is a rate-limiting step in catalysis. Presence of 30S subunits under ribosome assembly conditions promotes the dissociation of RrmJ from the modified A-loop, thereby significantly accelerating the methylation reaction.

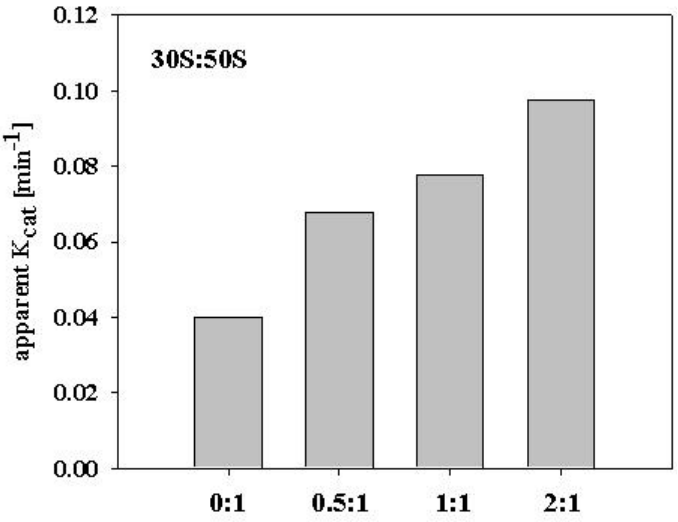

Figure 24: 30S ribosomal subunits increase RrmJ's turnover number *in vitro*
100 nM purified wild type RrmJ was incubated with various amounts of 30S ribosomal subunits prepared from the *rrmJ* deletion strain HB23 in reconstitution buffer (20 mM Hepes-KOH [pH 7.5], 100 mM KCl, 20 mM $MgCl_2$, 4 mM β-mercaptoethanol, 40 U of RNasIn) in the presence of 50 µM [^{3}H]AdoMet (200µC/ml). The methylation reaction was started by the addition of 5 µM 50S ribosomal subunits prepared from the *rrmJ* deletion strain HB23. At defined time points, aliquots were taken and the [^{3}H]methyl incorporation was determined as described.

2.6.7 RrmJ exerts a methyltransferase independent function as a ribosome assembly helper protein

Binding of RrmJ to 50S ribosomal subunits was found to be a very stable process, which was rapidly disrupted by the association of 50S ribosomal subunits with their 30S subunits to form functional 70S ribosomes. This suggested that the binding of RrmJ to 50S ribosomal subunits might affect 70S assembly. To test this idea, 55S reconstitution assays were conducted using isolated ribosomal subunits from both *rrmJ* deletion and wild type strains. Reconstitution experiments using isolated subunits from the *rrmJ* deletion strain HB23 gave ill-reproducible results and no clear indication whether RrmJ is involved in the 70S assembly process. Reconstitution experiments using wild type 50S and 30S ribosomal subunits, however, revealed that RrmJ plays indeed a role in 70S assembly. In wild type lysates, about 5% of the isolated 50S ribosomal subunits are associated with endogeneous RrmJ (Hager et al., 2004). When these 50S ribosomal subunits were incubated with 30S ribosomal subunits from wild type strains, a substantial part of the ribosomal subunits associated into the reported ~55S particles (Fig. 25, left column, II) within 5 min of incubation. This was in excellent agreement with the literature that described about 30% association within the first 5 min of incubation at 40^{o}C (Blaha et al., 2002). Significantly larger amounts of 30S and 50S associated in the ~55S particle, however, when wild type 50S ribosomal subunits were supplemented with stoichiometric amounts of purified RrmJ (Fig. 25, left column, III). This result suggested that the ribosome assembly process was indeed accelerated by the presence of RrmJ bound to the 50S subunit *in vitro* and suggested that RrmJ works as an assembly helper protein.

Irritating, however, was that phenotypical studies of the *rrmJ* deletion strain expressing the K38A mutant protein revealed the typical ribosome defect (see section 2.3.3, Hager et al., 2002), although this inactive mutant of RrmJ is still able to bind to the 50S ribosomal subunit (section 2.6.3). The ribosomal defect of this strain could, however, be explained by a non-productive interaction of the K38A mutant protein with its 23S rRNA methylation substrate and the inability of 30S ribosomal subunits to release RrmJ to form functional 70S ribosomes. This would prevent RrmJ from its productive interactions with 50S ribosomal subunits as assembly helper protein and would result in the observed ribosome defect. To test this model, reconstitution experiments were conducted using isolated 30S and 50S subunits prepared from the inactive K38A mutant strain. As shown in Fig. 25 (right

column, II) these mutant ribosomal subunits associated less efficiently than wild type subunits, suggesting that the binding of the mutant RrmJ might prevent the 70S assembly. This became even more obvious when these ribosomal subunits were supplemented with stoichiometric amounts of purified inactive K38A. This inhibited the ribosome assembly process even more and very few ribosomal subunits associated to the ~55S particle within the 5 min incubation period at 40^{o}C (Fig. 25, right column, III). These results suggested a very tight interaction of the methyltransferase inactive K38A mutant protein with the 50S ribosomal subunits, which apparently prevents these subunits from association to the 70S ribosomes. This interaction would titrate away the cellular pool of RrmJ and might explain why the methyltransferase inactive mutant of RrmJ exerts a *rrmJ* deletion like ribosomal defect in spite of its ability to bind to the 50S ribosomal subunit.

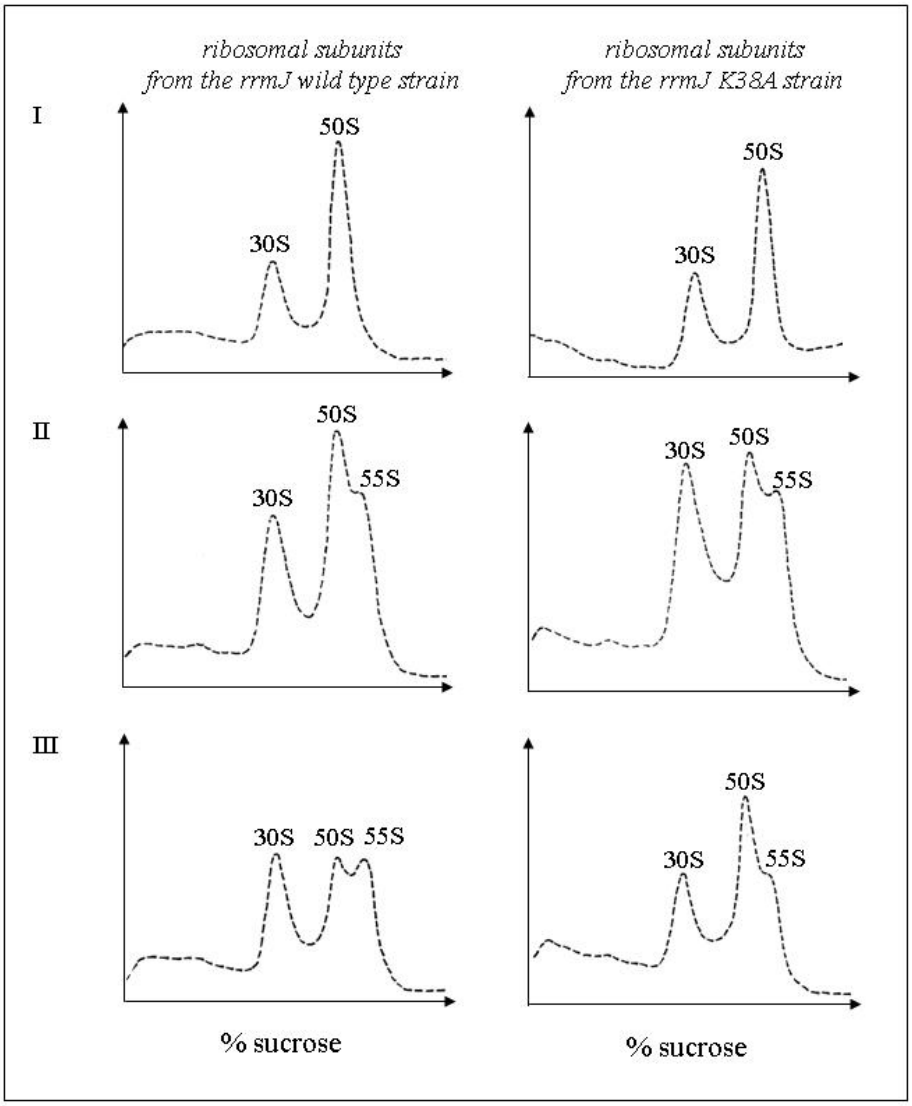

Figure 25: RrmJ acts as ribosome assembly helper protein independent from its methyltransferase activity

Comparison of ribosome assembly *in vitro* using 30S and 50S ribosomal subunits prepared from the *rrmJ* wild type strain HB24 (left column) as well as the *rrmJ* deletion strain expressing the K38A mutant (JuH25) (right column) supplemented with (III) and without (II) stoichiometric amounts of wild type RrmJ or K38A mutant, respectively. Ribosomal subunits were incubated under non-reconstitution conditions (I) or in reconstitution buffer (20mM Hepes-KOH, pH7.5, 20 mM $MgCl_2$, 100 mM KCl, 4 mM β-mercaptoethanol, 40 U of RNasIn) in the presence of 50 µM AdoMet at 40 ºC (II + III). The assembly process was stopped after 5 min by shock-freezing the samples in liquid nitrogen.

2.6.8 The inactive mutant K38A is able to compete with wild type RrmJ

To further corroborate the finding that the inactive mutant RrmJ-K38A causes the ribosome defect due to a nonproductive but tight binding to the 50S ribosomal subunit competition experiments were performed. *In vitro* methylation assays were carried out in order to investigate whether wild type RrmJ and the RrmJ-K38A mutant are able to compete for their ribosomal substrate. The concentrations of purified wild type RrmJ (100 nM) and 50S ribosomal subunits prepared from the *rrmJ* deletion strain (2 μM) were kept constant. The 50S ribosomal subunits, however, were pre-incubated with various amounts of the inactive mutant K38A. The K38A mutant protein was chosen to be used in concentrations of 1 μM, 1.5 μM, 2 μM and 4μM, which, in turn, would leave 1 μM, 0.5 μM, and no free 50S ribosomal subunits as substrate for wild type RrmJ if the binding of K38A is strong enough to compete. As shown in Fig. 26, adding the inactive mutant K38A to the methylation reaction has clearly an inhibitory defect. Already by using the RrmJ-K38A mutant in half stoichiometric amounts to 50S ribosomal subunits the methylation activity of wild type RrmJ decreases drastically and continues to decrease when using higher concentrations of K38A.

This together with the results of the previous section led us to conclude, that RrmJ has at least two functions *in vivo*; one, which is methyltransferase dependent and involves the methylation of Um_{2552} in the A-loop of the ribosome. Absence of Um_{2552} presumably causes the observed growth defect and decreased translational efficiency that is observed in *rrmJ* deletion strains. The second function of RrmJ involves the stoichiometric binding of RrmJ to 50S ribosomal subunits and appears to play a role in ribosome assembly. Lack of this second, methyltransferase independent function of RrmJ seems to be the cause for the observed ribosome defect in *rrmJ* deletion strains.

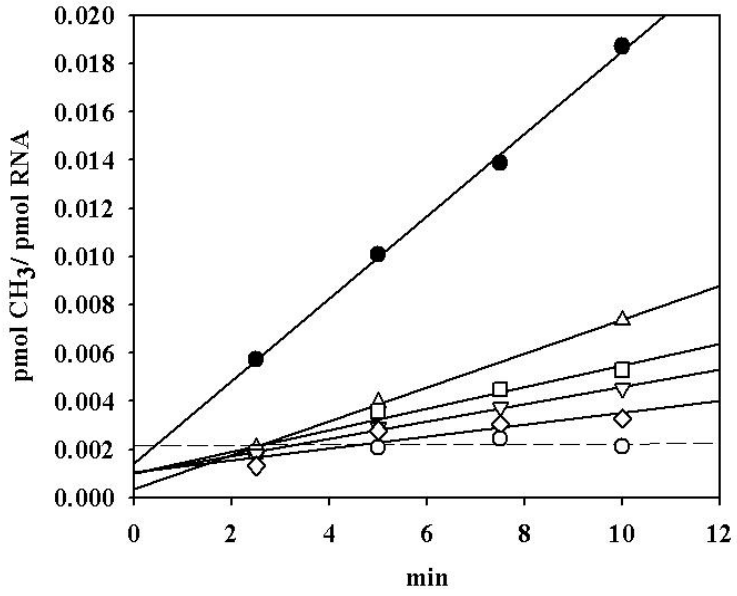

Figure 26: The inactive mutant is able to compete with wild type RrmJ for the ribosomal substrate

2 µM 50S ribosomal subunits were supplemented with 1 µM, 1.5 µM, 2 µM and 4 µM purified K38A mutant protein and incubated at 37°C for 10 min prior to starting the methylation reaction.

Then, 0.1 µM wild type RrmJ was incubated with 50 µM ^{3}H-AdoMet (200 µC/ml) in methylation buffer (50 mM HEPES•KOH, pH 7.5, 100 mM NH_4Cl, 3 mM $MgCl_2$, 2 mM β-mercaptoethanol; 40 U RNasIn) at 37^{o}C and the reaction was started by adding 50S ribosomal subunits supplemented either without (closed circles) or with (open symbols) 1 µM (triangles up), 1.5 µM (squares), 2 µM (triangles down) and 4 µM (diamonds) purified K38A mutant protein. 4 µM K38A alone does not show any methylation activity at all (open circles and dashed line). Aliquots were taken at defined time points and the ^{3}H-methyl incorporation was measured as described.

2.7 The N-terminus of RrmJ

2.7.1 The N-terminus of RrmJ contains a specificity domain for rRNA binding

In order to investigate the binding of RrmJ to the 50S ribosomal subunit in more detail, the binding affinity of several other RrmJ mutants from the mutant collection was analyzed. The one mutant protein that appeared to have completely lost its ability to interact with the 50S ribosomal subunit was a fragment of RrmJ, which lacks the first 29 aa (RrmJΔ1-29) (Fig. 27). This RrmJ variant corresponds to the RrmJ fragment, whose structure has been solved (Bügl et al., 2000). Analysis of sucrose gradients performed with lysates from the *rrmJ d*eletion strain HB23 expressing the RrmJΔ1-29 truncation mutant protein to wild type protein levels (HB43), revealed that the RrmJΔ1-29 truncation mutant does no longer co-fractionate with the 50S ribosomal subunits. This mutant protein was exclusively found at the top of the gradient (Fig. 27A). However, the observed lack of RrmJ association could not be due to the expression of a folding deficient RrmJ variant since the purified protein co-crystallized with AdoMet and folded into the previously determined core structure of RrmJ within 24 h (data not shown) (Bügl et al., 2000).

Therefore, the inability of the RrmJΔ1-29 to bind to its 50S ribosomal subunits could be either due to the fact that the N-terminus of RrmJ plays a role in 50S binding or due to differences in the composition and/or conformation of the 50S ribosomal subunits that were prepared from this mutant strain. To distinguish between these possibilities, the ability of purified wild type RrmJ to bind to 50S ribosomal subunits prepared from the *rrmJ* deletion strain expressing truncated RrmJ was analyzed. Lysates prepared from this strain were supplemented with a 0.5:1 ratio of purified wild type RrmJ to 50S ribosomal subunits. As shown in Fig. 27B, all of the wild type RrmJ co-fractionated with the 50S ribosomal subunits. This suggested that the N-terminus of RrmJ is indeed involved in the stable interaction of RrmJ with the 50S ribosomal subunit. It furthermore showed that RrmJ is not able to bind to ~40S ribosomal particles.

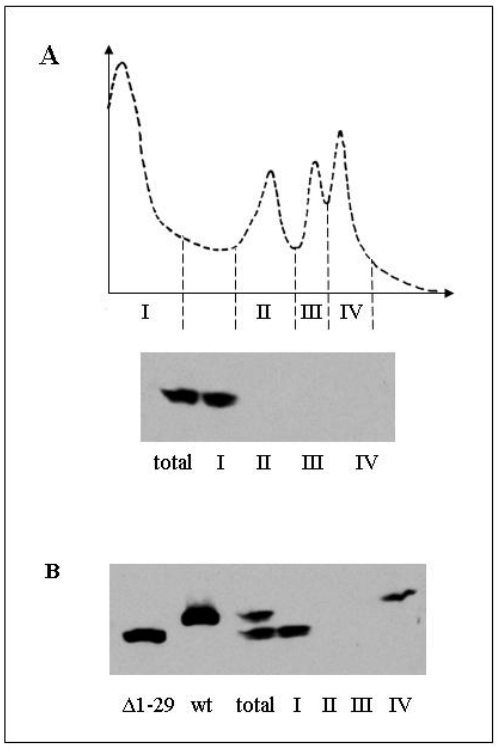

Figure 27: The N-terminal truncated RrmJ mutant is unable to bind to 50S ribosomal subunits
A, The lysate of the *rrmJ d*eletion strain HB23 expressing the RrmJΔ1-29 truncation mutant protein was applied onto a 10-50% sucrose gradient under stringent salt conditions. The marked fractions were collected and analyzed by western blot. B, The lysate of the RrmJΔ1-29 truncation strain was supplemented with 80 ng wild type RrmJ and applied onto a 10-50% sucrose gradient under stringent salt conditions. Western blots of the collected fractions were performed to detect the wild type RrmJ as well as truncated RrmJ protein.

2.7.2 N-terminal ribosome binding domain of RrmJ is required for methyltransferase activity

To analyze whether the ability of RrmJ to stably associate with the 50S ribosomal subunit is required for the successful methylation of 23S rRNA, *in vitro* methylation assays were performed. In this assay, the activity of RrmJ to methylate 23S rRNA in intact 50S ribosomes prepared from the *rrmJ* deletion strain HB23 is tested. As shown in Fig. 28, the RrmJΔ1-29 mutant protein was completely unable to methylate 23S rRNA in intact 50S ribosomal subunits. While the rate of methyl incorporation approximately doubled from 0.01 pmol/min to 0.018 pmol/min when the concentration of wild type RrmJ was raised from 100 to 200 nM, only a very low background incorporation of 0.0008 pmol/min was observed when the truncation mutant was used. This low background incorporation of methyl groups into 23S rRNA did also not increase with increasing mutant enzyme concentration. These results suggested that the deletion of the first 29 aa in RrmJ renders the enzyme unable to methylate 23S rRNA in 50S ribosomal subunits *in vitro*. This inability to methylate 23S rRNA provided additional evidence that the N-terminus of RrmJ serves as a specificity domain for the binding of RrmJ to 50S ribosomal subunits.

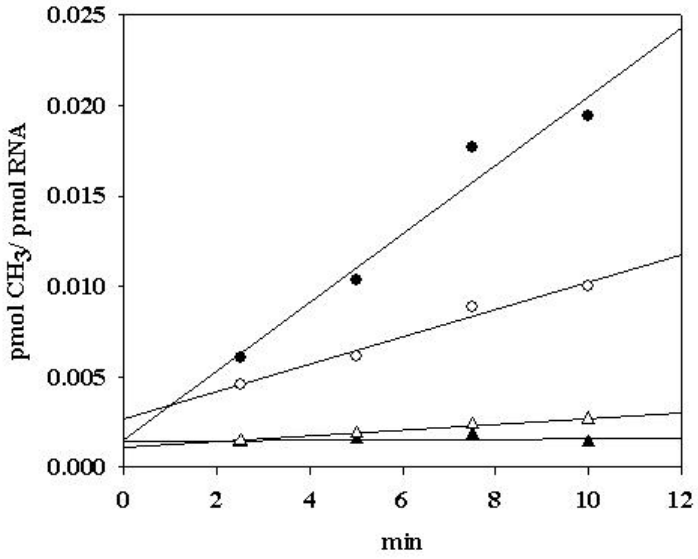

Figure 28: The RrmJΔ1-29 truncation mutant is methyltransferase inactive
100 nM (open symbols) and 200 nM (closed symbols) of wild type (circles) or mutant (triangles) was incubated with 50 µM [^{3}H]AdoMet (200µC/ml) in methylation buffer (50 mM Hepes-KOH [pH 7.5], 100 mM NH_4Cl, 3 mM $MgCl_2$, 2 mM β-mercaptoethanol, 40 U of RNasIn). The methylation reaction was started by adding 5 µM 50S ribosomal subunits prepared from the *rrmJ* deletion strain HB23. At defined time points aliquots were taken and the [^{3}H] methyl incorporation was determined as described previously.

2.7.3 The N-terminal truncation mutant points towards a possible second function of RrmJ

The N-terminal truncation mutant was found to be unable to bind and methylate 50S ribosomal subunits *in vitro*. Consistent with this finding seemed to be, that the *rrmJ* deletion strain expressing the N-terminal truncation mutant revealed a ribosomal defect comparable to the one exerted by the *rrmJ* deletion strain (Fig 29A). However, growth in liquid LB (Fig 29B) as well as on plate (data not shown) seemed to be partially restored in an *rrmJ* deletion strain expressing Δ1-29 RrmJ from a plasmid. Since the crystal structure of the N-terminal truncated RrmJ mutant showed an intact active site, this result suggested that RrmJ might have a second substrate and that the methylation status of this substrate accounts for the partially rescued growth in this strain. Because Pintard et al. showed that the yeast homologue Trm7p methylates tRNA and furthermore, Bügl et al also showed that RrmJ is indeed able to recognize tRNA as *in vitro* substrate to some extent this may reveal a possible second function for RrmJ (Bügl et al., 2000).

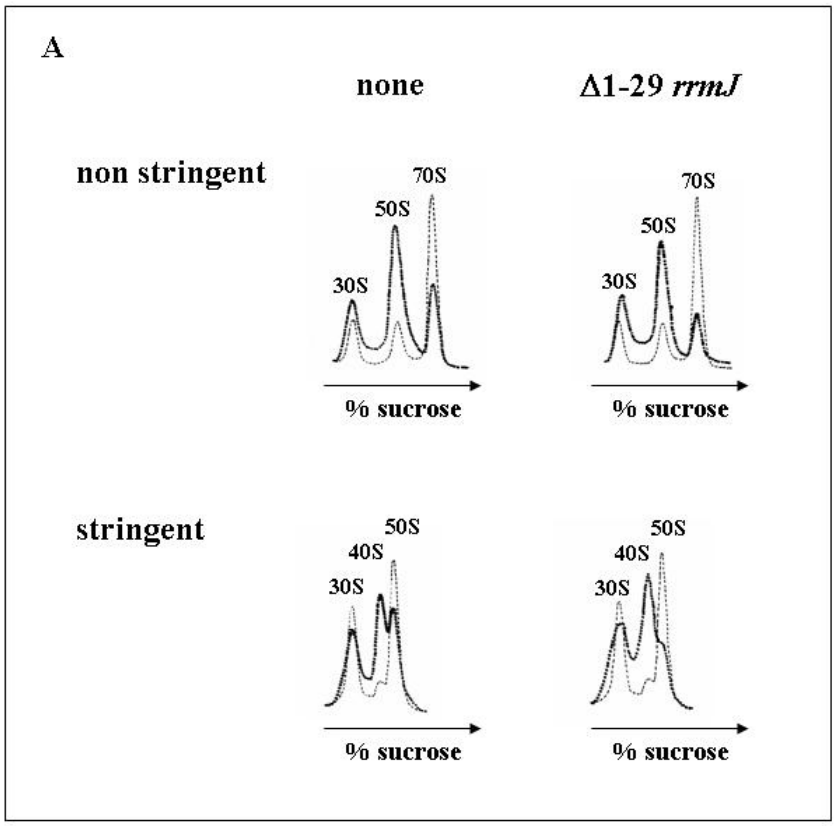

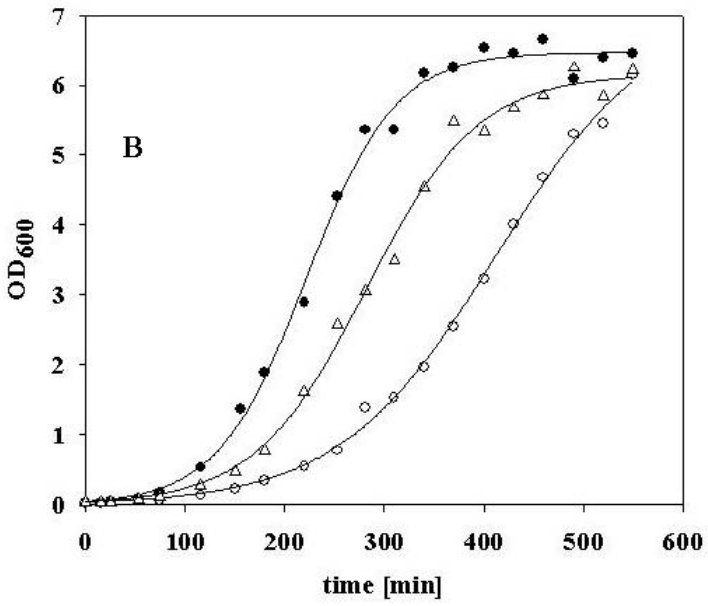

Figure 29: Phenotype of the *rrmJ* truncation mutant

A, Polysome profiles of the *rrmJ* deletion strain HB23 expressing no plasmid (left column) or pHB1 derived plasmids encoding the *rrmJ* truncation mutant (right column) under non stringent (10 mM $MgCl_2$, 100 mM NH_4Cl) and stringent salt conditions (1 mM $MgCl_2$, 200 mM NH_4Cl), as indicated, in 10% - 50% sucrose gradients. In the absence of functional RrmJ, ribosomal subunits accumulate under associating salt conditions whereas the 70S peak decreases significantly and under dissociating salt conditions ~40S ribosomal particles accumulate at the expense of intact 50S ribosomal subunits.

B, Comparison of growth in liquid LB of the *rrmJ* wild type (closed circles), *rrmJ* deletion (open circles) and *rrmJ* truncation strain (open triangles) at 37°C.

3 Discussion

3.1 The Active Site

3.1.1 Reaction mechanism of RrmJ

The investigation concerning the reaction mechanism of RrmJ has been guided by the high structural similarity of RrmJ and the two *O*-methyltransferases COMT and VP39. As described before (section 1.4), the methylation reaction of COMT has been extensively investigated and shown to follow a S_N2 reaction mechanism. The crystal structure of COMT revealed that Mg^{2+} is bound to the active site, which was proposed to play a crucial role in substrate binding and positioning the hydroxyl group close to the methyl group of AdoMet (Vidgren et al., 1994; Jeffery and Roth, 1987). The methyltransferase activity of RrmJ has also been shown to be dependent on the presence of Mg^{2+} ions (Caldas et al., 2000b). However, we found that Mg^{2+} may rather be important for stabilizing the 50S ribosomal substrate than for the catalytic mechanism of RrmJ. Because the crystal structure of RrmJ does not show any Mg^{2+} ions bound to the active site and because the active site of RrmJ superimposes very well with the active site of the Mg^{2+}-independent 2'-*O*-methyltransferase VP39 (see Fig. 3A and Bujnicki and Rychlewski, 2001), we concluded that the methyltransferase activity of RrmJ works independent of Mg^{2+}.

The crystal structure of VP39 reveals that in the active site the target 2'-*O* is hydrogen bonded to the highly conserved Lys175 and is positioned in close proximity to two additional positive charges, namely the sulfur atom of AdoHcy and the Lys41. The proximity of these positive charges carried by the two Lysines and the sulfur atom of bound AdoMet presumably lowers the pK_a of the target 2'-*O*-ribose and takes over the function that is carried out by the Mg^{2+} ion in COMT. Therefore, in analogy to COMT, Hodel et al. proposed that in VP39 a general base catalyzed deprotonation of the 2'-OH group of the ribose activates the nucleophilic oxygen, which attacks the methyl group of AdoMet in a S_N2 type reaction (Hodel et al., 1998).

Based on the geometry of the catalytic center in RrmJ and VP39, two highly conserved lysine residues Lys-38 (VP39: Lys-41*)* and Lys-164 (VP39: Lys-175*)* were identified as likely candidates to be involved in either deprotonating the hydroxyl group

directly or in lowering the p*Ka* of the hydroxyl group (Hodel et al., 1998). Superposition of RrmJ and VP39 and modeling of the ribose substrate of VP39 into the potential active site of RrmJ also revealed the presence of two highly conserved negatively charged residues, Asp-124 and Glu-199 in close proximity to the substrate (Fig. 6A and Staker, 2000). From a comparison of the methyltransferase domains of reovirus λ2 protein, VP39, and RrmJ, Bujnicki and Rychlewski have proposed that these four conserved residues form a catalytically active K-D-K-E tetrad (Bujnicki and Rychlewski, 2001). Simultaneous superposition of all three structures revealed a perfect conservation of these four residues. In addition, alanine mutagenesis scans that were performed with VP39 suggested that some of these residues are involved in AdoMet binding and methyltransferase activity (Schnierle et al., 1994). These alanine scans and additional structure and sequence comparisons also suggested a possible involvement of Tyr-201, a highly conserved residue that lies underneath the putative active site of RrmJ.

In this work these five, potentially crucial amino acids in RrmJ were individually mutated to alanine residues and the activity of the mutants was analyzed both *in vivo* and *in vitro*. The introduced mutations did not significantly decrease the expression level and solubility of the mutant proteins *in vivo* or the AdoMet binding affinity of the purified proteins *in vitro*, suggesting that no major structural rearrangements occurred in the mutant proteins. The results that were obtained in this study clearly show that lysine residues Lys-38 and Lys-164 both play critical roles in the methyltransfer reaction of RrmJ (Hager et al., 2002). RrmJ variants with alanine substitutions for either of these two lysine residues were unable to rescue the *rrmJ* deletion phenotype when expressed at wild type level and revealed a significant decrease in the methyltransfer activity *in vitro*. Substitution of residue Asp-124 also caused a severe phenotype and the accumulation of ~40S ribosomal subunits, indicating that the methyltransfer reaction is severely impaired *in vivo*. Mutations in Glu-199, however, did not reveal a *rrmJ* deletion like phenotype *in vivo*, although the mutated protein showed a reduced specific activity *in vitro*. These results suggest that Glu-199 plays a more minor role in the methyltransfer reaction than anticipated from the structural considerations. Tyr-201 also seems not to be directly involved in the catalytic reaction. The function of the Y201A variant of RrmJ was not significantly impaired *in vivo* or *in vitro*. We, therefore, concluded that RrmJ and VP39 function with the use of a catalytic K-D-K triad rather than a catalytic K-D-K-E tetrad as proposed previously (Bujnicki and Rychlewski, 2001).

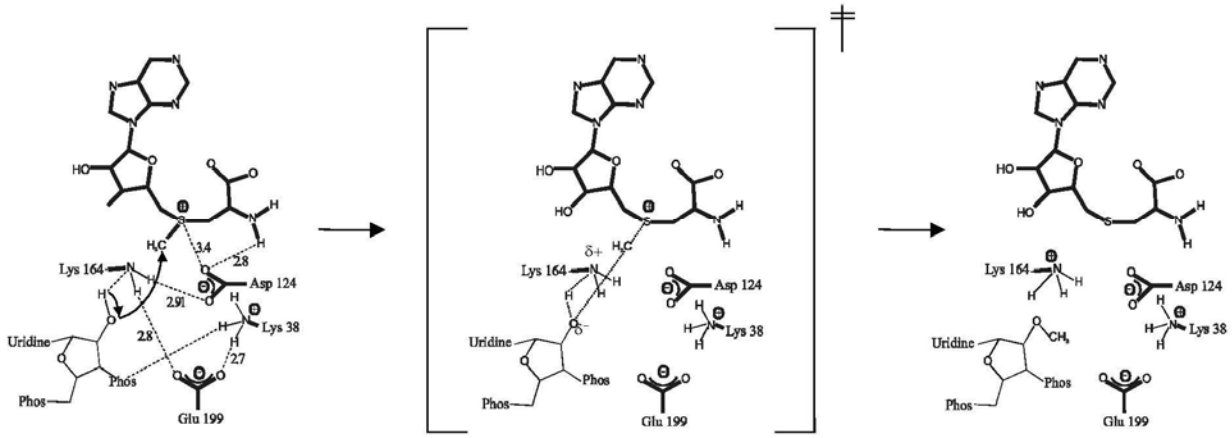

Figure 30: Proposed reaction mechanism of RrmJ (Hager et al., 2002).
After deprotonation of the target hydroxyl group, the nucleophilic attack occurs at the reactive methyl group of AdoMet in a S_N2 reaction, and the methyl group is transferred onto the 2'-OH group of the ribose.

Based on these results, structural considerations and comparisons to the proposed mechanism of the small molecule 2'-*O*-methyltransferase COMT, we suggested the model shown in Fig. 30. In analogy to COMT (Vidgren, 1999) where Lys-144 has been proposed to act as general base, Lys-164 is suggested to act as a general base in RrmJ. The ε-NH2 of Lys-164 is oriented to directly face the target hydroxyl group of the ribose molecule and is within hydrogen bonding distance of the 2'-hydroxyl group. This model requires that Lys-164 is in its deprotonated form and suggests, therefore, that the pK_a of this amino group is lowered. This decrease in pK_a has also been suggested for VP39 by Hodel *et al.* (Hodel, 1999) and has been found to be the case in aldolases (Barbas et al., 1997) and amidases (Hodel, 1999). In RrmJ, the pK_a for Lys-164 may be lowered because of the proximity of the amine to the positively charged sulfur atom of AdoMet and the amine group of Lys-38. This could also explain the important catalytic role of Lys-38, the second residue in RrmJ, whose substitution causes a substantial decrease in the methyltransferase activity. In addition, the surroundings of Lys-164 are dominated by non-polar amino acids like Met-125, Ala-126, Leu-143, Val-144, Val-163, Val-165, Phe-166, Val-200, and Tyr201 that might destabilize the protonated amine group and thereby lower the pK_a of this side chain (Fersht, 2000). The general base-activated hydroxyl group of the RNA substrate then attacks the reactive methyl group to form the S_N2-like transition state as shown in Fig. 30. Asp-124 is positioned in the crystal structure

to stabilize the positive charge on the sulfur atom of AdoMet and the amino group of Lys-164. It is conceivable that a proton from protonated Lys-164 is transferred to Asp-124 during catalysis. We found that substitution of this central residue causes the protein to aggregate upon overexpression. Glu-199, which is in hydrogen bond contact with Lys-38, might play a role by positioning the ε-NH2 group of Lys-164, thereby ensuring that the free electron pair of Lys-164 is located next to the target hydroxyl.

3.1.2 The proposed reaction mechanism of VP39 and RrmJ

Although 2'-*O*-methylations are ubiquitous, the catalytic mechanism of RNA 2'-*O*-methyltransferases has until recently not been characterized at the atomic level (Li et al., 2004). However, the most common assumption for reactions involving an oxygen methyl acceptor was that the reaction takes place as a straightforward S_N2 reaction. This means that an electron pair of the nucleophile attacks the methyl group leading to a linear arrangement of the nucleophile, the methyl carbon and the thioester leaving group as transition state. Although the crystal structure of COMT's active site underlines the idea that the attacking nucleophile is an oxyanion due to the positioning of the Mg^{2+} ion, as well as due to the very low pK_a (see section 1.4) (Hegazi et al., 1976; Vidgren et al., 1994; Vidgren, 1999), it has not been directly shown if the initial attack requires the formation of a 2'-oxyanion.

The reaction mechanism for VP39 has been proposed based on the reaction mechanism of COMT as described in section 3.1.1. However, while VP39 is functionally related to COMT as 2'-*O*-methyltransferase, VP39 is unrelated at the same time since its target hydroxyl is an aliphatic hydroxyl instead of an aromatic hydroxyl. Furthermore, VP39 does not use an Mg^{2+} ion in its active site, which would be capable of lowering the pK_a of the target hydroxyl. Therefore, in a recently published study by Li and coworkers, VP39's reaction mechanism was reconsidered and argued against a general base catalyzed reaction involving a nucleophilic oxyanion (Li et al., 2004).

This was based on two dimensional (2D) NMR studies, which probed for enzyme dependent and pH dependent changes in the ionization status of VP39's substrate in complex with the enzyme and cofactor. These studies did not show the expected deprotonation of the target hydroxyl (Li et al., 2004). Therefore, Li et al. proposed an alternative model for the enzyme-catalyzed 2'-*O*-methylation reaction, in which a non-deprotonating hydrogen bond

between VP39's K175 side chain and the 2'-OH proton catalyzes the methyl transfer by freezing the rotation of the 2'-OH proton and steering an oxygen lone pair of the 2'-OH proton directly towards the methyl center (Li et al., 2004). This orbital steering mechanism agrees with the results of the 2D NMR studies as well as with the position of the K175 side chain in the active site (Li et al., 2004).

Because of the high structurally resemblance between the active sites of VP39 and RrmJ, this newly proposed model might also apply for the methylation reaction of RrmJ. This refined model would be consistent with the results of our mutational analysis and, therefore, with the proposed function of the catalytic triad KDK.

3.2 The Substrate of RrmJ

3.2.1 Substrate binding site of RrmJ

Structure predictions, structural modeling approaches and structure based sequence alignments have been used to identify highly conserved, surface exposed residues that could be involved in the binding of the 2'-*O*-methyltransferase RrmJ to its 23S rRNA substrate. The identified residues were mutated and after careful *in vivo* and *in vitro* analysis of the respective mutants, we are proposing that a positively charged ridge built by the highly conserved arginines 32/34 and 194 plays an important role in the coordination of the rRNA sugar phosphate backbone (Fig. 31). In addition to the positively charged ridge in RrmJ, the highly conserved serine 197 appears to also contribute to the binding of the RNA substrate. Moreover, co-fractionation studies of RrmJ with the 50S ribosomal subunit on sucrose gradients revealed that the 29 N-terminal amino acids are crucial for substrate binding. However, the position of these 29 amino acids cannot be shown in the crystal structure of RrmJ, because they got cleaved off during the crystallization process.

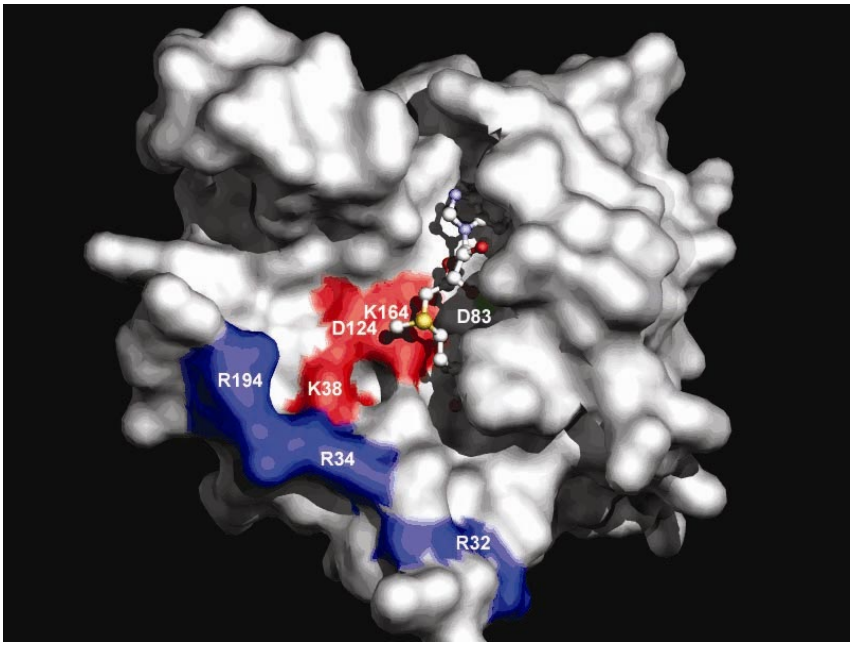

Figure 31:
Putative substrate binding site of RrmJ
Surface of RrmJ colored according to alanine mutagenesis results. Residues that when mutated to alanine result in decreased substrate binding are colored blue. Residues, that when mutated to alanine result in perturbations of the catalytic mechanism, are colored red. Figure done by Bart Staker.

Both, the crystal and solution structures of the 19 residue A-loop were modeled into RrmJ (Hager et al., 2004). In neither case was it possible to position the 2'-hydroxyl of U_{2552} into the active site of RrmJ without significant clashes with the surrounding protein. However, for both the crystal and NMR structures, which differ mainly in those parts of the RNA that do not contact the protein, it was possible to model the A-loop into RrmJ by overlaying the U_{2552} nucleotide in the active site with the 5' m^7G-capped reactive nucleotide in the VP39 structure, and then simply turning the whole A-loop into a cleft in the surface of RrmJ. This positioned the phosphodiesters into the same position as the phosphodiesters of the mRNA hexamer substrate in VP39. The residues that are in closest contact to the A-loop structure in this model were found to be the active site residues K38, and the surface residues R34, G131, F166, R194 and S197. Except for the less conserved G131, all amino acids are highly conserved and have been found to alter the catalytic activity of the enzyme (K38), the apparent AdoMet affinity (F166) or the apparent K_m for substrate binding (R34, R194, S197) when mutated. The finding that the A-loop modeling positions exactly those surface exposed amino acids closest to the A-loop that have been found to cause increased K_m values for 23S rRNA when mutated in RrmJ, was very suggestive that we have indeed identified the 23S rRNA binding site in RrmJ. This model now positions the ribose of the target U_{2552} next to

the active site Lys164 and to the reactive methyl group of AdoMet. The suggested substrate binding site in RrmJ, which is very similar to the known substrate binding site of VP39, also resembles other predicted RNA binding sites in methyltransferases. Although lacking co-crystallization studies with its substrate, the substrate binding site of the 23S rRNA methyltransferase ErmC' in *B. subtilis* has been extensively investigated by alanine-scanning mutagenesis and a model for protein-RNA interaction has been proposed (Maravic et al., 2003). Since RrmJ's K_m for its rRNA substrate is very similar to the K_m that has been published for ErmC', this model might be important for elucidating the substrate binding site of RrmJ (Denoya and Dubnau, 1987). The crystal structure of ErmC' has been solved in the complex of AdoMet (Bussiere et al., 1998; Schluckebier et al., 1999). Due to analysis of the distribution of electrostatic potential on the protein surface it was previously proposed that the small C-terminal domain was responsible for substrate binding (Yu et al., 1997). The alanine-scanning mutagenesis however, redefined this prediction by localizing the important RNA binding residues in the large catalytic domain instead. Kinetic analysis of the mutants showed that residues building a positively charged ridge are crucial for substrate binding (Maravic et al., 2003). Moreover, the crystal structure of a putative RNA methyltransferase from *Mycobacterium tuberculosis*, Rv2118c, also displays a groove lined with positively charged residues, which is wide enough to fit the RNA (Gupta et al., 2001).

3.2.2 The A-loop has to loop out of the tightly packed 50S structure

The methylation target of RrmJ is U_{2552}, one of the five highly conserved A-loop residues that form part of the peptidyltransferase center in the ribosome. The residues of the A-loop are thought to play a role in tRNA selection and accommodation. In the context of the ribosome, U_{2552} is positioned on the bottom of a deep cleft and, although solvent accessible, appears not to be accessible to the 23 kDa protein RrmJ. This raised the intriguing question about the mechanism of substrate recognition and binding by RrmJ. It was suggested that docking of the A-loop might be a reversible process and that undocking is required for tRNA binding (Blanchard and Puglisi, 2001). Our findings that the A-loop, when it adopts its solution structure, can be modeled into the substrate binding site of RrmJ, and, even more importantly, can be recognized by RrmJ as a substrate *in vitro*, supports this hypothesis. This reversible undocking of the A-loop out of the 50S ribosome could explain

how RrmJ can gain access to the A-loop structure and can methylate U_{2552} so late in the maturation process of the ribosome assembly.

3.2.3 A base flipping event may be involved in the RrmJ mediated reaction

Modeling studies of the A-loop into the putative substrate binding site of RrmJ revealed that a base flipping of U_{2552} is likely to be required for the methylation reaction (see Fig. 17B). A base flip would conserve both the active site orientation of the methylated U_{2552} and the phosphodiester contacts, as well as prevent a clash with the extended α_4-helix, which is uniquely longer in RrmJ and VP39 as compared to structurally related catechol *O*-methyltransferases (Bügl et al., 2000). Base flipping was first discovered when a DNA cytosine 5-methyltransferase was co-crystallized with its DNA-substrate (Klimasauskas et al., 1994). Since then, base flipping has been shown or suggested for many other DNA modifying enzymes. Now, there are several indications that base flipping is a mechanism that can occur in RNA as well (Cheng and Blumenthal, 2002). Base flipping of RNA has recently been shown to be induced by the binding of initiation factor IF1 to the 30S ribosomal subunit. Here, binding of IF1 causes the bases A1492 and A1493 of the 16S rRNA to flip out of helix 44. This buries the bases in specific pockets of the initiation factor 1 (Carter et al., 2001). Furthermore, tRNA and rRNA modifying enzymes, which modify within base-paired regions, have been suggested to induce base flipping as well. The recently solved structure of the tRNA pseudouridine synthase TruB, in complex with its tRNA substrate revealed that the target base U55 flips out completely, thereby disrupting the U55-G18 base pair and with that the tertiary structure of the tRNA (Hoang and Ferre-D'Amare, 2001). This could give misfolded tRNAs the chance to correct their tertiary structure. RrmJ's target nucleotide U_{2552} forms an unusual pyrimidine-pyrimidine base pair with C_{2556}, which gives the A-loop its compact loop structure (Blanchard and Puglisi, 2001). A base flip would also disrupt this base pair and possibly the A-loop structure. Most importantly also for ErmC' it has been reported that the binding of the target alanine to the catalytic center presumably involves a base flipping mechanism (Maravic et al., 2003). This underlines the resemblance in terms of substrate binding features between RrmJ and ErmC'. Furthermore, also for Trm7p, the yeast cytosolic homologue of RrmJ, a nucleotide flipping mechanism has been proposed in order to present the target C32 of the tRNA anticodon loop to the active site

of Trm7p (Pintard et al., 2002b).

3.2.4 Recognition of the methylation target

RrmJ recognizes its target nucleotide only in fully assembled 50S ribosomal subunits (Bügl et al., 2000). Naked 23S rRNA does not serve as a substrate for RrmJ. The fact that the RrmJ mediated methylation occurs at a late stage of ribosome maturation may be either due to the requirement of additional protein-protein interactions or due to the specific loop structure of the region harboring the target nucleotide. Because RrmJ is able to recognize its methylation target in the isolated A-loop *in vitro* as shown in section 2.5.2, the latter consideration appears more likely. Comparison of RrmJ to other related 2'-*O*-methyltransferases that have been investigated in regard to substrate recognition revealed the necessity for a specific RNA fold and showed similarities in terms of substrate requirements.

Trm7p, the cytosolic homologue of RrmJ in yeast, has been shown to methylate the anticodon loop of tRNA (Pintard et al., 2002b). The structure of the anticodon loop has been found to be very similar to the structure of the A-loop of the 23S rRNA (see section 1.2.4). Furthermore, NMR studies of the 23S rRNA substrate of the bacterial rRNA methyltransferase $RlmA^{II}$ revealed that the region of the target nucleotide folds spontaneously into a hairpin loop as a compact and stable structure (Lebars et al., 2003). This specific loop structure folds independently of the rest of the 23S rRNA and resembles strongly the anticodon loop of tRNA. This loop structure seems only to be required for the methylation process, because it later undergoes major conformational changes during the maturation process of the 50S ribosomal subunit. Similar to the A-loop structure that is recognized by RrmJ, this loop structure also involves a non-canonical base pair. While in the A-loop of the 23S rRNA a uridine base pairs with a cytosine, it has been shown that in case of Rlm^{II} a purine-purine G-A base pair stabilizes the loop structure (Blanchard and Puglisi, 2001; Lebars et al., 2003).

3.3 RrmJ – a protein with more than one function

Over the course of this study, it became evident that RrmJ has a quite complex spectrum of phenotypes that could no longer be explained with RrmJ exerting a single function as a methyltransferase, modifying U_{2552} in the A-loop of the 23S rRNA. Because RNA modifying enzymes have been shown to be able to exert both dual substrate specificity as well as methyltransferase independent functions, it was conceivable that RrmJ also performs more than one function in the cell. Based on the results obtained with wild type RrmJ as well as with the numerous RrmJ mutants, we were able to suggest the following model of RrmJ's various functions in the cell.

3.3.1 RrmJ does not only act as a methyltransferase but also as a ribosome assembly helper protein

It has been shown that RrmJ is able to specifically bind to free 50S ribosomal subunit (Hager et al., 2004; Pintard et al., 2002a). This binding appears to be independent of RrmJ's methyltransferase activity as well as of the methylation status of the A-loop. 30S ribosomal subunits were found to replace RrmJ during the course of ribosome assembly explaining why RrmJ is not found in 70S ribosomal fractions. Importantly, *in vitro* reconstitution of 70S ribosomes was enhanced when additional wild type RrmJ was added to 30S and 50S ribosomal subunits prepared from the *rrmJ* wild type strain. This result suggested that RrmJ is involved in the ribosome assembly process. Because the methylation of U_{2552} goes to completion *in vivo* (Bügl et al., 2000), this result could not be due to an increase in methyl incorporation and enabled us to separate the putative assembly helper function of RrmJ from its enzymatic activity. Therefore, RrmJ's influence on ribosome assembly appears to be methyltransferase activity independent.

This result allowed us to explain a number of observations (see below), but was contradicted by results with methyltransferase inactive mutants of RrmJ. Methyltransferase inactive mutants such as K38A bound to 50S ribosomal subunits, yet still revealed a ribosome defect *in vivo*. Further investigation of the inactive mutant K38A showed, however, that this mutant is no longer able to enhance the ribosome assembly process *in vitro* and even exerted an inhibitory effect. This could be due to a tight binding of the K38A mutant to the

23S rRNA. As discussed in section 3.2.2, methylation of U_{2552} presumably requires the A-loop to loop out of the tightly packed structure of the 50S ribosomal subunit in order for RrmJ to access its methylation target (Hager et al., 2004). Based on our modeling studies, U_{2552} has been furthermore proposed to undergo base flipping to fit into the active site of RrmJ (section 3.2.3) (Hager et al., 2004). The inactive mutant K38A might, therefore, interact with the 23S rRNA but because the methylation reaction cannot further proceed, the K38A remains bound to the 50S ribosomal subunit. Locking K38A to the ribosomal subunit might prevent association of the 50S with the 30S ribosomal subunit and, therefore, might block the ribosome assembly process. This presumably tight interaction between K38A and 50S ribosomal subunit would titrate away the cellular pool of RrmJ and would explain why the inactive mutants of RrmJ exert a ribosomal defect despite their ability to bind to the 50S ribosomal subunit. This explanation is supported by competition studies, in which *in vitro* methylation assays were performed with pre-incubated K38A-50S complexes and purified wild type RrmJ. Wild type RrmJ was not able to replace the bound K38A mutant on the 50S ribosomal subunit and the measured methyl incorporation decreased with increasing K38A concentrations.

Mutagenesis studies performed by Caroline Kumsta in our lab finally confirmed very nicely the conclusion that the ribosomal defect observed in an *rrmJ* deletion strain is methyltransferase activity independent. She constructed mutant strains that lack all 7 endogenous rRNA operons and express either wild type rRNA or rRNA mutated at position U_{2552} from a single operon encoded on a plasmid. Strains expressing a single copy of 23S rRNA from a plasmid harboring either U_{2552}A or U_{2552}C substitution did not exert any defect in ribosome assembly. This clearly showed that the methylation of the highly conserved U_{2552} is dispensable for ribosome assembly.

3.3.1.1 Further support that RrmJ function as ribosome assembly helper

As described before, the *rrmJ* deletion strain reveals a severe growth disadvantage, a substantial decrease in protein synthesis as well as a significant ribosomal defect. Latter is exerted by the accumulation of 30S and 50S ribosomal subunits under associating, non stringent salt conditions and an additional ~40S peak at the expense of the 50S peak under dissociating, stringent salt conditions (Bügl et al., 2000). This ribosomal defect is usually

very characteristic for strains lacking a ribosomal assembly helper protein and only one other 23S rRNA methyltransferase mutant in *E. coli* was found to have a similar phenotype (Gustafsson and Persson, 1998).

Although fully active 70S ribosomes can be reconstituted *in vitro* using isolated 30S and 50S ribosomal subunits (Nierhaus, 1991), non-physiological conditions like heat activation steps and high Mg^{2+} concentrations are required (Blaha et al., 2002). *In vivo*, the ribosomal assembly process has been shown to be dependent on several auxiliary proteins (Williamson, 2003). These ribosome assembly helper proteins are mostly associated with ribosomal subunits and are usually not found in complete 70S ribosomes (Bylund et al., 1998). This is very similar to our observations with RrmJ. Even more so, like deletion of RrmJ, deletion of assembly proteins leads to a defect in ribosome maturation as well as to a decrease in growth rate and translational efficiency (Bylund et al., 1997; Charollais et al., 2004; Charollais et al., 2003; Dammel and Noller, 1995; Lovgren et al., 2004; Wower et al., 1998). Known ribosome assembly helper proteins include the cold shock proteins CsdA and SrmB, which are both involved in the biogenesis of the large ribosomal subunit (Charollais et al., 2004; Charollais et al., 2003). They associate with different precursor intermediates of the 50S ribosomal subunit at low temperatures. Deletion mutants, like the *rrmJ* deletion strain, show a slow growth phenotype and accumulate free ribosomal subunits. In addition, ~40S ribosomal particles accumulate that consist of pure 23S rRNA precursor and a decreased amount of distinct ribosomal proteins. A similar defect in assembly and activity of the 50S ribosomal subunit can be observed in strains that lack the 50S ribosomal protein L27 (Wower et al., 1998). Although functional 50S ribosomal subunits are being formed in this mutant strain, an accumulation of ~40S precursor particles has been reported and the peptidyl transferase activity of 70S ribosomes was found to be decreased. In addition, deletion of L27 led to a severe growth defect and a cold- and heat-sensitive phenotype (Wower et al., 1998). Caroline Kumsta, a diploma student in our lab, has demonstrated a similar cold sensitive growth phenotype on LB plates for the *rrmJ* deletion strain. This cold sensitive phenotype was nicely reflected by the ribosomal defect of the *rrmJ* deletion strain, which was also significantly more severe at lower temperatures. Furthermore, the cold sensitive phenotype was independent of the U_{2552} methylation.

Although some other rRNA modifying enzymes have been reported to be important for ribosome assembly as well, it is still unclear whether this is due to their enzymatic

activity. It has been suggested that the proteins might have a second function, which can be separated from their enzymatic activity and which influences the assembly process. For instance, deletion of Pet56p, a yeast 2'-*O*-methyltransferase specific for G_{2251} (*E. coli* numbering) in mitochondria, leads to a ribosomal defect, which can be rescued by expressing a methyltransferase inactive mutant of Pet56p (Sirum-Connolly and Mason, 1993; Lovgren and Wikstrom, 2001). Similarly, the 23S rRNA methyltransferase $RlmA^I$ has been shown to cause a slow growth phenotype when deleted, which is methyltransferase activity independent. This led to the conclusion that $RlmA^I$ has another primary function, supposedly a chaperone like role helping ribosomes to assemble (Liu et al., 2004). Also Dim1, which methylates 18S rRNA in yeast (Lafontaine et al., 1998), is essential for cell viability although its methyltransferase activity is dispensable. Furthermore, it has been demonstrated for the 23S rRNA pseudouridine synthetase RluD that the enzymatic activity is not the main but a secondary function of the protein (Gutgsell et al., 2001).

Thus, it is conceivable that RrmJ's enzymatic activity is actually only a secondary function while the primary function of RrmJ is to support ribosome assembly. This would also be in agreement with the work by Lapeyre et al. who have already suggested that the late time point at which RrmJ and its nucleolar yeast homologue Spb1p act on the 50S ribosomal subunit might be an indication that not the methyl incorporation but the recruitment of modifying proteins are important for ribosome assembly (Lapeyre and Purushothaman, 2004).

That RrmJ functions as ribosome assembly protein would also explain the somewhat surprising result that the ribosomal defect exerted by the *rrmJ* deletion strain can be rescued by the overexpression of the small GTPase Obg or Eng (Tan et al., 2002). Recent studies showed that Obg binds to the 50S ribosomal subunit and interacts with the SpoT protein (Wout et al., 2004). Similarly, the ribosomal assembly defect caused by the deletion of the 30S ribosomal binding protein RbfA can be restored by overexpression of the essential GTPase Era, which has been shown to bind to the 30S ribosomal subunit (Inoue et al., 2003; Sayed et al., 1999). Furthermore, ribosomal defects caused by deletion of various other assembly helper proteins have also been found to be restored by overexpression of other ribosomal subunit binding proteins (Bylund et al., 1998; Lovgren et al., 2004). Overexpression of the 50S ribosomal subunit binding protein CsdA, for example, has been shown to correct the ribosome defect in a *srmB* deletion strain (Charollais et al., 2004).

Therefore, it is conceivable that the binding of the small GTPase Obg is sufficient to take over RrmJ's role in ribosome assembly. This would explain why the overexpression of Obg rescued the ribosomal assembly defect in the *rrmJ* deletion strain although the Um_{2552} modification was still lacking.

On a similar note, we found that the ribosome defect of an *rrmJ* deletion strain is partially restored when cells are grown at high temperatures (data not shown). It is possible, that under these conditions, heat shock proteins such as DnaK and GroEL, that are known to bind to the ribosomal subunits and are involved in ribosome biogenesis, can take over RrmJ's assembly helper function. This would then be similar to the effects of overexpressing the small GTPase Obg in an *rrmJ* deletion strain at non-stress temperatures. DnaK has been shown to bind to 5S rRNA in 50S and 70S ribosomes (Ghosh et al., 2003). A DnaK temperature sensitive (ts) mutant strain is defective in the late stages of ribosome biogenesis at high temperatures, thereby accumulating 21S, 32S and 45S ribosomal particles. These ribosomal particles have been confirmed to be true precursors instead of dead end particles (Hage and Alix, 2004). While the 21S and 32S ribosomal particles harbor precursor types of 16S and 23S rRNA, the 23S rRNA in 45S ribosomal particles has undergone further maturation (Hage and Alix, 2004). This is comparable to the ~40S ribosomal particles of RrmJ that also do not seem to contain any precursor type of 23S rRNA (data not shown). Moreover, because 50S ribosomal subunits prepared from a *rrmJ* deletion strain under dissociating salt conditions do not further dissociate into ~40S when subjected to stringent salt conditions, ~40S ribosomal particles that accumulate in lysates of the *rrmJ* deletion strain, appear also to be precursors rather than dissociating products of 50S ribosomal subunits. Interestingly, five of the seven late assembly proteins that have been shown to be present in significant diminished amounts in ~40S ribosomal particles of an *rrmJ* deletion strain, are also absent from the 45S ribosomal particles of a DnaK-ts mutant strain (Hage and Alix, 2004). With this resemblance in phenotype, it is conceivable that DnaK, when overexpressed at high temperatures, may be able to take over RrmJs function in ribosome maturation. In addition, GroEL has also been shown to be involved in ribosome biogenesis at high temperatures. GroEL seems to be necessary for the 45S → 50S step in the maturation of the large subunit at high temperatures. Overexpression of the GroES/GroEL system has been found to partially compensate for the lack of DnaK/DnaJ at 44ºC (El Hage et al., 2001).

RrmJ's function under heat shock conditions is still unknown but does not seem to require that RrmJ is bound to the 50S ribosomal subunit. We could, furthermore, exclude that RrmJ's increased expression under heat shock is due to the thermal instability of the protein. Moreover, it has been reported that the number of free ribosomal subunits does not change between 37°C and 43°C. This excludes the possibility that the concentration of RrmJ in the cell needs to be adjusted to an increased pool of ribosomes at elevated temperatures. Therefore, the reason for RrmJ's heat shock induction is still very speculative, but might be linked to a putative second methylation target of RrmJ as it is discussed in the next section.

3.3.2 RrmJ may have an additional methylation target

As described before, the *rrmJ* deletion strain exerts a ribosome assembly defect, which is independent of the methylation status of U_{2552} but depends on the presence of the first 29 amino acids of RrmJ that function as a specific domain for ribosome binding. Co-fractionation studies revealed that the 29 N-terminal amino acids seem to be crucial for 50S ribosomal subunit binding and expression of this mutant protein in the *rrmJ* deletion strain caused a severe ribosome assembly defect. The inability of the N-terminal truncated RrmJ mutant to bind to 50S ribosomal subunits also prevented this mutant protein from methylating 50S ribosomal subunits *in vitro* although its active site was intact as confirmed by the crystal structure. Despite these defects both in U_{2552} methylation and ribosome assembly, the *rrmJ* deletion strain expressing the Δ1-29 RrmJ mutant protein revealed a significantly healthier growth than the *rrmJ* deletion strain at all temperatures tested. This was especially apparent at 43°C, where the *rrmJ* deletion strain is unable to grow while the *rrmJ* deletion strain expressing the Δ1-29 RrmJ mutant protein formed single colonies. Because strains that lack the RrmJ methylation target U_{2552} do not show a temperature sensitive phenotype either, we must assume that RrmJ might exert a third function that becomes particular evident at heat shock temperatures. This function appears, however, to depend on the methyltransferase activity of RrmJ, because the methyltransferase inactive mutant shows a growth defect similar to the *rrmJ* deletion strain. The methylation of the putative second substrate does not seem to require the binding to the 50S ribosomal subunit. This leads to the assumption that the severe growth phenotype of the *rrmJ* deletion strain or the *rrmJ* deletion strain expressing an inactive mutant of RrmJ appears to be the combination of two minor slow growth

phenotypes, one, which is caused by the ribosome assembly defect and one, which might be due to the missing methylation of the putative second substrate.

A dual substrate specificity for RrmJ in *E. coli* is certainly conceivable given the recent studies that showed that the eukaryotic homologues of RrmJ differ significantly in their substrate specificity, both in terms of target nucleotides and target RNAs. The main methylation target for Spb1p, the nucleolar homologue of RrmJ in yeast, has been shown to be G_{2553} (*E. coli* numbering) in 23S rRNA, while the mitochondrial homologue, Mrm2p, methylates the U_{2552} equivalent nucleotide in mitochondrial 21S rRNA. In contrast Trm7p, the cytosolic homologue of RrmJ in yeast, Trm7p, has been shown to methylate certain tRNAs instead of rRNAs. Because earlier studies have shown that RrmJ is also able to methylate tRNA *in vitro* it is conceivable that certain *E. coli* tRNAs are possible candidates for a second substrate (Bügl et al., 2000). Methylation of tRNAs does not require RrmJ's binding to the ribosome. This would suggest that while yeast harbors three different RrmJ homologues that methylate different RNA targets *in vivo*, *E. coli* might have combined this dual substrate specificity within one protein. Dual substrate specificity for RNA modifying enzymes has been reported before. The first enzyme that has been shown to be specific for a single site in two different classes of RNA (16S rRNA and four tRNAs) is the pseudouridine synthase RluA in *E. coli* (Wrzesinski et al., 1995). Furthermore, dual substrate specificity has also been shown for the pseudouridine synthase Pus1p in yeast, which is specific for acting on both tRNAs and U2 snRNA (Massenet et al., 1999). Analysis of TrmA revealed that during normal cell growth about half of this tRNA methyltransferase is covalently bound to both tRNA and rRNA (Gustafsson and Bjork, 1993). In addition, TrmA has been shown to be able to also methylate 16S rRNA *in vitro*, although the physiological relevance of this methylation remains to be elucidated (Gu et al., 1994). According to Massenet and coworkers, cells might have developed a strategy to minimize the number of enzymes that are required to account for the numerous Ψ and 2'-*O*-methylated nucleotides. In prokaryotes, this strategy appears to involve the use of multisite-specific enzymes while in eukaryotic cells, the involvement of guide RNAs confers different specificities to a single enzymatic machinery (Massenet et al., 1999).

3.3.3 The final conclusion: the heat shock protein RrmJ might have three distinct functions *in vivo*

According to the results and considerations presented here, we conclude that the highly conserved protein RrmJ in *E. coli* most likely exerts at least three different functions *in vivo*. RrmJ functions as 23S rRNA methyltransferase, which methylates the highly conserved U_{2552} in the A-loop of the 23S rRNA. This methylation appears to decrease the translational accuracy and, therefore, allows frame shifts and read-through. This observation supports the idea that translational accuracy is rather optimal than maximal (Widerak et al., 2005), and would also serve as the first explanation why U_{2552} and its ribose modification are so highly conserved in pro- and eukaryotes. Absence of U_{2552} or its methylated ribose, however, seems not to be the cause for the ribosome defect or growth defect on McConkey plates observed with the *rrmJ* deletion strain. Strains that express a homogenous population of 23S rRNA with mutations at position U_{2552} do not exert a ribosome assembly defect and grow indistinguishable from cells expressing wild type 23S rRNA.

Responsible for the observed ribosomal defect of the *rrmJ* deletion strain appears to be the methyltransferase independent function of RrmJ as ribosome assembly protein. This function of RrmJ is conferred by its N-terminal 29 amino acids, which allow RrmJ to bind tightly to free 50S ribosomal subunits. Upon 70S ribosome assembly, the 30S ribosomal subunit causes the release of RrmJ. This enables RrmJ to bind and methylate the next free 50S ribosomal subunit. This reveals a mechanism, by which all 50S ribosomal subunits that are being assembled into 70S ribosomes carry the Um_{2552} methylation, which allows optimal translation accuracy under normal growth conditions.

Absence of the N-terminal ribosome-binding region of RrmJ prevents RrmJ from acting as a ribosome assembly helper protein as well as a 23S rRNA methyltransferase. Nevertheless, *rrmJ* deletion strains expressing this truncated RrmJ mutant protein grow significantly better than the *rrmJ* deletion strain, indicating that RrmJ harbors a third ribosome independent function. This function of RrmJ seems to involve another methylation target and might be the function that RrmJ carries out upon heat shock. Under heat shock conditions, we found that the binding of RrmJ to the 50S ribosomal subunit, like other ribosomal helper proteins (Charollais et al., 2004; Charollais et al., 2003) is no longer required. RrmJ would be free in the cytosol and able to methylate its second ribosome independent target.

3.3.4 A model of RrmJ's functions in the cell

In *E. coli*, RrmJ is responsible for the methylation of the highly conserved nucleotide U_{2552} in the A-loop of the 23S rRNA. RrmJ recognizes 50S ribosomal subunits independent of the methylation status of U_{2552}. Upon binding to the 50S ribosomal subunit, RrmJ methylates U_{2552}. This methylation does not cause the release of RrmJ. Bound to the 50S ribosomal subunit, RrmJ carries out its methyltransferase independent function as ribosome assembly helper protein. Like other assembly helper proteins, RrmJ is being replaced by the 30S ribosomal subunit during the assembly process and is, therefore, not found in complete 70S ribosomes. Due to the replacement by the 30S ribosomal subunit, RrmJ is able to bind and methylate the next free 50S ribosomal subunit and to support their assembly. Under stress conditions and similar to other ribosomal assembly helper proteins, RrmJ binding appears to no longer be required for ribosome assembly and RrmJ might dissociate from the 50S ribosomal subunit after the methylation process. Now, RrmJ is free in the cytosol where it can methylate a second not yet identified substrate.

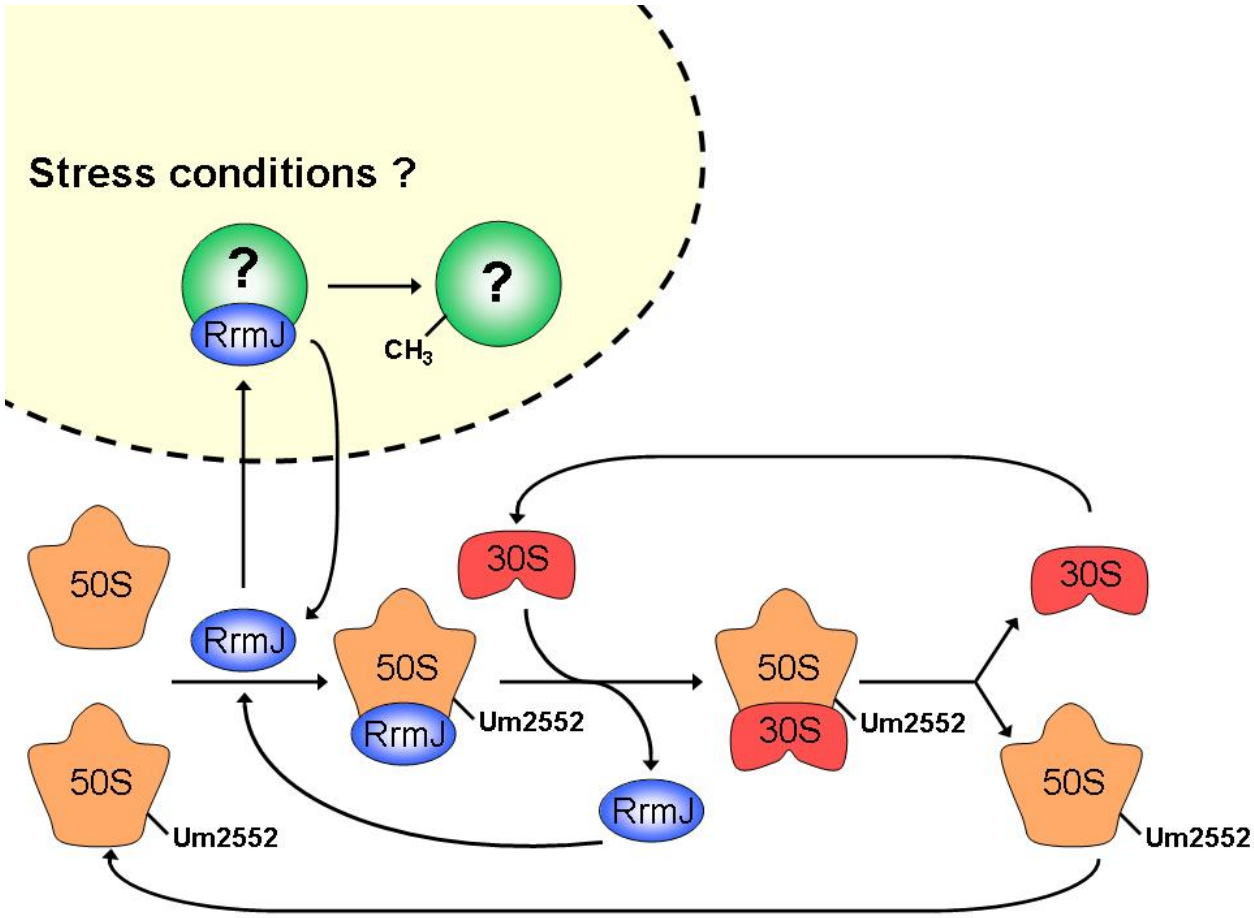

Figure 32: Model of RrmJ's various functions in the cell.
Under normal conditions RrmJ binds to 50S ribosomal subunits independent of the methylation status of the A-loop in order to methylate the U_{2552} as well as to act as ribosome assembly helper protein. Upon ribosome assembly RrmJ is being replaced by the 30S ribosomal subunit and, therefore, able to bind to the next free 50S ribosomal subunit. Under stress conditions, RrmJ's binding to the 50S ribosomal subunit is no longer needed and cellular RrmJ methylates now a second not yet identified substrate in the cytosol.

3.4 Future directions

Using gene chip technology, Blattner and co-workers have shown that RrmJ's mRNA level increases up to 20 fold upon heat shock induction (Richmond et al., 1999). We have now provided some preliminary evidence that RrmJ's heat shock function might involve the methylation of a second RNA substrate, which appears to be independent from the ribosome. Therefore, it is likely that the putative second substrate of RrmJ is located free in the cytosol. RrmJ's cytosolic yeast homologue, Trm7p, has been shown to be responsible for the 2'-*O*-ribose methylation at the positions 32 and 34 of certain tRNAs (Pintard et al., 2002b). Moreover, it has been shown by Hans Bügl that RrmJ is able to recognize tRNA as methylation substrate *in vitro* (Bügl et al., 2000). Therefore, it is not unreasonable to assume that tRNA might serve as the possible second methylation target for RrmJ. In order to identify the RNAs, that might be modified by RrmJ under heat shock conditions, a combination of HPLC and mass spectrometry of *rrmJ* wild type and deletion strain grown at heat shock temperatures should be performed. While in strains grown under normal conditions, all tRNA modifications have been identified successfully with this method (Rozenski et al., 1999; Sprinzl and Vassilenko, 2005), RNA modifications in strains that have been subjected to heat shock have not yet been analyzed. However, there have been studies that reveal the importance of tRNA modifications in regard to heat shock. Most importantly, studies with the pseudouridine synthetase TruB as well as the tRNA methyltransferase Trm1 in *E. coli* have demonstrated that tRNA nucleoside modifications in the elbow region of tRNA is important for the thermal stability of tRNA *in vivo* and, therefore, crucial for the survival of the cell upon heat shock (Kinghorn et al., 2002). Furthermore, unmodified *in vitro* transcribed tRNA has been shown to be thermal instable (Kintanar et al., 1994) and susceptible for nucleases (Davanloo et al., 1979). Therefore, RrmJ's heat shock function might be important for tRNA stability at elevated temperatures. If RrmJ, however, methylates only very few distinct tRNAs like its cytosolic homologue Trm7p in yeast, this difference in modification pattern between the *rrmJ* wild type and *rrmJ* deletion strain may not be detectable by HPLC/mass spectrometry. In that case, thin layer chromatography could be performed. This approach has been successfully used by Pintard and coworkers in order to identify the tRNA substrates for Trm7p (Pintard et al., 2002b). This method is based on the RNase T2 digestion of total tRNA extracted from strains grown in the presence of

[^{32}P]orthophosphate. RNase T2 cleaves all phosphodiester linkages between nucleotides, except those that are 2'-*O*-methylated. The result of the RNase T2 digestion can then be analyzed on thin layer chromatography and the methylated nucleotides can be identified. Due to their 3'-neighboring nucleotide, it should be possible to assign these identified methylated nucleotides to distinct tRNAs. *In vitro* methylation assays with total tRNA prepared from the *rrmJ* wild type and *rrmJ* deletion strain that have been grown under heat shock conditions could serve as another possibility to test if RrmJ's heat shock function involves methylating tRNAs. If free RrmJ methylates certain tRNAs, these should be modified in the *rrmJ* wild type strain when subjected to heat stress and RrmJ is not bound to the ribosome. They should, however, be unmethylated in the *rrmJ* deletion strain and serve as *in vitro* substrate.

RrmJ has been shown to act as ribosome assembly protein by binding tightly to the 50S ribosomal subunit. However, the exact location of RrmJ on the surface of the 50S ribosomal subunit has not yet been identified. Although it was possible to crosslink RrmJ to the 50S ribosomal subunit using glutaraldehyde as chemical crosslinker it was not possible to upscale this crosslinking reaction in quantities, which is necessary to identify of the crosslinked complexes by mass spectrometry. Therefore, it may be useful to test different crosslinking reagents and techniques. The Trigger Factor (TF), for example, could be successfully crosslinked to the ribosomal proteins L23 and L29 using the crosslinking reagent benzophenone-4-iodoacetamide (BPIA) (Kramer et al., 2002). The crosslinking was done by substituting an aspartate adjacent to the putative ribosomal binding site of TF with a cysteine. Because TF lacks additional cysteine residues, it was then possible to couple the thiol-specific ultraviolet-activatable crosslinker BPIA specifically to this site of the TF mutant protein. This renders a nice strategy that would be also possible for RrmJ. RrmJ has two cysteine residues in its amino acid sequence. The 3D structure of RrmJ, however, reveals that both of them are buried inside the protein. Therefore, in analogy to the study with TF, it would be possible to mutate an amino acid, which has been shown to be in a region that is important for the binding of RrmJ to the 50S ribosomal subunit. However, this substitution should not influence the binding, therefore, it is important to choose a non-conserved amino acid for this mutagenesis. I showed that the N-terminus of RrmJ is crucial for 50S binding. Therefore, it would be reasonable to substitute an amino acid within this region with a cysteine and couple BPIA specifically to this residue. Then, RrmJ could be crosslinked to ribosomal proteins via the crosslinker BPIA by ultraviolet irradiation and the bands could be

made visible on a one dimensional SDS PAGE. Subsequently the crosslinked complexes could be identified by mass spectrometry.

4 Materials and Methods

4.1 Constructing the various mutants of RrmJ

4.1.1 Site directed mutagenesis

Site directed mutagenesis was performed according to the protocol of the QuickChange Kit (Stratagene, La Jolla, CA). This kit allows to introduce point mutations by using double-stranded DNA plasmid as template, in contrast to several other techniques that require single-stranded DNA (ssDNA) (Kunkel, 1985; Sugimoto et al., 1989; Taylor et al., 1985; Vandeyar et al., 1988). By using a thermal temperature cycler, the plasmid is denatured and the two complementary oligonucleotide primers containing the desired mutation are annealed. The oligonucleotide primers are extended during temperature cycling by using the non-strand displacing action of *PfuTurbo* DNA polymerase. Extension and incorporation of the mutagenic primers results in nicked circular strands. Subsequently, the product is treated with *Dpn I*. The *Dpn I* endonuclease (target sequence: 5'-Gm6ATC-3') is specific for methylated and hemimethylated DNA and is therefore used to exclusively digest the parental *dam* methylated DNA template (Nelson & McClelland, 1992). To repair the nicks in the mutated plasmid, the circular, nicked dsDNA containing the desired mutation is then transformed into XL1-Blue supercompetent cells. The success rate of the site directed mutagenesis is greater than 80%.

4.1.1.1 Primer Design

Complementary coding and non coding strand primers were designed with the desired mutations in the center of the oligonucleotides flanked by 10 – 15 bases of complimentary sequence. An appropriate restriction site was introduced with the mutation to screen the obtained plasmids. The melting temperature of the primer was calculated according to equation (1):

(1) $T_m = 81.5 + 0.41(\%\ GC) – 675/N - \%$

and was equal or greater than 75°C for the primers used. N is the primer length in base pairs.

4.1.1.2 Polymerase chain reaction (PCR)

For the PCR, the samples were prepared containing 1 µl of the dsDNA template, 200 ng forward primer, 200 ng reverse primer and 0.8 mM dNTP mix. The template vector (here pJuH1) was isolated from a *dam*$^+$ *E.coli* strain (here JuH1).
The samples (final volume: 49 µl) were overloaded with 30 µl liquid wax. After a hot start of 5 min at 95°C, 1 µl *PfuTurbo* DNA polymerase was added. The cycling parameters used for pJuH1 are shown in table 3. To verify that the PCR-reaction was successful, the PCR product was visualized on a 1% TAE-agarose gel.

#	*Temperature [°C]*	*Incubation time [min]*	*Step*
1	95	5	Hot start
2	80	2	Addition of 1µl *PfuTurbo* polymerase
3	95	0.5	Initial denaturing
4	95	0.5	Denaturing
5	55	1	Annealing
6	68	12	Elongation

17 cycles 4 – 6

Table 3: Cycling parameters used for site directed mutagenesis according to the QuickChange Kit (Stratagen, La Jolla, CA)

After the PCR amplification, the samples were incubated for 1 hour at 37°C with 10 U *Dpn* I to digest the Dam-methylated parental supercoiled dsDNA (Lacks and Greenberg, 1975). The plasmids were transformed into heat shock competent *E.coli* XL1-blue cells. Subsequently, restriction analysis of the plasmids (section 4.1.1.3) and sequencing (section 4.1.1.4) was used to verify the correct introduction of the mutations.

4.1.1.3 Restriction analysis

The primers which were used for the site directed mutagenesis (section 4.1.1.1) were designed to introduce new restriction sites, which were not present in the template plasmid. Therefore, restriction analysis could be utilized as a screening step for the clones obtained. Restriction endonucleases were used according to the protocol of the manufacturer. 2 µl plasmid DNA was digested with the respective restriction enzyme in the appropriate buffer

system for 2 h at the recommended temperature. The samples were supplemented with loading buffer (final concentration: 0.05% bromophenol-blue, 0.05% xylene cyanol FF, 6% glycerol) (Sambrook, 1989) and the DNA fragments were separated in 1% TAE-agarose gels (Sharp et al., 1973) or precast 4-20% TBE-polyacrylamide gels. TAE gel electrophoresis buffer (40 mM Tris-acetate, 1 mM EDTA) was used for agarose gels, while TBE buffer (45 mM Tris-borate, 1 mM EDTA) was used for polyacrylamide gels. Agarose gels were run at 120 V for 50 min and polyacrylamide gels were run at 200 V for 50 min. The DNA was visualized by staining the gels with ethidium bromide, a fluorescent dye that intercalates into nucleic acids.

4.1.1.4 DNA sequencing

For DNA sequencing, the chain termination method by (Sanger et al., 1992) was used.
10 µl of a DNA preparation (see section 2.8.1) and 5µl of standardized T7 primers (3.2 pmol/µl of T7-forward (5'- TAA TAC GAC TCA CTA TAG GG -3') and T7 reverse (5'- ACC GCT GAG CAA TAA CTA – 3')) were used to sequence pET11a derivatives. Sequencing reactions and gel runs were performed at the DNA sequencing core facilities of the University of Michigan in Ann Arbor.

4.1.2 Expression Analysis

To investigate the expression level of wild type RrmJ in HB24 and of the mutant proteins in the transformed HB23 (*rrmΔJ567*) strains, Western blot analysis using polyclonal antibodies against RrmJ was performed. The transformed strains were grown in LB medium supplemented with 100 µg/ml ampicillin until an A_{600} of 0.5 was reached. Then, a 2-ml aliquot of cells was taken, resuspended in 85 µl of 2 x SDS-Laemmli buffer, and boiled for 20 min. The proteins were separated on a 14% Tris-glycine PAGE (NOVEX), and RrmJ was visualized using Western blot analysis. To investigate whether the RrmJ mutant proteins are expressed in a soluble form in HB23 cells, cell lysates were prepared (see below), and the presence of RrmJ in the soluble supernatant was determined with Western blot analysis.

4.2 Constructing the BL21 *rrmJ* deletion strain JuH47

4.2.1 Preparation of a high titer P1-lysate

The preparation of a high titer P1-lysate was performed according to Silhavy (Silhavy, 1984). To prepare a transducing P1-Lysate, 2 ml of an overnight culture of the *rrmJ*-deletion strain (HB23) was pelleted at 13,500 x g for 1 min. The cells were then resuspended in 1 ml 5 mM $CaCl_2$, 5 mM $MgCl_2$ and 100 µl aliquots were prepared.
0 µl, 10 µl undiluted, 10 µl 1: 10 diluted, 10 µl 1:100 diluted, 10 µl 1:1000 diluted P1-lysate was added to 100 µl cells. 2 ml warm top agar containing 5 mM $CaCl_2$ and 5 mM $MgCl_2$ was added to each sample and plated onto LB-plates. These plates were incubated overnight at 37°C. To obtain the phages, 2-3 ml LB was added onto the plate which showed a lawn of individual plaques. The top agar was scratched of the plate and transferred into a centrifugation tube. 100 µl chloroform was added, the suspension was vortexed and centrifuged at 8,000 x g for 5 min. The supernatant harboring the P1-phages was transferred into a falcon tube and again 100 µl chloroform was added. The P1-Lysate was stored at 4°C.

4.2.2 Titer determination

A sample of 100 µl *rrmJ*-deletion cells in 2 ml topagar containing 5 mM $CaCl_2$ and 5 mM $MgCl_2$ was plated onto a LB-plate and 2 µl of the P1-Lysate in dilutions of 10^{-4}, 10^{-5}, 10^{-6}, 10^{-7} were spotted onto the cell lawn. The plate was incubated overnight at 37°C. Subsequently the titer was determined according to equation (2):
(2) λ/μ = N plaques * dilution / 2µl,
where N equals the number of plaques. A titer of 5-30 x 10^6 phages/µl was obtained.

4.2.3 P1 – transduction

4 ml overnight culture (here BL21(DE3)) was supplemented with 40 µl 1 M $CaCl_2$ and the culture was divided into four 1 ml aliquots. 0µl, 50µl, 100µl or 200µl of the high titer P1-lysate was added to each of the aliquots. One sample was prepared containing only P1-lysate without cells. The samples were incubated without shaking at 37°C for exactly 20 min. Then,

100 µl of a 1 M sodium citrate solution was added and the cells were incubated for the phenotypic expression in a roller drum for 1 h at 37°C.
The cells were plated onto LB-plates supplemented with 12.5 µg/µl tetracyclin and 1.5 mM sodium citrate and incubated at 37°C overnight. Individual colonies were streaked out for single colonies and permanent cultures were prepared. The tetracycline resistance cassette is linked with the *rrmJ*-deletion to 90%. The result of the transduction revealed a 75% linkage.

4.3 Purification of RrmJ

4.3.1 Ion exchange chromatography

Separation of proteins with an ion exchange chromatography is based on Columb interaction between the ions of the gel matrix and the charged side chains of the protein.
The netto charge of a protein is dependent on the isoelectric point of the protein and the pH of the chosen buffer system. Is the pH above the isoelectric point of the protein, the nettocharge will be negative and the protein will bind onto an anion exchange chromatographer. A pH lower than the isoelectric point of the protein leads to a positive nettocharge of the protein and the protein will bind to a cation exchange chromatographer. For binding of a protein to the column a difference of $| pH-pI | > 1$ is required. The elution of the protein from the column is performed by either variation of the pH or by changing the ionic strength.

4.3.2 Purification of the RrmJ mutants

The purification of the RrmJ mutants was performed according to Bügl et al. (Bügl et al., 2000). However, slight modifications were applied to optimize the purification protocol.
To prepare the soluble cell proteins, the cell pellet was resuspended in 20 ml of buffer A (40 mM HEPES•KOH, 150 mM KCl, pH 8.0, 1 mM DTT, 2% v/v glycerol) and lysed twice by using a French press cell at 1,200 psi. After each round of lysis, 0.5 ml of a Protease Inhibitor Cocktail Complete^{TM} tablet (Boehringer) dissolved in 1 ml ddH_2O was added to the crude extract to inactivate proteases. The cell lysate was cleared from membranes and other insoluble cellular components by centrifugation (40,000 x g, 40 min, 4°C). The supernatant

was additionally cleared by a passage through a 0.8 µm syringe filter. For separating RrmJ from the other cellular proteins, the supernatant was applied onto a tandem anion exchanger (Q-Sepharose), followed by a cation exchanger (S-Sepharose). At the given pH of 8.0, the RrmJ protein and all the point mutants bound exclusively to the S-Sepharose. This is due to their high isoelectric point (pI) of 9.44. Since the truncated RrmJ mutant protein, however, exerts a pI of 8.57, I used a pH of 7.0 in order to purify this protein. In contrast to Bügl et al. (Bügl et al., 2000), a tandem 5 ml HiTrap™ Q Sepharose™ High Performance (Pharmacia) connected to a 5 ml HiTrap™ SP Sepharose™ High Performance (Pharmacia) column was used. The special design of these columns, together with a modern chromatography matrix, provides fast separations. The columns are made of medical grade polypropylene, which is biocompatible and non-interactive with biomolecules. The Q sepharose and SP sepharose columns were equilibrated with 5 column volumes of buffer A (40 mM HEPES•KOH, pH 8.0, 150 mM KCl, 1 mM DTT, 2% v/v glycerol). For all steps, a flow rate of 4 ml/min was used. The lysate of approximately 20 ml volume was loaded onto the tandem column using a syringe. After loading the lysate, the columns were washed with buffer A until an OD of 0.2 was reached. Then, a linear 300 ml gradient from 0 to 30 % of buffer B (40 mM HEPES•KOH, pH 8.0, 2 M KCl, 1 mM DTT, 2% v/v glycerol) was applied. The eluate was collected in 6 ml fractions. The fractions were analyzed by SDS-PAGE and the RrmJ containing fractions were pooled. The pooled fractions were concentrated to approximately 6 ml using an Amicon Ultrafiltration Cell with an ultrafiltration membrane of 10 kDa exclusion size (YM-10). The buffer was changed to 150 mM KCl, 40 mM HEPES•KOH, pH 7.5, 2% v/v glycerol, 1 mM DTT (storage buffer) by a 1:20 dilution with subsequent concentration to approximately 6 ml. Since the mutants were shown to be > 95% pure, the gelfiltration chromatography was omitted. The protein concentration was determined by UV absorbance (see section 2.9.3) and aliquots of the protein were frozen and stored at - 80°C.

4.4 AdoMet titration

To establish a calibration curve for determining the amount of AdoMet present in the various RrmJ preparations, a spectrum of the purified RrmJ D83A was measured. This mutant of RrmJ is unable to bind AdoMet and served as a standard for this calibration curve. Then, AdoMet was titrated in 1 µM steps and the OD at 280 nm, 260 nm and 257 nm was

measured. The exact AdoMet concentration of the stock solution was determined using the molar AdoMet extinction coefficient of ε_{257nm}= 15,400 mM^{-1} cm^{-1}

The 280 nm/260 nm ratio was plotted against the amount of titrated AdoMet by adjusting the final volume. Subsequently, the unknown amount of bound AdoMet was calculated using this standard curve and an $A_{280/260}$ ratio of each RrmJ mutant.

4.5 Preparation of ribosomal subunits

4.5.1 Preparation of the lysate

To prepare ribosomal subunits, 4 liters of the *rrmJ* deletion strain, HB23 (Bügl et al., 2000), were grown at 37°C in LB-Media until an OD_{600} of 0.7 was reached. The cells were harvested in 1 l centrifugation buckets in which half of the volume was supplied by ice to cool down the cells as fast as possible.

The cell cultures were spun down at 2,000 x g for 20 min at 4°C. The cell pellet was resuspended in 20 ml 20 mM HEPES•KOH buffer, pH 7.5 under associating, high magnesium conditions (10 mM $MgCl_2$, 100 mM NH_4Cl, 4 mM β-mercaptoethanol; see Table 4) (Korber et al., 2000). To lyse the cells, 15 µl of 50 mg/ml lysozyme solution was added per 100 ml starting culture (Korber et al., 2000). To prevent degradation of the RNA, the cell lysate was supplemented with 80 U RNAse inhibitor (RnaseIn, Promega). Additional to the lysozyme treatment, the cells were lysed by two freezing and thawing cycles of the cells using dry ice/EtOH and ice water, respectively. The lysed cells were ultracentrifuged at 100,038 x g for 30 min at 2°C (RP80AT rotor) and the DNA was removed. The supernatant was transferred into 2 ml eppendorf tubes and stored at -80°C Before use the lysates were again clarified by 45 min centrifugation at 13,000 x g at 4°C. For determination of the RNA concentration, the OD of the lysates at 260 nm was measured. RNA concentrations were determined using an extinction of 0.1 (A_{260}) for a 40 µg/ml solution.

4.5.2 Preparative sucrose gradients

To be able to collect the individual ribosomal subunits, dissociating sucrose gradients were prepared with sucrose concentrations of 10%, 15%, 20% and 25% w/v in 20 mM

HEPES•KOH, pH 7.5, 4 mM β-mercaptoethanol, 1 mM $MgCl_2$, 100 mM NH_4Cl (Korber et al., 2000). From each of the sucrose solutions, 7 ml were used overlaying each other and starting with the highest sucrose concentration. The sucrose gradients were incubated o/n at 4°C or at least 2.5 h at 37°C to obtain equal diffusion. The gradients were loaded with 1 ml of 4 mg/ml lysate and then centrifuged at 21,000 rpm for 20 h at 4°C ($\omega_2 t = 3.3\ e^{11}\ rad^2/sec$, Beckman L8-70 centrifuge with SW28 Ti rotor). When speed and time was changed, equation (3) was used to calculate the new parameters.

(3) $rpm^2_1 * t_1 = rpm^2_2 * t_2$,

where t equals the time and rpm are the rotations per minute.

Fractions containing the ribosomal subunits were obtained by using a gradient pump (sensitivity 1.0, 1.5 ml/min). The complete 30S peak was collected. The 50S subunits were collected as late fractions starting at the top of the 50S peak. The subunits were pelleted by ultracentrifugation at 33,000 x g for 20 h at 4°C ($\omega_2 t = 8.65\ e^{11}\ rad^2/sec$, Beckman L8-70 centrifuge with SW40 Ti rotor). The pellet was resuspended in a 20 mM HEPES•KOH, pH 7.5, 4 mM β-mercaptoethanol buffer containing 6 mM $MgCl_2$ and 30 mM NH_4Cl. To determine the subunit concentrations, the absorbance at 260 nm was measured and the concentrations were calculated (1 A_{260} unit is equivalent to about 69 pmol, 34.5 pmol and 23 pmol for 30S, 50S and 70S, respectively (Spedding, 1990)). The obtained subunits were stored at -80°C.

Table 4: Various buffers for preparation of ribosomal subunits and analytical polysome profiles.

	10-100 buffer associating buffer	*1-200 buffer dissociating buffer*	*6-30 buffer storage buffer*
HEPES•KOH, pH 7.5	20 mM	20 mM	20 mM
$MgCl_2$	10 mM	1 mM	6 mM
NH_4Cl	100 mM	200 mM	30 mM
β-mercaptoethanol	4 mM	4 mM	4 mM

4.6 Methyltransferase activity assay

In order to determine apparent K_{cat} and K_m values for the various RrmJ mutants an activity assay with radioactive [^{3}H]-S-Adenosyl-L-Methionine (85.0 Ci/mmol; Amersham) was carried out (Tscherne et al., 1999) (Bügl et al., 2000).

If not noted differently, 100 nM RrmJ mutant was preincubated in a 20 µl volume for 40 sec at 37°C with a defined concentration of cold (47 µM) and hot (3 µM) [^{3}H]-S-Adenosyl-L-Methionine (^{3}H-AdoMet) in 50 mM HEPES·KOH, pH 7.5, 85 mM NH_4Cl, 2 mM β-mercaptoethanol, 40 U RnaseIn (Promega). This preincubation was necessary to allow the exchange of the RrmJ-bound AdoMet with radioactive AdoMet. After the 40 sec preincubation reaction, 20 µl 50S subunits in 20 mM HEPES·KOH, pH 7.5, 6 mM $MgCl_2$, 30 mM NH_4Cl and 4 mM β-mercaptoethanol were added. To measure initial rates, 8 µl samples were taken out at four time points: 2.5 min, 5 min, 7.5 min, 10 min. These samples were immediately precipitated with 1 ml ice cold TCA (5% w/v final concentration). Subsequently, the samples were incubated on ice for 15 min and centrifuged at 13,000 x g for 15 min. The supernatant was discarded, the pellet was washed with 1 ml 5% w/v ice cold TCA and spun down. The pellet was finally resuspended in 80 µl 200 mM Tris, pH 8.5. Then, 80 µl of 10% w/v TCA was added and after a 15 minutes incubation on ice, the acid-insoluble material was collected on nitrocellulose filters (Millipore). The filters were washed with 10 ml 5% w/v TCA, air-dried and counted in a Beckman LS6800 liquid scintillation counter using EcoLite^{TM} as liquid scintillation cocktail (ICN). The slopes of the methyl incorporation versus time were calculated.

To measure the apparent K_m for 50S ribosomal subunits, 100 nM enzyme, 50 µM AdoMet and various concentrations of 50S ribosomal subunits ranging from 0.25 µM to 10 µM were used. The various V_{max} values obtained were plotted against the respective substrate concentrations and the apparent K_m values were calculated.

To determine the apparent K_{cat} values for the mutated RrmJ proteins, the assay was carried out using 100 nM enzyme, 50 µM AdoMet and 5 µM 50S ribosomal subunits. In order to test the stability of RrmJ at elevated temperatures the assay was performed at temperatures ranging from 25ºC to 80ºC. To investigate the influence of Mg^{2+} on the enzymatic activity of RrmJ, Mg^{2+} concentrations between 0.9 mM and 6 mM were used in the methylation buffer. Competition assays were carried out by pre-incubating the 50S ribosomal subunits prepared

from the *rrmJ* deletion strain (HB23) with various concentrations of purified RrmJ-K38A mutant protein for 10 min at 37°C. Then, the assay was carried out as described.

To study the influence of 30S ribosomal subunits on the methylation activity of RrmJ, buffer conditions were adjusted to reflect conditions optimal for both ribosome assembly and specificity of RrmJ. The assay buffer used for these reactions contained 20 mM HEPES·KOH, pH 7.5, 100 mM KCl, 20 mM $MgCl_2$ and 4 mM β-mercaptoethanol. The initial rate for methylation was measured at 40 ^oC in the presence of 100 nM RrmJ, 5 µM 50S ribosomal subunits prepared from HB23, 50 µM AdoMet supplemented with [^{3}H] S-adenosyl-L-methionine (85.0 Ci/mmol; Amersham) either in the absence or presence of increasing amounts of 30S ribosomal subunits prepared from HB23. At defined time points (0.5, 1, 2, 3, 4, 6 min) after initiating the methylation reaction, 6 µl aliquots were taken and the [^{3}H]-methyl incorporation into 23S rRNA was determined.

Methylation reactions with the A-loop as substrate were performed in 50 mM HEPES•KOH, pH 7.5, 50 mM NaCl, 10 mM EDTA, 1 mM DTT, 40 U RNase inhibitor RNasIn (Promega), 0.1 mg/ml BSA at 37^oC. RrmJ (5 µM) was incubated with 50 µM ^{3}H-AdoMet (85 Ci/mmol) and the reaction was started by adding 1 µM purified A-loop (nucleotides 2545-2563 of *E.coli* 23S rRNA, kindly provided by Dr. Joseph Puglisi, Stanford) (Blanchard and Puglisi, 2001). Defined time points after initiating the methylation reaction, 8 µl aliquots were taken, supplemented with 40 µg tRNA (Sigma) as carrier for precipitation and the ^{3}H-methyl incorporation was determined.

4.7 Analytical polysome profiles

4.7.1 Associating and dissociating polysome profiles

Gradients were poured with overlaying sucrose solutions ranging from 50% on the bottom to 10% w/v sucrose on the top in 10% steps (Korber et al., 2000). 1.8 ml of the 50% sucrose solution and 2.5 ml of the other sucrose solutions were used in 12.5 ml tubes. Associating or dissociating polysome profile were obtained by using either 10 mM $MgCl_2$ and 100 mM NH_4Cl or 1 mM $MgCl_2$ and 200 mM NH_4Cl in 20 mM HEPES•KOH, 4 mM β-mercaptoethanol buffer (see table 4). Equal diffusion was obtained by incubating the gradients o/n at 4°C or at least 2.5 h at 37°C.100 µg Lysate was loaded onto the gradients and

the gradients were ultracentrifuged for 4 h at 35,000 rpm at 2°C ($\omega_2 t$ = 2.87 e^{11} rad^2/sec, Beckman L8-70 centrifuge with SW40 Ti rotor). The polysome profile was analysed using the gradient pump at a sensitivity of 0.5 and a speed of 0.75 ml/min (Korber et al., 2000).

4.8 RrmJ binding to the ribosome

Preparation of 50S ribosomal subunits from wild type (HB24) or the *rrmJ* deletion strain expressing no RrmJ (HB23) or the RrmJ-D136N mutant protein was performed under stringent, high salt conditions (1 mM $MgCl_2$, 200 mM NH_4Cl) as described in section 4.5.2. Aliquots of 2 µM 50S ribosomal subunits alone or supplemented with various concentrations of purified wild type RrmJ were prepared. 10 µl of those aliquots were loaded onto a 14% Tris-glycine SDS-PAGE (Invitrogen) and western blot analysis was performed using polyclonal antibodies against RrmJ.

4.9 Co-fractionation experiments

To analyze the localization of endogenous RrmJ, lysates of either the *rrmJ* wild type strain HB24 or the *rrmJ* Δ1-29 strain HB43 were prepared. To test the binding of purified wild type RrmJ to ribosomal subunits in a HB43 strain, 200 µg lysate of HB43 was supplemented with 80 ng purified wild type RrmJ protein. For titration studies using isolated 50S ribosomal subunits, 50S ribosomal subunits were prepared from HB23 as described in section 4.5.2. 4.5 µM isolated 50S ribosomal subunits were supplemented with defined concentrations of either wild type or the RrmJ mutant proteins and incubated in 50 mM HEPES·KOH, pH 7.5, 3mM $MgCl_2$, 100 mM NH_4CL, 2 mM β-mercaptoethanol, 50 µM AdoMet for 10 min at 37 ºC (final volume: 20 µl). The complete samples were then analyzed using 12 ml 10 - 50% sucrose gradients under stringent (1 mM $MgCl_2$, 200 mM NH_4Cl) or non stringent (10 mM $MgCl_2$, 100 mM NH_4Cl) salt conditions. The complete peak fractions as well as the "top of the gradient" were collected and the proteins were precipitated with 5% v/v TCA. The pellets were resuspended in 500 µl SDS-Laemmli buffer, separated on 14% SDS PAGE (Novex) and RrmJ was detected by western blot using polyclonal antibodies against RrmJ.

4.10 *In vitro* reconstitution of the ribosome

The reconstitution experiments were performed according to Blaha et al. with slight modifications (Blaha et al., 2002). 30S and 50S ribosomal subunits prepared from the *rrmJ* deletion strain HB23 or wild type strain HB24 either in a ratio of 2:1 or in stoichiometric amounts were incubated with or without 1 µM wild type RrmJ in 20 mM HEPES·KOH, pH 7.5, 100 mM KCl, 20 mM MgCl2, 4 mM β-mercaptoethanol, 50 µM AdoMet in a total volume of 40 µl at 40ºC for 5 and 10 min. To stop the ribosome assembly process after 5 min, samples were shock-frozen in liquid nitrogen. The complete samples were then analyzed on a 12 ml 10-50% sucrose gradient under the same buffer conditions. Fractions were collected and analyzed for the presence of RrmJ by western blot analysis as described in section 4.9.

4.11 Crosslinking

Chemical crosslinking of RrmJ with the 50S ribosomal subunit was performed using Glutaraldehyde (GA) as crosslinking reagent. To determine the optimal GA concentration titration experiments were performed and resulted in an optimal concentration of 600 µM. For crosslinking, 200 nM RrmJ and 200 nM 50S ribosomal subunits (or concentrations as indicated) prepared from either the *rrmJ* wild type HB24 or *rrmJ* deletion strain HB23 were incubated with GA either in buffer containing 20 mM HEPES·KOH, pH 7.5, 30 mM KCL, 20 mM Mg Cl_2, 4 mM β-mercaptoethanol or containing 50 mM HEPES·KOH, pH 7.5, 100 mM NH_4Cl, 3 mM $MgCl_2$, 4 mM β-mercaptoethanol for 2 min at 37ºC. After 2 min Tris-HCl, pH 8.0, in a final concentration of 20 mM was added to stop the crosslinking process and the samples were kept on ice. The crosslinking reaction was checked by visualizing the crosslinked bands on a 14% SDS PAGE (Novex) followed by western blot analysis using polyclonal antibodies against RrmJ.

4.12 Escherichia coli strains

Strains	*Genotype*	*Source of Reference*
MG1655	*rph-1*	Lab collection
BL21(DE3)	F^- ompT $hsdS_B(r_B^-m_B^-)$ gal dcm(DE3)	Novagene, Madison, WI
HB24	Mg1655, *zgi*-203::Tn*10*,TC^R	(Bügl et al., 2000)
HB23	Mg1655, *zgi*-203::Tn*10*,TC^R, *rrmJ*Δ567	(Bügl et al., 2000)
HB25	HB23, pHB1	(Bügl et al., 2000)
HB43	HB23, pHB16	(Bügl, 2001)
JuH 3	HB23, pJuH 3	(Hager et al., 2004)
JuH 5	HB23, pJuH 5	(Hager et al., 2004)
JuH 6	HB23, pJuH 6	(Hager et al., 2004)
JuH 7	HB23, pJuH 7	(Hager et al., 2004)
JuH 8	HB23, pJuH 8	(Hager et al., 2002)
JuH 10	HB23, pJuH10	(Hager et al., 2004)
JuH 11	HB23, pJuH11	(Hager et al., 2002)
JuH 25	HB23, pJuH12	(Hager et al., 2002)
JuH 26	HB23, pJuH13	(Hager et al., 2002)
HB101	HB23, pHB30	(Bügl, 2001)
HB102	HB23, pHB31	(Bügl, 2001)
JuH 33	HB23, pJuH18	(Hager et al., 2002)
JuH 34	HB23, pJuH19	(Hager et al., 2004)
JuH 35	HB23, pJuH20	(Hager et al., 2004)
JuH 36	HB23, pJuH21	(Hager et al., 2002)
JuH 37	HB23, pJuH22	(Hager et al., 2004)
JuH 38	HB23, pJuH23	(Hager et al., 2004)
JuH 12	BL21(DE3), pHB 1	(Hager et al., 2002)
JuH 47	JuH47, rrmJΔ567, Tet^R	(Hager et al., 2002)
JuH 56	JuH47, pJuH 18	(Hager et al., 2002)
JuH 57	JuH47, pJuH 21	(Hager et al., 2002)
JuH 58	JuH47, pHB16	This study
JuH 59	JuH47, pJuH 12	(Hager et al., 2002)
JuH 60	JuH47, pJuH 8	(Hager et al., 2002)
JuH 61	JuH47, pJuH 13	(Hager et al., 2002)
JuH 62	JuH47, pJuH11	(Hager et al., 2002)
JuH 63	JuH47, pJuH5	(Hager et al., 2004)
JuH 64	JuH47, pJuH20	(Hager et al., 2004)
JuH 65	JuH47, pJuH22	(Hager et al., 2004)
JuH 66	JuH47, pJuH19	This study
JuH 67	JuH47, pJuH23	(Hager et al., 2004)
JuH 68	JuH47, pJuH3	(Hager et al., 2004)
JuH 69	JuH47, pHB30	(Hager et al., 2004)
JuH 70	JuH47, pJuH6	(Hager et al., 2004)
JuH 71	JuH47, pJuH7	(Hager et al., 2004)

JuH 72	JuH47, pJuH10	(Hager et al., 2004)
JuH 73	JuH47, pHB31	(Hager et al., 2004)
XL-1blue	F'::Tn10 $proA^+B^+$ $lacI^q$ Δ(lacZ)M15/recA1 endA1 gyrA96 (Nal^r) thi hsdR17 ($r_K^-m_K^+$) glnV44 relA1 lac	Bullock et al. (1987); Stratagene, La Jolla, CA

4.13 Plasmids

Plasmids	*Relevant Features*	*Source of Reference*
pET 11a	pBR 322 derived, ColE1 compatibility group origin of replication; promotor, Shine Dalgarno sequence and terminator from T7 Φ10, promotor containing lac operator; lacI, Amp^r	Novagene, Madison, WI
pHB1	pET11a/*rrmJ*	(Bügl et al., 2000)
pHB16	pET11a/ *rrmJ* Δ29	(Bügl, 2001)
pJuH 3	pET11a/ *rrmJ* D20A	(Bügl, 2001)
pJuH 5	pET11a/ *rrmJ* R32A/R34A	(Bügl, 2001)
pJuH 6	pET11a/ *rrmJ* F37A/L39A	(Bügl, 2001)
pJuH 7	pET11a/ *rrmJ* Q67A/Y68A	(Bügl, 2001)
pJuH 8	pET11a/ *rrmJ* D124A	(Bügl, 2001)
pJuH10	pET11a/ *rrmJ* R194A	(Bügl, 2001)
pJuH11	pET11a/ *rrmJ* Y201A	(Bügl, 2001)
pJuH12	pET11a/ *rrmJ* K38A	(Hager et al., 2002)
pJuH13	pET11a/ *rrmJ* E199A	(Hager et al., 2002)
pHB30	pET11a/ *rrmJ* Y22A	(Bügl, 2001)
pHB31	pET11a/ *rrmJ* S197A	(Bügl, 2001)
pJuH18	pET11a/ *rrmJ* D83A	(Hager et al., 2002)
pJuH19	pET11a/ *rrmJ* P127V	(Hager, 2001)
pJuH20	pET11a/ *rrmJ* D136N	(Hager et al., 2004)
pJuH21	pET11a/ *rrmJ* K164A	(Hager et al., 2002)
pJuH22	pET11a/ *rrmJ* F166A	(Hager et al., 2004)
pJuH23	pET11a/*rrmJ* K189A	(Hager et al., 2004)

5 Literature

Agarwalla, S., Kealey, J. T., Santi, D. V., and Stroud, R. M. (2002). Characterization of the 23 S ribosomal RNA m5U1939 methyltransferase from Escherichia coli. J Biol Chem *277*, 8835-8840.

Agarwalla, S., Stroud, R. M., and Gaffney, B. J. (2004). Redox reactions of the iron-sulfur cluster in a ribosomal RNA methyltransferase, RumA: optical and EPR studies. J Biol Chem *279*, 34123-34129.

Ban, N., Nissen, P., Hansen, J., Moore, P. B., and Steitz, T. A. (2000). The complete atomic structure of the large ribosomal subunit at 2.4 A resolution. Science *289*, 905-920.

Barbas, C. F., 3rd, Heine, A., Zhong, G., Hoffmann, T., Gramatikova, S., Bjornestedt, R., List,
B., Anderson, J., Stura, E. A., Wilson, I. A., and Lerner, R. A. (1997). Immune versus natural selection: antibody aldolases with enzymic rates but broader scope. Science *278*, 2085-2092.

Barbosa, E., and Moss, B. (1978). mRNA(nucleoside-2'-)-methyltransferase from vaccinia virus. Characteristics and substrate specificity. J Biol Chem *253*, 7698-7702.

Bjoerk, G. R. (1996). E.coli and Salmonella. Cellular and Molecular Biology (Washington, D.C., ASM Press).

Blaha, G., Burkhardt, N., and Nierhaus, K. H. (2002). Formation of 70S ribosomes: large activation energy is required for the adaptation of exclusively the small ribosomal subunit. Biophys Chem *96*, 153-161.

Blanchard, S. C., and Puglisi, J. D. (2001). Solution structure of the A loop of 23S ribosomal RNA. Proc Natl Acad Sci U S A *98*, 3720-3725.

Brecht, B. (1938). Das Leben des Galilei, Edition Suhrkamp).

Brimacombe R., Mitchell P., Osswald M., Stade K., Bochkariov D. (1993). Clustering of modified nucleotides at the functional center of bacterial ribosomal RNA. FASEB J. *7(1)*:161-7.

Brunger, A. T., Adams, P. D., Clore, G. M., DeLano, W. L., Gros, P., Grosse-Kunstleve, R. W., Jiang, J. S., Kuszewski, J., Nilges, M., Pannu, N. S.*, et al.* (1998). Crystallography & NMR system: A new software suite for macromolecular structure determination. Acta Crystallogr D Biol Crystallogr *54 (Pt 5)*, 905-921.

Bügl, H. (2001) Funktionelle und strukturelle Analyse des Hitzeschockproteins FtsJ aus *Escherichia coli*, Universitaet Regensburg, Regensburg.

Bügl, H., Fauman, E. B., Staker, B. L., Zheng, F., Kushner, S. R., Saper, M. A., Bardwell, J. C., and Jakob, U. (2000). RNA methylation under heat shock control. Mol Cell *6*, 349-360.

Bujnicki, J. M., and Rychlewski, L. (2001). Reassignment of specificities of two cap methyltransferase domains in the reovirus lambda 2 protein. Genome Biol *2*, RESEARCH0038.

Bussiere, D. E., Muchmore, S. W., Dealwis, C. G., Schluckebier, G., Nienaber, V. L., Edalji, R. P., Walter, K. A., Ladror, U. S., Holzman, T. F., and Abad-Zapatero, C. (1998). Crystal structure of ErmC', an rRNA methyltransferase which mediates antibiotic resistance in bacteria. Biochemistry *37*, 7103-7112.

Bylund, G. O., Persson, B. C., Lundberg, L. A., and Wikstrom, P. M. (1997). A novel ribosome-associated protein is important for efficient translation in Escherichia coli. J Bacteriol *179*, 4567-4574.

Bylund, G. O., Wipemo, L. C., Lundberg, L. A., and Wikstrom, P. M. (1998). RimM and RbfA are essential for efficient processing of 16S rRNA in Escherichia coli. J Bacteriol *180*, 73-82.

Caldas, T., Binet, E., Bouloc, P., Costa, A., Desgres, J., and Richarme, G. (2000a). The FtsJ/RrmJ heat shock protein of Escherichia coli is a 23 S ribosomal RNA methyltransferase. J Biol Chem *275*, 16414-16419.

Caldas, T., Binet, E., Bouloc, P., Costa, A., Desgres, J., and Richarme, G. (2000b). The FtsJ/RrmJ heat shock protein of Escherichia coli is a 23 S ribosomal RNA methyltransferase. J Biol Chem *275*, 16414-16419.

Caldas, T., Binet, E., Bouloc, P., and Richarme, G. (2000c). Translational defects of Escherichia coli mutants deficient in the Um(2552) 23S ribosomal RNA methyltransferase RrmJ/FTSJ. Biochem Biophys Res Commun *271*, 714-718.

Carson, M. (1997). Ribbons (New York, Academic Press).

Carter, A. P., Clemons, W. M., Jr., Brodersen, D. E., Morgan-Warren, R. J., Hartsch, T., Wimberly, B. T., and Ramakrishnan, V. (2001). Crystal structure of an initiation factor bound to the 30S ribosomal subunit. Science *291*, 498-501.

Charollais, J., Dreyfus, M., and Iost, I. (2004). CsdA, a cold-shock RNA helicase from Escherichia coli, is involved in the biogenesis of 50S ribosomal subunit. Nucleic Acids Res *32*, 2751-2759.

Charollais, J., Pflieger, D., Vinh, J., Dreyfus, M., and Iost, I. (2003). The DEAD-box RNA helicase SrmB is involved in the assembly of 50S ribosomal subunits in Escherichia coli. Mol Microbiol *48*, 1253-1265.

Cheng, X., and Blumenthal, R. M. (2002). Cytosines do it, thymines do it, even pseudouridines do it--base flipping by an enzyme that acts on RNA. Structure (Camb) *10*, 127-129.

Ching, Y. P., Zhou, H. J., Yuan, J. G., Qiang, B. Q., Kung Hf, H. F., and Jin, D. Y. (2002). Identification and characterization of FTSJ2, a novel human nucleolar protein homologous to bacterial ribosomal RNA methyltransferase. Genomics *79*, 2-6.

Curran, J. F. (1998). Modified Nucleotides in Translation (Washington D>C>, AMS Press).

Dammel, C. S., and Noller, H. F. (1995). Suppression of a cold-sensitive mutation in 16S rRNA by overexpression of a novel ribosome-binding factor, RbfA. Genes Dev *9*, 626-637.

Das, K., Acton, T., Chiang, Y., Shih, L., Arnold, E., and Montelione, G. T. (2004). Crystal structure of RlmAI: implications for understanding the 23S rRNA G745/G748-methylation at the macrolide antibiotic-binding site. Proc Natl Acad Sci U S A *101*, 4041-4046.

Davanloo, P., Sprinzl, M., Watanabe, K., Albani, M., and Kersten, H. (1979). Role of ribothymidine in the thermal stability of transfer RNA as monitored by proton magnetic resonance. Nucleic Acids Res *6*, 1571-1581.

Decatur, W. A., and Fournier, M. J. (2002). rRNA modifications and ribosome function. Trends Biochem Sci *27*, 344-351.

Denoya, C. D., and Dubnau, D. (1987). Site and substrate specificity of the ermC 23S rRNA methyltransferase. J Bacteriol *169*, 3857-3860.

El Hage, A., Sbai, M., and Alix, J. H. (2001). The chaperonin GroEL and other heat-shock proteins, besides DnaK, participate in ribosome biogenesis in Escherichia coli. Mol Gen Genet *264*, 796-808.

Fauman, E. B., Blumenthal, R. M., Cheng, X. (1999). Structure and evolution of AdoMet-dependent methyltransferases (Singapore, World scientific).

Fersht, A. (2000). Structure and Mechanism in Protein Science, a Guide to Enzyme Catalysis and Protein Folding (New York, W. H. Freeman and Company).

Freude, K., Hoffmann, K., Jensen, L. R., Delatycki, M. B., des Portes, V., Moser, B., Hamel, B., van Bokhoven, H., Moraine, C., Fryns, J. P.*, et al.* (2004). Mutations in the FTSJ1 gene coding for a novel S-adenosylmethionine-binding protein cause nonsyndromic X-linked mental retardation. Am J Hum Genet *75*, 305-309.

Ghosh, J., Basu, A., Pal, S., Chowdhuri, S., Bhattacharya, A., Pal, D., Chattoraj, D. K., and DasGupta, C. (2003). Ribosome-DnaK interactions in relation to protein folding. Mol Microbiol *48*, 1679-1692.

Green, R., and Noller, H. F. (1996). In vitro complementation analysis localizes 23S rRNA posttranscriptional modifications that are required for Escherichia coli 50S ribosomal subunit assembly and function. Rna *2*, 1011-1021.

Gregory, S. T., and Dahlberg, A. E. (1999). Mutations in the conserved P loop perturb the conformation of two structural elements in the peptidyl transferase center of 23 S ribosomal RNA. J Mol Biol *285*, 1475-1483.

Gu, X., Ofengand, J., and Santi, D. V. (1994). In vitro methylation of Escherichia coli 16S rRNA by tRNA (m5U54)-methyltransferase. Biochemistry *33*, 2255-2261.

Gu, X. R., Gustafsson, C., Ku, J., Yu, M., and Santi, D. V. (1999). Identification of the 16S rRNA m5C967 methyltransferase from Escherichia coli. Biochemistry *38*, 4053-4057.

Gupta, A., Kumar, P. H., Dineshkumar, T. K., Varshney, U., and Subramanya, H. S. (2001). Crystal structure of Rv2118c: an AdoMet-dependent methyltransferase from Mycobacterium tuberculosis H37Rv. J Mol Biol *312*, 381-391.

Gustafsson, C., and Bjork, G. R. (1993). The tRNA-(m5U54)-methyltransferase of Escherichia coli is present in two forms in vivo, one of which is present as bound to tRNA and to a 3'-end fragment of 16 S rRNA. J Biol Chem *268*, 1326-1331.

Gustafsson, C., and Persson, B. C. (1998). Identification of the rrmA gene encoding the 23S rRNA m1G745 methyltransferase in Escherichia coli and characterization of an m1G745-deficient mutant. J Bacteriol *180*, 359-365.

Gutgsell, N. S., Del Campo, M. D., Raychaudhuri, S., and Ofengand, J. (2001). A second function for pseudouridine synthases: A point mutant of RluD unable to form pseudouridines 1911, 1915, and 1917 in Escherichia coli 23S ribosomal RNA restores normal growth to an RluD-minus strain. Rna *7*, 990-998.

Hage, A. E., and Alix, J. H. (2004). Authentic precursors to ribosomal subunits accumulate in Escherichia coli in the absence of functional DnaK chaperone. Mol Microbiol *51*, 189-201.

Hager, J. (2001) Mutational analysis of a heat shock inducible methyltransferase from *E. coli*, Universität Konstanz, Konstanz.

Hager, J., Staker, B. L., Bügl, H., and Jakob, U. (2002). Active site in RrmJ, a heat shock-induced methyltransferase. J Biol Chem *277*, 41978-41986.

Hager, J., Staker, B. L., and Jakob, U. (2004). Substrate binding analysis of the 23S rRNA methyltransferase RrmJ. J Bacteriol *186*, 6634-6642.

Hansen, L. H., Kirpekar, F., and Douthwaite, S. (2001). Recognition of nucleotide G745 in 23 S ribosomal RNA by the rrmA methyltransferase. J Mol Biol *310*, 1001-1010.

Hansen, M. A., Kirpekar, F., Ritterbusch, W., and Vester, B. (2002). Posttranscriptional modifications in the A-loop of 23S rRNAs from selected archaea and eubacteria. Rna *8*, 202-213.

Harms, J., Schluenzen, F., Zarivach, R., Bashan, A., Gat, S., Agmon, I., Bartels, H., Franceschi, F., and Yonath, A. (2001). High resolution structure of the large ribosomal subunit from a mesophilic eubacterium. Cell *107*, 679-688.

Hegazi, M. F., Borchard, R. T., and Schowen, R. L. (1976). Letter: SN2-like transition state for methyl transfer catalyzed by catechol-O-methyl-transferase. J Am Chem Soc *98*, 3048-3049.

Hoang, C., and Ferre-D'Amare, A. R. (2001). Cocrystal structure of a tRNA Psi55 pseudouridine synthase: nucleotide flipping by an RNA-modifying enzyme. Cell *107*, 929-939.

Hodel, A. E., Gershon, P. D., and Quiocho, F. A. (1998). Structural basis for sequence-nonspecific recognition of 5'-capped mRNA by a cap-modifying enzyme. Mol Cell *1*, 443-447.

Hodel, A. E., Gershon, P. D., Shi, X., and Quiocho, F. A. (1996). The 1.85 A structure of vaccinia protein VP39: a bifunctional enzyme that participates in the modification of both mRNA ends. Cell *85*, 247-256.

Hodel, A. E., Quiocho, F. A., Gershon, P. D. (1999). S-Adenosylmethionine-dependent Methyltransferases: Structure and Functions (Riveredge, N. J., World Scientific).

Holm, L., and Sander, C. (1997). Dali/FSSP classification of three-dimensional protein folds. Nucleic Acids Res *25*, 231-234.

Hu, G., Gershon, P. D., Hodel, A. E., and Quiocho, F. A. (1999). mRNA cap recognition: dominant role of enhanced stacking interactions between methylated bases and protein aromatic side chains. Proc Natl Acad Sci U S A *96*, 7149-7154.

Hu, G., Oguro, A., Li, C., Gershon, P. D., and Quiocho, F. A. (2002). The "cap-binding slot" of an mRNA cap-binding protein: quantitative effects of aromatic side chain choice in the double-stacking sandwich with cap. Biochemistry *41*, 7677-7687.

Inoue, K., Alsina, J., Chen, J., and Inouye, M. (2003). Suppression of defective ribosome assembly in a rbfA deletion mutant by overexpression of Era, an essential GTPase in Escherichia coli. Mol Microbiol *48*, 1005-1016.

Jeffery, D. R., and Roth, J. A. (1987). Kinetic reaction mechanism for magnesium binding to membrane-bound and soluble catechol O-methyltransferase. Biochemistry *26*, 2955-2958.

Kim, D. F., and Green, R. (1999). Base-pairing between 23S rRNA and tRNA in the ribosomal A site. Mol Cell *4*, 859-864.

Kinghorn, S. M., O'Byrne, C. P., Booth, I. R., and Stansfield, I. (2002). Physiological analysis of the role of truB in Escherichia coli: a role for tRNA modification in extreme temperature resistance. Microbiology *148*, 3511-3520.

Kintanar, A., Yue, D., and Horowitz, J. (1994). Effect of nucleoside modifications on the structure and thermal stability of Escherichia coli valine tRNA. Biochimie *76*, 1192-1204.

Klimasauskas, S., Kumar, S., Roberts, R. J., and Cheng, X. (1994). HhaI methyltransferase flips its target base out of the DNA helix. Cell *76*, 357-369.

Knippers, R. (1995). Molekulare Genetik (New York, Georg Thieme Verlag Stuttgart).

Korber, P., Stahl, J. M., Nierhaus, K. H., and Bardwell, J. C. (2000). Hsp15: a ribosome-associated heat shock protein. Embo J *19*, 741-748.

Kramer, G., Rauch, T., Rist, W., Vorderwulbecke, S., Patzelt, H., Schulze-Specking, A., Ban, N., Deuerling, E., and Bukau, B. (2002). L23 protein functions as a chaperone docking site on the ribosome. Nature *419*, 171-174.

Kunkel, T. A. (1985). Rapid and efficient site-specific mutagenesis without phenotypic selection. Proc Natl Acad Sci U S A *82*, 488-492.

Lacks, S., and Greenberg, B. (1975). A deoxyribonuclease of Diplococcus pneumoniae specific for methylated DNA. J Biol Chem *250*, 4060-4066.

Lafontaine, D. L., Preiss, T., and Tollervey, D. (1998). Yeast 18S rRNA dimethylase Dim1p: a quality control mechanism in ribosome synthesis? Mol Cell Biol *18*, 2360-2370.

Lapeyre, B., and Purushothaman, S. K. (2004). Spb1p-directed formation of Gm2922 in the ribosome catalytic center occurs at a late processing stage. Mol Cell *16*, 663-669.

Lebars, I., Yoshizawa, S., Stenholm, A. R., Guittet, E., Douthwaite, S., and Fourmy, D. (2003). Structure of 23S rRNA hairpin 35 and its interaction with the tylosin-resistance methyltransferase RlmAII. Embo J *22*, 183-192.

Lee, T. T., Agarwalla, S., and Stroud, R. M. (2004). Crystal structure of RumA, an iron-sulfur cluster containing E. coli ribosomal RNA 5-methyluridine methyltransferase. Structure (Camb) *12*, 397-407.

Li, C., Xia, Y., Gao, X., and Gershon, P. D. (2004). Mechanism of RNA 2'-O-methylation: evidence that the catalytic lysine acts to steer rather than deprotonate the target nucleophile. Biochemistry *43*, 5680-5687.

Liu, M., and Horowitz, J. (1994). Functional transfer RNAs with modifications in the 3'-CCA end: differential effects on aminoacylation and polypeptide synthesis. Proc Natl Acad Sci U S A *91*, 10389-10393.

Liu, M., Kirpekar, F., Van Wezel, G. P., and Douthwaite, S. (2000). The tylosin resistance gene tlrB of Streptomyces fradiae encodes a methyltransferase that targets G748 in 23S rRNA. Mol Microbiol *37*, 811-820.

Liu, M., Novotny, G. W., and Douthwaite, S. (2004). Methylation of 23S rRNA nucleotide G745 is a secondary function of the RlmAI methyltransferase. Rna *10*, 1713-1720.

Lotta, T., Vidgren, J., Tilgmann, C., Ulmanen, I., Melen, K., Julkunen, I., and Taskinen, J. (1995). Kinetics of human soluble and membrane-bound catechol O-methyltransferase: a revised mechanism and description of the thermolabile variant of the enzyme. Biochemistry *34*, 4202-4210.

Lovgren, J. M., Bylund, G. O., Srivastava, M. K., Lundberg, L. A., Persson, O. P., Wingsle, G., and Wikstrom, P. M. (2004). The PRC-barrel domain of the ribosome maturation protein RimM mediates binding to ribosomal protein S19 in the 30S ribosomal subunits. Rna *10*, 1798-1812.

Lovgren, J. M., and Wikstrom, P. M. (2001). The rlmB gene is essential for formation of Gm2251 in 23S rRNA but not for ribosome maturation in Escherichia coli. J Bacteriol *183*, 6957-6960.

Madsen, C. T., Mengel-Jorgensen, J., Kirpekar, F., and Douthwaite, S. (2003). Identifying the methyltransferases for m(5)U747 and m(5)U1939 in 23S rRNA using MALDI mass spectrometry. Nucleic Acids Res *31*, 4738-4746.

Maravic, G., Bujnicki, J. M., Feder, M., Pongor, S., and Flogel, M. (2003). Alanine-scanning mutagenesis of the predicted rRNA-binding domain of ErmC' redefines the substrate-binding site and suggests a model for protein-RNA interactions. Nucleic Acids Res *31*, 4941-4949.

Martz, E. (2002). Protein Explorer: easy yet powerful macromolecular visualization. Trends Biochem Sci *27*, 107-109.

Massenet, S., Motorin, Y., Lafontaine, D. L., Hurt, E. C., Grosjean, H., and Branlant, C. (1999). Pseudouridine mapping in the Saccharomyces cerevisiae spliceosomal U small nuclear RNAs (snRNAs) reveals that pseudouridine synthase pus1p exhibits a dual substrate specificity for U2 snRNA and tRNA. Mol Cell Biol *19*, 2142-2154.

McRee, D. F. (1993). Practical Protein Crystallography (San Diego, CA, Academic Press).
Michel, G., Sauve, V., Larocque, R., Li, Y., Matte, A., and Cygler, M. (2002). The structure of the RlmB 23S rRNA methyltransferase reveals a new methyltransferase fold with a unique knot. Structure (Camb) *10*, 1303-1315.

Nierhaus, K. H. (1991). The assembly of prokaryotic ribosomes. Biochimie *73*, 739-755.
O'Connor, M., and Dahlberg, A. E. (1995). The involvement of two distinct regions of 23 S ribosomal RNA in tRNA selection. J Mol Biol *254*, 838-847.

Ovaska, M., and Yliniemela, A. (1998). A semiempirical study on inhibition of catechol O-methyltransferase by substituted catechols. J Comput Aided Mol Des *12*, 301-307.

Pintard, L., Bujnicki, J. M., Lapeyre, B., and Bonnerot, C. (2002a). MRM2 encodes a novel yeast mitochondrial 21S rRNA methyltransferase. Embo J *21*, 1139-1147.

Pintard, L., Kressler, D., and Lapeyre, B. (2000). Spb1p is a yeast nucleolar protein associated with Nop1p and Nop58p that is able to bind S-adenosyl-L-methionine in vitro. Mol Cell Biol *20*, 1370-1381.

Pintard, L., Lecointe, F., Bujnicki, J. M., Bonnerot, C., Grosjean, H., and Lapeyre, B. (2002b). Trm7p catalyses the formation of two 2'-O-methylriboses in yeast tRNA anticodon loop. Embo J *21*, 1811-1820.

Poldermans, B., Roza, L., and Van Knippenberg, P. H. (1979). Studies on the function of two adjacent N6,N6-dimethyladenosines near the 3' end of 16 S ribosomal RNA of Escherichia coli. III. Purification and properties of the methylating enzyme and methylase-30 S interactions. J Biol Chem *254*, 9094-9100.

Porse, B. T., and Garrett, R. A. (1995). Mapping important nucleotides in the peptidyl transferase centre of 23 S rRNA using a random mutagenesis approach. J Mol Biol *249*, 1-10.

Ramser, J., Winnepenninckx, B., Lenski, C., Errijgers, V., Platzer, M., Schwartz, C. E., Meindl, A., and Kooy, R. F. (2004). A splice site mutation in the methyltransferase gene FTSJ1 in Xp11.23 is associated with non-syndromic mental retardation in a large Belgian family (MRX9). J Med Genet *41*, 679-683.

Richmond, C. S., Glasner, J. D., Mau, R., Jin, H., and Blattner, F. R. (1999). Genome-wide expression profiling in Escherichia coli K-12. Nucleic Acids Res *27*, 3821-3835.

Rozenski, J., Crain, P. F., and McCloskey, J. A. (1999). The RNA Modification Database: 1999 update. Nucleic Acids Res *27*, 196-197.

Sambrook, J., Fritsch, E. F., Maniatis, T. (1989). Molecular Cloning - A Laboratory Manual., Cold Spring Habor Laboratory Press).

Sanger, F., Nicklen, S., and Coulson, A. R. (1992). DNA sequencing with chain-terminating inhibitors. 1977. Biotechnology *24*, 104-108.

Sayed, A., Matsuyama, S., and Inouye, M. (1999). Era, an essential Escherichia coli small G-protein, binds to the 30S ribosomal subunit. Biochem Biophys Res Commun *264*, 51-54.

Schluckebier, G., Kozak, M., Bleimling, N., Weinhold, E., and Saenger, W. (1997). Differential binding of S-adenosylmethionine S-adenosylhomocysteine and Sinefungin to the adenine-specific DNA methyltransferase M.TaqI. J Mol Biol *265*, 56-67.

Schluckebier, G., Zhong, P., Stewart, K. D., Kavanaugh, T. J., and Abad-Zapatero, C. (1999). The 2.2 A structure of the rRNA methyltransferase ErmC' and its complexes with cofactor and cofactor analogs: implications for the reaction mechanism. J Mol Biol *289*, 277-291.

Schnierle, B. S., Gershon, P. D., and Moss, B. (1992). Cap-specific mRNA (nucleoside-O2'-)-methyltransferase and poly(A) polymerase stimulatory activities of vaccinia virus are mediated by a single protein. Proc Natl Acad Sci U S A *89*, 2897-2901.

Schnierle, B. S., Gershon, P. D., and Moss, B. (1994). Mutational analysis of a multifunctional protein, with mRNA 5' cap-specific (nucleoside-2'-O-)-methyltransferase and 3'-adenylyltransferase stimulatory activities, encoded by vaccinia virus. J Biol Chem *269*, 20700-20706.

Sharp, P. A., Sugden, B., and Sambrook, J. (1973). Detection of two restriction endonuclease activities in Haemophilus parainfluenzae using analytical agarose--ethidium bromide electrophoresis. Biochemistry *12*, 3055-3063.

Silhavy, T. J., Berman, M. L., Enquist, L. W. (1984). Experiments with gene fusions, Cold Spring Habor Laboratory Press).

Sirum-Connolly, K., and Mason, T. L. (1993). Functional requirement of a site-specific ribose methylation in ribosomal RNA. Science *262*, 1886-1889.

Sirum-Connolly, K., Peltier, J. M., Crain, P. F., McCloskey, J. A., and Mason, T. L. (1995). Implications of a functional large ribosomal RNA with only three modified nucleotides. Biochimie *77*, 30-39.

Skinner, R., Cundliffe, E., and Schmidt, F. J. (1983). Site of action of a ribosomal RNA methylase responsible for resistance to erythromycin and other antibiotics. J Biol Chem *258*, 12702-12706.

Spedding, G. (1990). Isolation and analysis of ribosomes from procaryotes, eucaryotes, and organelles (New York, Oxford University Press).

Sprinzl, M., and Vassilenko, K. S. (2005). Compilation of tRNA sequences and sequences of tRNA genes. Nucleic Acids Res *33*, D139-140.

Staker, B. L. (2000) X-ray crystallographic studiies of three nucleic acid binding protins., University of Michigan, Ann Arbor.

Sugimoto, M., Esaki, N., Tanaka, H., and Soda, K. (1989). A simple and efficient method for the oligonucleotide-directed mutagenesis using plasmid DNA template and phosphorothioate-modified nucleotide. Anal Biochem *179*, 309-311.

Tan, J., Jakob, U., and Bardwell, J. C. (2002). Overexpression of two different GTPases rescues a null mutation in a heat-induced rRNA methyltransferase. J Bacteriol *184*, 2692-2698.

Taylor, J. W., Ott, J., and Eckstein, F. (1985). The rapid generation of oligonucleotide-directed mutations at high frequency using phosphorothioate-modified DNA. Nucleic Acids Res *13*, 8765-8785.

Tollervey, D., Lehtonen, H., Carmo-Fonseca, M., and Hurt, E. C. (1991). The small nucleolar RNP protein NOP1 (fibrillarin) is required for pre-rRNA processing in yeast. Embo J *10*, 573-583.

Tollervey, D., Lehtonen, H., Jansen, R., Kern, H., and Hurt, E. C. (1993). Temperature-sensitive
mutations demonstrate roles for yeast fibrillarin in pre-rRNA processing, pre-rRNA methylation, and ribosome assembly. Cell *72*, 443-457.

Tscherne, J. S., Nurse, K., Popienick, P., Michel, H., Sochacki, M., and Ofengand, J. (1999). Purification, cloning, and characterization of the 16S RNA m5C967 methyltransferase from Escherichia coli. Biochemistry *38*, 1884-1892.

VanBogelen, R. A., Abshire, K. Z., Moldover, B., Olson, E. R., and Neidhardt, F. C. (1997). Escherichia coli proteome analysis using the gene-protein database. Electrophoresis *18*, 1243-1251.

Vandeyar, M. A., Weiner, M. P., Hutton, C. J., and Batt, C. A. (1988). A simple and rapid method for the selection of oligodeoxynucleotide-directed mutants. Gene *65*, 129-133.

Vidgren, J., Ovaska, M., Tenhunen, J., Tilgmann, C., Lotta, T., and Maennistoe, P. T. (1999). S-Adenosylmethionine-dependent Methyltransferases: Structure and Functions (Riveredge, N. J., World Scientific).

Vidgren, J., Svensson, L. A., and Liljas, A. (1994). Crystal structure of catechol O-methyltransferase. Nature *368*, 354-358.

Wang, H., Boisvert, D., Kim, K. K., Kim, R., and Kim, S. H. (2000). Crystal structure of a fibrillarin homologue from Methanococcus jannaschii, a hyperthermophile, at 1.6 A resolution. Embo J *19*, 317-323.

Weitzmann, C., Tumminia, S. J., Boublik, M., and Ofengand, J. (1991). A paradigm for local conformational control of function in the ribosome: binding of ribosomal protein S19 to Escherichia coli 16S rRNA in the presence of S7 is required for methylation of m2G966 and blocks methylation of m5C967 by their respective methyltransferases. Nucleic Acids Res *19*, 7089-7095.

Widerak, M., Kern, R., Malki, A., and Richarme, G. (2005). U2552 methylation at the ribosomal A-site is a negative modulator of translational accuracy. Gene.

Williamson, J. R. (2003). After the ribosome structures: how are the subunits assembled? Rna *9*, 165-167.

Wout, P., Pu, K., Sullivan, S. M., Reese, V., Zhou, S., Lin, B., and Maddock, J. R. (2004). The Escherichia coli GTPase CgtAE cofractionates with the 50S ribosomal subunit and interacts with SpoT, a ppGpp synthetase/hydrolase. J Bacteriol *186*, 5249-5257.

Wower, I. K., Wower, J., and Zimmermann, R. A. (1998). Ribosomal protein L27 participates in both 50 S subunit assembly and the peptidyl transferase reaction. J Biol Chem *273*, 19847-19852.

Wrzesinski, J., Nurse, K., Bakin, A., Lane, B. G., and Ofengand, J. (1995). A dual-specificity pseudouridine synthase: an Escherichia coli synthase purified and cloned on the basis of its specificity for psi 746 in 23S RNA is also specific for psi 32 in tRNA(phe). Rna *1*, 437-448.

Yu, L., Petros, A. M., Schnuchel, A., Zhong, P., Severin, J. M., Walter, K., Holzman, T. F., and Fesik, S. W. (1997). Solution structure of an rRNA methyltransferase (ErmAM) that confers macrolide-lincosamide-streptogramin antibiotic resistance. Nat Struct Biol *4*, 483-489.

6 Acknowledgement

My time in Ann Arbor at the University of Michigan has been of great value to me. I have learned a lot – not only in and for the lab but also for life in general.

I would like to thank all the people who made this experience possible for me.

I would like to thank my “Doktorvater” Prof. Hans-Werner Hofer very much for supporting me in doing the research for my PhD thesis at the University of Michigan. Without him, I could never have started this adventure in the first place. We had mostly stayed in email contact during those years, and it always seemed to me that it was equally important to him to be filled in on the progress of my research as well as to hear that I am doing fine.

Especially I would like to thank Prof. Ursula Jakob who invited me to stay in Ann Arbor after my diploma thesis and to continue working on the RrmJ project in her lab. Besides being an exceptionally good supervisor, continuously pushing me to do things I do not like to do and helping me to get better at those, Ursula also grew to be a very good friend outside the lab and a confidant I could talk to. I owe her very much!

I certainly would like to thank all the lab members of the Jakob lab for a great time, especially Jörg Hoffmann and Paul Graf as well as my bench neighbor Katrin Linke who were in Ann Arbor almost the whole time I was there and who are, therefore, associated with many fond memories. I would also like to thank Dr. Jeannette Winter and Lars Leichert for answering my many questions. Furthermore, I would like to thank Prof. James Bardwell as well as his lab members for their help and support. Both, the Jakob and Bardwell labs work very closely together, and I would like to thank Jim and Ursula for creating a great working environment and fun atmosphere.

Moreover, I was very happy when Caroline Kumsta joined our lab and decided she wanted to work on RrmJ as the subject of her diploma thesis. With her decision, I was not left alone anymore with the RrmJ project, which was quite different from the main interest of the lab. It was certainly good to have someone to talk to when either excited about recent results or discouraged due to technical problems and unexpected outcomes of experiments. I also would like to thank her for making the nice figure showing the model of RrmJ’s various functions in the cell.

I would like to thank the lab managers Tina Kelley, Aaron Kleinjans and Christie Parish as well as all the ‘work studies’ for their tremendous help.

I would like to thank Bart Staker very much for his modeling studies and all the beautiful figures of RrmJ’s substrate binding site.

I am very grateful for the time I have been able to spend with my boyfriend Everett, who not only introduced me to the joy of following sports as well as encouraged me to become a runner. Much more important, he helped me to open my mind to the world around me, which was, at times, a rather painful and slow process.

I would like to thank my parents very much for supporting me in every way possible during all those years even though they longed for me to come back home. I am also very happy about the time we were able to spend together here in Ann Arbor and its surroundings.

I would like to thank my friends Anja and Wencke as well as my sister Britta, who always encouraged me with emails or packages when I was feeling down and who visited me in Ann Arbor as well. I also would like to thank my friend Kerstin who was my last and faithful link to the University of Konstanz for her help.

The time in Ann Arbor has been exceptional for me and although the future is still uncertain, I am sure my experiences will help me to get through many challenges.
Recent occurrence had made it clear to me how important it is to not take things for granted and to live intensively. Being worried too much as well as putting things off is a waste of valuable time. Therefore, I will end my “story” with a quote by Bert Brecht: „Stell die Milch auf den Tisch, aber schlag kein Buch zu.” (Brecht, 1938).

7 Publications

Most of this work has been published in the following papers:

Hager, J., Staker, B. L., Bügl, H., and Jakob, U. (2002) Active site in RrmJ, a heat shock induced methyltransferase. *J. Biol. Chem.* **277**:41978-41986.

Hager, J., Staker, B. L., and Jakob, U. (2004) Substrate binding analysis of the 23S rRNA methyltransferase RrmJ. *J. Bacteriol.* **186**(19): 6634-6642.

Hager, J., Kumsta C., and Jakob, U. (2005) The RNA methyltransferase RrmJ - A ribosome assembly helper protein. *manuscript in preparation.*

THE JOURNAL OF BIOLOGICAL CHEMISTRY
Vol. 277, No. 44, Issue of November 1, pp. 41978–41986, 2002

Printed in U.S.A.

Active Site in RrmJ, a Heat Shock-induced Methyltransferase*

Received for publication, May 31, 2002, and in revised form, July 11, 2002
Published, JBC Papers in Press, August 13, 2002, DOI 10.1074/jbc.M205423200

Jutta Hager‡, Bart L. Staker§, Hans Bügl‡, and Ursula Jakob‡¶

From the ‡Department of Molecular, Cellular and Developmental Biology, University of Michigan, Ann Arbor, Michigan 48109-1048 and §Emerald BioStructures Inc., West Bainbridge Island, Washington 98110

The heat shock protein RrmJ (FtsJ), highly conserved from eubacteria to eukarya, is responsible for the 2′-*O*-ribose methylation of the universally conserved base U2552 in the A-loop of the 23 S rRNA. Absence of this methylation, which occurs late in the maturation process of the ribosome, appears to cause the destabilization and premature dissociation of the 50 S ribosomal subunit. To understand the mechanism of 2′-*O*-ribose methyltransfer reactions, we characterized the enzymatic parameters of RrmJ and conducted site-specific mutagenesis of RrmJ. A structure based sequence alignment with VP39, a structurally related 2′-*O*-methyltransferase from vaccinia virus, guided our mutagenesis studies. We analyzed the function of our RrmJ mutants *in vivo* and characterized the methyltransfer reaction of the purified proteins *in vitro*. The active site of RrmJ appears to be formed by a catalytic triad consisting of two lysine residues, Lys-38 and Lys-164, and the negatively charged residue Asp-124. Another highly conserved residue, Glu-199, that is present in the active site of RrmJ and VP39 appears to play only a minor role in the methyltransfer reaction *in vivo*. Based on these results, a reaction mechanism for the methyltransfer activity of RrmJ is proposed.

RrmJ (FtsJ) is a well conserved heat shock protein present in prokaryotes, archaea, and eukaryotes (1). Functional studies revealed that RrmJ is responsible for methylating 23 S rRNA at position U2552 in the aminoacyl (A)[1]-site of the ribosome (1, 2). U2552 is one of the five universally conserved A-loop residues and has been shown to be methylated at the ribose 2′-OH group in the majority of organisms investigated so far (3). This suggests that this modification plays an important role in the A-loop function. Analysis of *rrmJ* deletion mutants in *Escherichia coli* supports this view, because these cells show a severe growth disadvantage and ribosome defects (1, 4). Polysome profiles of *rrmJ* deletion strains prepared under non-stringent salt conditions reveal the accumulation of 30 S and 50 S ribosomal subunits at the expense of functional 70 S ribosomes (1, 4). In addition, lower $MgCl_2$ concentrations in the lysate buffer cause the accumulation of 40 S ribosomal particles and a concomitant reduction in 50 S ribosomal subunits (1). This ribosomal defect is also reflected in the significantly decreased translational efficiency of S_{30} extracts prepared from *rrmJ* deletion strains (4). Interestingly, the absence of Mrm2p, the mitochondrial RrmJ homologue that has recently been identified to modify the corresponding U2791 in 21 S rRNA does not cause a mitochondrial ribosome assembly or stability defect (5). Yeast mitochondria in the absence of Mrm2p do, however, reveal instability of their genome, a feature that is often associated with defects in mitochondrial translation (5). All these observations point to an important role of RrmJ in ribosome biology, and the simplest interpretation of these results is that the ribosome defect that is observed in *rrmJ* deletion strains is directly caused by the absence of the Um2552 modification in 23 S rRNA. It also is possible, however, that RrmJ has a second methyltransferase-independent function. Such dual function modes for methyltransferases have been observed in the past. For instance, Pet56p, the methyltransferase that is responsible for methylating the other universally conserved residue in mitochondrial 21 S rRNA, has been shown to be essential for the *in vivo* maturation of the large ribosomal subunit in mitochondria (3). This phenotype, however, seems to be independent of the methylation activity of Pet56p, because *S*-adenosylmethionine (AdoMet) binding mutants of Pet56p, which completely eliminate methyltransferase activity, still support ribosome assembly *in vivo* (6).

In vitro methylation assays have revealed that RrmJ recognizes its methylation target only when the 23 S rRNA is present in 50 S ribosomal subunits (1, 2). This has been confirmed in studies revealing that Mrm2p modifies mitochondrial 21 S rRNA only when assembled with proteins of the large subunit (5). This suggests that the RrmJ-mediated methylation must occur late in the maturation process of the ribosome (1). This is in contrast to other known 23 S rRNA modifications that occur in earlier maturation steps (7).

The reaction mechanism of 2′-*O*-ribose methyltransferases such as RrmJ has not been analyzed experimentally. We have crystallized RrmJ in the presence of its AdoMet cofactor and have solved the structure of the RrmJ·AdoMet complex to a 1.5-Å resolution (1). Comparison of the structure of RrmJ with structures of other methyltransferases revealed homology to 1FBN, the fibrillarin homologue from *Methanococcus jannaschii* (8), catechol-*O*-methyltransferase (COMT) (9), and vaccinia mRNA 2′-*O*-methyltransferase VP39 (10). VP39, in particular, shows a highly homologous core domain and an RNA binding groove that shares numerous features with RrmJ (1). These structural and sequence comparisons have allowed us and others (11) to predict which residues in RrmJ might be directly involved in the methyltransfer reaction and to postulate a reaction mechanism.

Here, we have prepared a number of site-specific mutants of RrmJ to investigate which residues participate in catalysis. We have conducted phenotypical studies and enzymatic analyzes to characterize the activity of our mutants *in vivo* and *in vitro*. We have identified two lysine and one aspartate residues that are important for catalyzing the methyltransfer reaction; RrmJ mutants at these positions show a significant decrease in meth-

* This work was supported in part by the Burroughs Wellcome Fund Career Award (to U. J.). The costs of publication of this article were defrayed in part by the payment of page charges. This article must therefore be hereby marked "*advertisement*" in accordance with 18 U.S.C. Section 1734 solely to indicate this fact.

¶ To whom correspondence should be addressed. Tel.: 734-615-1286; Fax: 734-647-0884; E-mail: ujakob@umich.edu.

[1] The abbreviations used are: A, aminoacyl; AdoMet, *S*-adenosylmethionine; COMT, catechol-*O*-methyltransferase; WT, wild type; 2D, two-dimensional.

TABLE I
Strains and plasmids used in this study

Strains	Genotype	Source
MG1655	*rph-1*	Lab collection
HB24	MG1655; *zgi*-203::Tn*10*,-TC^R	(1)
HB23	MG1655, *zgi*-203::Tn*10*,TC^R, *rrmJΔ567*	(1)
HB25	HB23, pHB1	(1)
HB1	BL21 (DE3), pHB1	(1)
BL21 (DE3)	F$^-$ *ompT hsdS*$_B^-$ ($r_B^-m_B^-$) *gal dcm* (DE3)	Novagene
JUH47	BL21 (DE3), *rrmJΔ567*; Tc^R	BL21 × P1 (HB23)
Plasmids	**Relevant features**	**Source**
pET11a	pBR322-derived	Novagene
pHB1	pET11a/*rrmJ*	(1)
pJUH12	pET11a/*rrmJ* K38A	This study
pJUH18	pET11a/*rrmJ* D83A	This study
pJUH8	pET11a/*rrmJ* D124A	This study
pJUH21	pET11a/*rrmJ* K164A	This study
pJUH13	pET11a/*rrmJ* E199A	This study
pJUH11	pET11a/*rrmJ* Y201A	This study

yltransferase activity. These mutants allowed us to demonstrate that both the ribosome and growth defects observed in *rrmJ* deletion mutants are dependent on the methyltransfer activity of RrmJ.

EXPERIMENTAL PROCEDURES

Site-directed Mutagenesis—Site-directed mutagenesis was performed according to the QuickChange protocol (Stratagene, La Jolla, CA). Wild type *rrmJ* cloned into pET11a (pHB1) (1) was used as template DNA to generate the mutations. The primers used in this study were as follows: K38A, CGTTCCCGTGCCTGGTTTGCACTTGATGAAATACAGCAAAG; D83A, CCGCATCATCGCTTGCGCTCTTCTACCTATGGATCC; D124A, CAGGTTGTCATGTCCGCTATGGCCCCAAACATGAGCGG; K164A, GGTGGCAGTTTTGTAGTGGCGGTGTTCCAGGGCG; E199A, GACTCTTCTCGTGCACGTTCCCGGGCAGTGTATATTGTAGCG; Y201A, CGTGCACGTTCCCGGGAAGTGGCTATTGTAGCGACCGGG. All introduced mutations were confirmed by DNA sequencing. The plasmids that were generated and the strains that were used in this study are listed in Table I. For overexpression and purification of the mutant proteins, the plasmids that contained the mutated *rrmJ* genes were introduced into JUH47. This strain contained a deletion of the *rrmJ* gene to prevent the contamination of our purified mutant proteins by small amounts of WT protein. JUH47 was constructed by P1 transduction. The Tc^R of the Tn10 marker that is 90% linked to *rrmΔJ567* (1) was used to transfer the *rrmJΔ567* allele into BL21. We then selected for tet^R and screened for the slow growth phenotype observed in *rrmJ* deletion strains (1).

Expression Analysis—To investigate the expression level of wild type RrmJ in HB24 and of the mutant proteins in the transformed HB23 (*rrmΔJ567*) strains, Western blot analysis using polyclonal antibodies against RrmJ was performed. The transformed strains were grown in LB medium supplemented with 100 μg/ml ampicillin until an A_{600} of 0.5 was reached. Then, a 2-ml aliquot of cells was taken, resuspended in 85 μl of 2× SDS-Laemmli buffer, and boiled for 20 min. The proteins were separated on a 14% Tris-glycine PAGE (NOVEX), and RrmJ was visualized using Western blot analysis. To investigate whether the RrmJ mutant proteins are expressed in a soluble form in HB23 cells, cell lysates were prepared (see below), and the presence of RrmJ in the soluble supernatant was determined with Western blot analysis.

2D Gel Analysis—2D gel analysis of the protein composition of 50 S ribosomal subunits of HB24 (WT) and of 50 S and 40 S ribosomal particles of HB23 (*rrmΔJ567*) was performed according to Geyl *et al.* (12). The 40 S and 50 S ribosomal subunits were prepared as described previously (1).

Analytical Polysome Profiles—Analytical polysome profiles of the wild type strain HB24, the *rrmJ* deletion strain HB23, and HB23 expressing the individual *rrmJ* mutants were obtained by sucrose gradient centrifugation of the lysates under dissociating salt conditions (50 mM HEPES/KOH, pH 7.5, 200 mM NH_4Cl, 1 mM $MgCl_2$, 2 mM β-mercaptoethanol). The profiles were analyzed as described (1).

Purification of the RrmJ Mutants—The purification of the RrmJ mutants was performed according to Bügl *et al.* (1). Slight modifications were applied to optimize the purification protocol. JUH47 strains containing the *rrmJ* mutant plasmids were grown in 1 liter of LB medium containing 100 μg/ml ampicillin to an A_{600} = 0.7 at 37 °C. Induction of protein expression and cell lysis was performed as described (1). The lysis buffer was 40 mM HEPES/KOH, 150 mM KCl, pH 8.0, 1 mM dithiothreitol, 2% (v/v) glycerol. To purify the RrmJ mutant proteins, a tandem 5-ml HiTrap™ Q-Sepharose™ (Amersham Biosciences) connected to a 5-ml HiTrap™ SP-Sepharose™ (Amersham Biosciences) column was used. The cell lysate was applied (flow rate of 4 ml/min), and after washing the column with lysis buffer the proteins were eluted by applying a linear 300-ml gradient from 150 to 600 mM KCl in lysis buffer. The fractions were analyzed by SDS-PAGE, and the RrmJ-containing fractions were pooled and concentrated. The purity of the proteins was greater than 95%. The buffer was exchanged to RrmJ storage buffer (40 mM HEPES/KOH, pH 7.5, 150 mM KCl, 2% (v/v) glycerol, 1 mM dithiothreitol). The protein concentration was determined by UV absorbance using an extinction coefficient of 1.00 for a 1 mg/ml solution at A_{280} (1). Protein concentration determination was not significantly influenced by the presence of the absorbing cofactor AdoMet in the preparation. This was confirmed by performing a Bradford assay, using the AdoMet-free D83A mutant RrmJ protein as a standard protein (data not shown).

AdoMet Titration—To determine the amount of AdoMet present in the various RrmJ mutant preparations, we first generated an AdoMet titration curve. A 23 μM solution of our AdoMet-free D83A mutant RrmJ protein was prepared, and 1 μM AdoMet (ϵ_{257} = 15,400 M^{-1} cm^{-1}) was added per titration step. After each AdoMet addition, the A_{280}/A_{260} ratio of the protein/AdoMet mixture was determined. After volume correction, this ratio was plotted against the amount of titrated AdoMet. Then, the A_{280}/A_{260} ratio of the purified RrmJ mutants was determined, and the amount of bound AdoMet was calculated.

Preparation of Ribosomal Subunits and Methylation Assay—50 S ribosomal subunits of HB23 (*rrmΔJ567*) were prepared as described previously (1). Re-analysis of purified 50 S subunits on sucrose gradients revealed that the preparation is >98% pure. These subunits served as *in vitro* substrates for wild type RrmJ and the mutant proteins in the methylation assay (1). The RrmJ concentrations used in this assay were 20, 100, or 200 nM in 50 mM HEPES/KOH, pH 7.5, 85 mM NH_4Cl, 3 mM $MgCl_2$, 2 mM β-mercaptoethanol. The initial rate for methylation was measured in the presence of 5 μM 50 S ribosomal subunits and increasing amounts of radioactive [^{3}H]*S*-adenosyl-L-methionine (85.0 Ci/mmol; Amersham Biosciences). To determine the apparent K_m for 50 S ribosomal subunits, the methylation assay was performed in the presence of 50 μM AdoMet and varying concentrations of 50 S ribosomal subunits. To determine the specific activity of wild type RrmJ and the mutant proteins, the assay was carried out using 100 and 200 nM RrmJ mutant protein, 50 μM AdoMet, and either 5 or 8 μM 50 S ribosomal subunits, depending on the RrmJ mutant. The methylation reaction was performed at 37 °C. At defined time points (2.5, 5, 7.5, and 10 min) after initiating the methylation reaction, 8-μl aliquots were taken, and the [^{3}H]methyl incorporation into 23 S rRNA was determined as described (1). The slopes of the methyl incorporation *versus* time plots were calculated, and the initial velocities obtained were plotted against the respective substrate concentration. The curve was then fitted using a single rectangular hyperbola.

RESULTS

Enzymatic Characterization of RrmJ—To analyze the influence of our amino acid substitutions on the methyltransfer activity of RrmJ, we first needed to characterize the enzymatic properties of wild type RrmJ. The apparent V_{max} of the methyltransfer reaction, as well as the apparent K_m values for 50 S ribosomal subunits and AdoMet, were determined by *in vitro* methylation assays using purified RrmJ and radioactively labeled AdoMet. 50 S ribosomal subunits were prepared from the *rrmJ* deletion strain HB23, because their 23 S rRNA lacks the U2552 methylation catalyzed by RrmJ. We first established assay conditions (see "Experimental Procedures") in which the rate of [^{3}H]methyl incorporation from [^{3}H]AdoMet into 23 S rRNA was proportional to the RrmJ concentration and linear over more than 150 min (data not shown). Thus, the initial rate measurements represented true initial velocities, and the dependence of the rate on substrate concentration could be measured. Initial velocity data were first obtained with a fixed high concentration of AdoMet (50 μM) and varying concentrations of 50 S ribosomal subunits. The apparent K_m value for 23 S rRNA within 50 S ribosomal subunits was determined to be 0.8 + 0.1 μM with an apparent K_{cat} of 0.064 min^{-1} at 37 °C (Fig. 1*A*). This is a significantly higher K_m value than the one determined for the mRNA in VP39 (K_m = 5 nM) (13) but very similar to the K_m value determined for the 23 S rRNA methyltransferase ErmC′ from *Bacillus subtilis*. ErmC′ has been shown to dimethylate adenine 2058 (*E. coli* numbering) in naked 23 S rRNA, early in the ribosomal maturation process (13, 14). To determine the apparent K_m value for AdoMet, the 50 S ribosomal subunits were kept at saturating concentrations (5 μM), and AdoMet was varied (Fig. 1*A*, *inset*). The initial velocity experiments revealed an apparent K_m for AdoMet of 3.7 + 0.3 μM and the same K_{cat} of 0.064 min^{-1}. From these results it became clear that RrmJ and the 2′-*O*-ribose methyltransferase VP39 do not only share a very similar K_m for AdoMet, which is 2 μM for VP39 (13), but also a similarly low turnover number. The K_{cat} for VP39 has only very recently been determined to be 0.13 min^{-1} (15). As is the case for VP39, the RrmJ catalyzed reaction was linear over more than 150 min and, therefore, through more than 10 turnovers (data not shown). This excluded the possibility that the low K_{cat} observed for RrmJ is because of problems to multiple turnovers but may be because of slow chemical steps (15) or because of accessibility problems of the methylation site in the intact 50 S ribosomal subunits that are used in our *in vitro* studies (see below). Because of this low turnover number, however, our initial rate measurements that were followed over a 10-min time period need to be considered pre-steady state measurements rather than steady-state measurements.

RrmJ Is a Thermostable Heat Shock Protein—We considered that one possible reason for the heat shock induction of RrmJ could be a possible temperature lability of the enzyme. This would require the overexpression of RrmJ at heat shock temperatures to compensate for the potential loss of function. For this reason, we measured the activity of RrmJ under saturating substrate concentrations over a variety of temperatures (Fig. 1*B*). We found that the temperature optimum of the methyltransferase activity of RrmJ was at 55 °C. The decreased activity at temperatures beyond 55 °C is either because of instability of the 50 S ribosomal subunits or because of thermal inactivation of RrmJ. In either case, these results excluded the possibility that the heat shock regulation of RrmJ is based on thermal lability of the enzyme.

The Substrate of RrmJ—RrmJ is able to methylate 23 S rRNA in isolated 50 S ribosomal subunits, as well as in 70 S ribosomes (1, 2), but is unable to methylate naked 23 S rRNA

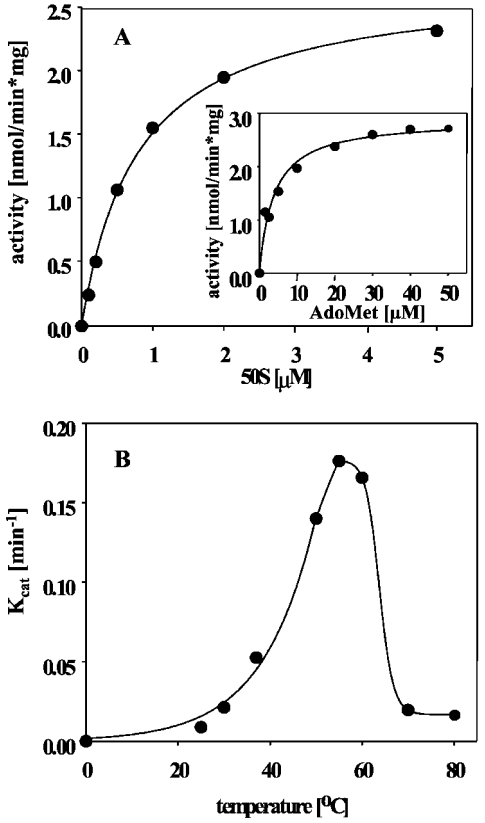

FIG. 1. **Characterization of the 2′-*O*-ribose methyltransferase RrmJ.** *A*, kinetic analysis of wild type RrmJ. The initial rate for methylation was measured in the presence of 20 nM purified RrmJ, 50 μM AdoMet (200 μC/ml), and increasing concentrations of 50 S ribosomal subunits prepared from the *rrmJ* deletion strain HB23 in 50 mM HEPES/KOH, pH 7.5, 85 mM NH_4Cl, 3 mM $MgCl_2$, 2 mM β-mercaptoethanol. *Inset*, the initial rate for catalysis of ribosome methylation was determined in the presence of saturating concentrations of 50 S ribosomal subunits (5 μM) and increasing concentrations of AdoMet in the presence of 20 nM RrmJ. At defined time points of the incubation reaction at 37 °C, aliquots were removed, and the incorporation of radioactivity due to methylation of 23 S rRNA of the 50 S subunit was determined as described (1). From fitting the Michaelis-Menten equation to the data, an apparent K_m of 0.8 + 0.1 μM was determined for 50 S ribosomal subunits. The apparent K_m for AdoMet was found to be 3.7 + 0.3 μM. The apparent K_{cat} of RrmJ under conditions of substrate saturation was found to be 0.064 min^{-1}. *B*, temperature optimum of the methyltransfer reaction of RrmJ. Wild type RrmJ (100 nM) was incubated with 5 μM 50 S ribosomal subunits and 50 μM AdoMet (200 μC/ml) at temperatures ranging from 25 to 80 °C. The initial rate of the methyl incorporation was determined as described above and was plotted against the temperature. The temperature optimum under these conditions was found to be 55 °C.

or 23 S rRNA that is present in 40 S ribosomal particles that have been shown to accumulate in cell lysates of *rrmJ* deletion strains under dissociating salt conditions (1). To analyze the substrate requirements of RrmJ in more detail, we performed 2D gel analysis to compare the protein composition of the 50 S ribosomal subunits of the *rrmJ* deletion strain with that of wild type strains. As shown in Fig. 2, all 30 ribosomal proteins were detectable at similar levels in the two strains (Fig. 2, *A* and *B*). These data reveal that the absence of methylation of the highly conserved U2552 does not affect the folding of the 23 S rRNA to an extent that impairs the correct assembly of the 50 S ribosomal subunit. To get some idea how accessible U2552 is in the intact 50 S ribosomal subunit, we performed modeling studies using the crystal structure of the *Deinococcus radiodurans* 50 S ribosomal subunit (16) and RrmJ. Although solvent-accessible, U2552 (*E. coli* nomenclature) is positioned at the bottom of a deep cleft. Assuming that this conserved residue has the same

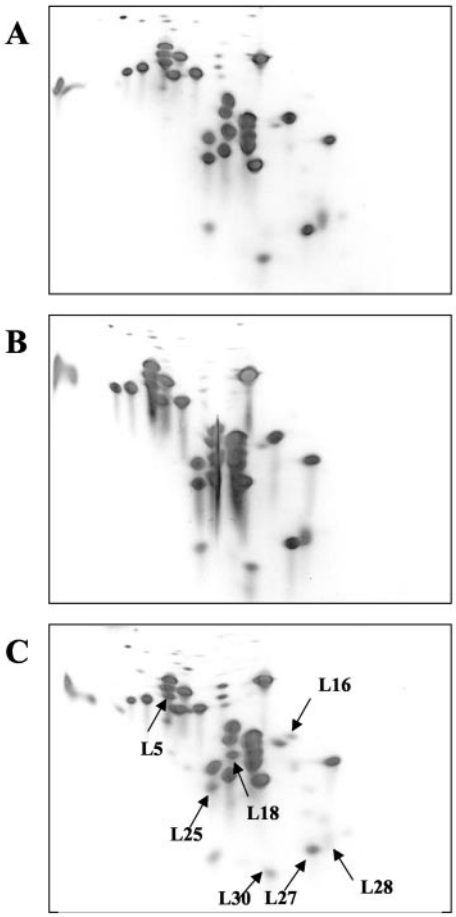

FIG. 2. **2D gel analysis of 50 S ribosomal subunits and 40 S particles prepared from WT and *rrmJ* deletion strains.** Protein composition of 50 S ribosomal subunits from HB24 (WT) (*A*), 50 S ribosomal subunits from HB23 (*rrmJΔ567*) (*B*), and 40 S ribosomal particles from HB23 is shown (*C*). 2D gel analysis revealed identical protein composition and concentration in 50 S ribosomes of wild type and *rrmJ* deletion strain. The 40 S ribosomal particles showed substantially decreased amounts of the late assembly proteins L5, L16, L18, L25, L27, L28, and L30, as indicated by the *arrows*.

position in the *E. coli* 50 S ribosomal subunits, this would make it rather inaccessible for RrmJ methylation and might require the 23 S rRNA to loop out so that RrmJ can gain access. This could certainly be a rate-limiting step that might occur *in vitro* but might not happen *in vivo* where RrmJ could methylate precursors whose A-loop is more accessible. This may explain the low turnover numbers we observe in our *in vitro* methylation reactions where completely assembled 50 S ribosomal subunits are used as substrates.

The 40 S ribosomal particles that accumulate under dissociating salt conditions in lysates prepared from *rrmJ* deletion strains are not *in vitro* substrates of RrmJ (1). 2D gel analysis of the 40 S peak reveals that at least seven different ribosomal proteins (L5, L16, L18, L25, L27, L28, L30) are present in significantly diminished amounts compared with 50 S ribosomal subunits (Fig. 2, *B* and *C*). All of these proteins belong to the group of late assembly proteins (17). While true ribosome precursors are also detectable under non-stringent, associating salt conditions, these 40 S particles only develop when the salt conditions become stringent. It is therefore more likely that they represent a mixture of destabilized 50 S particles that are lacking various late assembly proteins. Thus, the absence of Um2552 in the A-site of the ribosome appears to destabilize the 50 S ribosomal subunit and leads to premature dissociation of a number of ribosomal proteins probably causing structural changes in the 23 S rRNA that prevents RrmJ from recognizing it as a substrate.

The Active Site of RrmJ—Surprisingly little is known about the catalytic mechanism of any 2′-*O*-ribose methyltransferase. Although a reaction mechanism has been postulated for VP39 on the basis of its crystal structure (18), experimental data has not been obtained to support this hypothesis. We have, therefore, decided to combine structural analysis and site-specific mutagenesis to investigate the methyltransfer reaction of RrmJ. The first step in this analysis was to determine which residues are essential for catalysis.

Of all the methyltransferases that have been crystallized so far, VP39 and fibrillarin are the two enzymes whose structures resemble that of RrmJ the most (1). VP39 methylates the first transcribed nucleotide in mRNA following the m^7(5′)Gppp-cap (19). The structure of VP39, which was solved in complex with an mRNA substrate analog m^7(5′)Gppp-capped RNA hexamer and the inhibitor *S*-adenosyl homocysteine, showed that the mRNA binds to a groove on the surface of VP39 (20). Structural analysis of the RrmJ·AdoMet complex revealed that RrmJ has a very similar groove adjacent to the AdoMet binding site (1). We modeled the mRNA substrate analog of VP39 on the RrmJ structure and found that the ssRNA fits well into this putative substrate binding site of RrmJ. In this model, the 2′-hydroxyl group of the ribose to be methylated is positioned next to the reactive Cα group of AdoMet (Fig. 3*A*).

Lys-38, Asp-124, Lys-164, and Glu-199 of RrmJ are the most highly conserved amino acids among RrmJ homologues. A comparison of the crystal structures of RrmJ and VP39 indicate that these residues are located almost at the identical position as the homologous Lys-41, Asp-138, Lys-175 and Glu-207 residues in VP39 (Fig. 3, *A* and *B*). These residues, which form a hydrogen bond network that coordinates the phosphate atoms on each side of the methylated nucleoside, have been suggested by us and others (1, 21, 22) to play a critical role in the catalytic mechanism of RrmJ. In addition, Tyr-201 is highly conserved among RrmJ homologues and is located exactly underneath the putative active site, suggesting that it could play a catalytic role in RrmJ.

To analyze whether these residues are important for catalysis of the methyltransfer reaction, we performed site-specific mutagenesis and replaced the five amino acids in RrmJ (Lys-38, Asp-124, Lys-164, Glu-199, and Tyr-201) individually with alanine residues. We also substituted the highly conserved amino acid Asp-83 with alanine. This residue, which interacts with AdoMet via two hydrogen bonds, has been predicted to play a crucial role in AdoMet binding (1).

Growth Analysis of the RrmJ Mutants on McConkey Plates—After introducing the individual mutations into wild type *rrmJ* using site-specific mutagenesis, we transformed the *rrmJ* mutant plasmids into HB23 (*rrmJΔ567*) to investigate their *in vivo* function. All the mutant and wild type *rrmJ* genes are cloned into the pET11a expression system. Fortunately, the expression level of all of the mutated RrmJ proteins in the absence of induced T7 polymerase was found to be very similar to the level of RrmJ seen from a chromosomal copy (data not shown). This allowed us to be confident that any phenotype observed for the mutant proteins was not because of massive over- or underexpression of the protein.

As a first step in the *in vivo* characterization of our RrmJ mutants, we utilized the inability of *rrmJΔ567* cells to grow on McConkey plates at 37 °C (1). In contrast, strains that are *rrmJ*$^+$ because of their chromosomal copy (HB24) or *rrmJΔ567* strains that contain the pET11*rrmJ* plasmid (HB25) form large colonies. As shown in Fig. 4*A*, the D83A mutant, as well as the two lysine mutants, K38A and K164A, are unable to rescue the

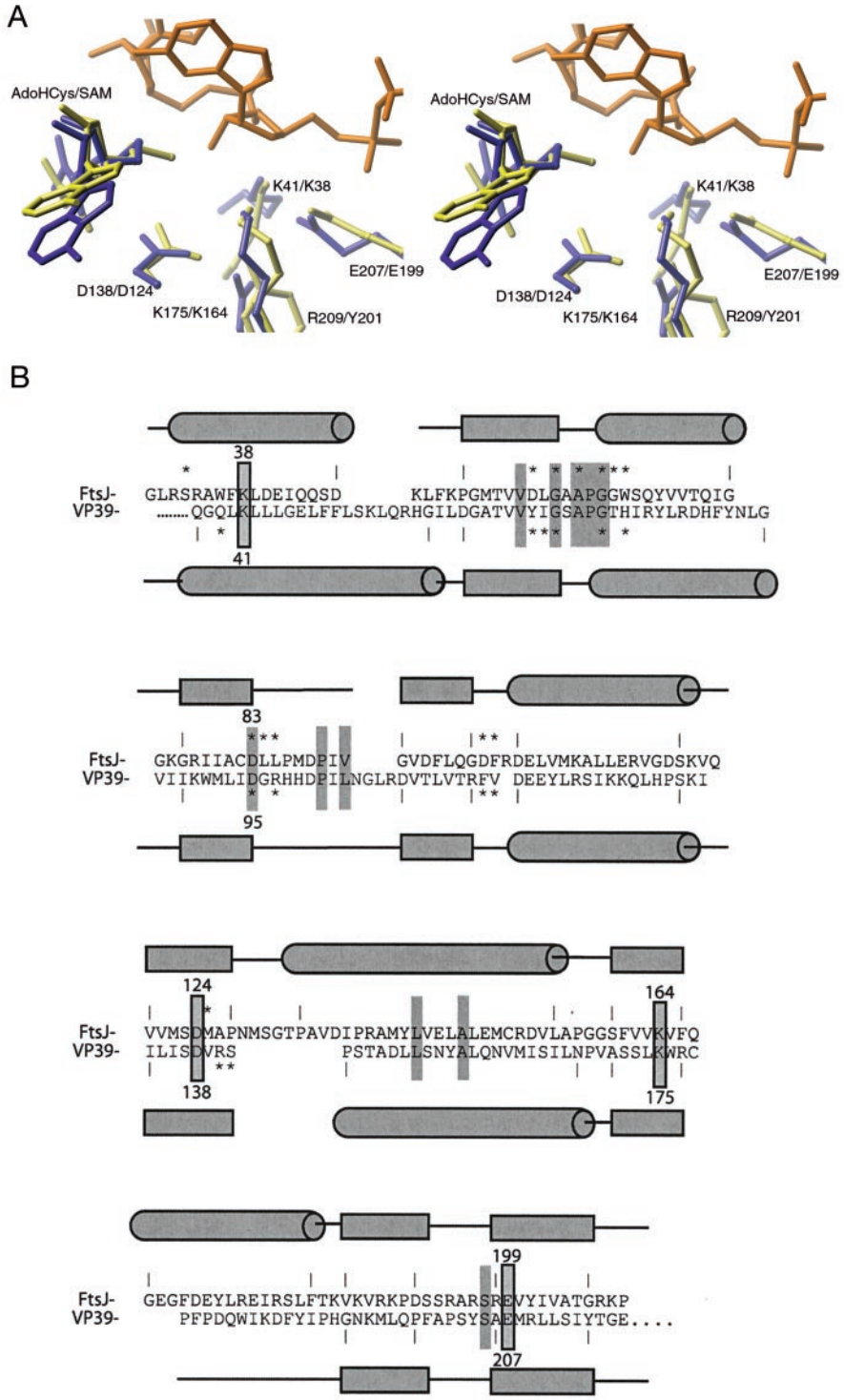

FIG. 3. **Structural comparison between RrmJ and VP39.** *A*, stereo view of the proposed active site in RrmJ and VP39. The active site residues of VP39 (*blue*) (19) and RrmJ (*yellow*) (1) were overlaid using a structural alignment calculated as described in the legend to Fig. 3*B*. The m^7G capped RNA hexamer from the structure of VP39 (20) is diagrammed in *orange*. The close structural alignment of the active site regions of VP39 and RrmJ suggests a similar mechanism of binding RNA substrate in the active site of RrmJ. *B*, structure-based sequence alignment of RrmJ and VP39. Amino acid sequence alignment is based on a three-dimensional structural alignment of RrmJ and VP39. Structural alignments were calculated using least squares difference between α-carbons of the β-strand portions of the methyltransferase core domains using the program Xtalview (28). *Tick marks* indicate beginning and end of secondary structure elements, α-helix (*rectangle*), and β-strand (*cylinder*). *Gray shaded* residues represent those residues that are conserved within homologues of the RrmJ (1) and VP39-related gene families, as well as structurally conserved in the methyltransferase fold of both proteins. *Boxed* residues are implicated in the catalytic mechanism. The residues that have been shown to make AdoMet contacts in the crystal structure (1) are labeled with an *asterisk*.

growth defect of the *rrmJ* deletion strain, indicating that all three mutations cause the inactivation of RrmJ *in vivo*. These results served as a first indication that the two lysine residues might be involved in the catalytic mechanism of RrmJ. Almost as severe was the phenotype of cells expressing the D124A mutant, suggesting that this amino acid also plays a crucial role in the function of RrmJ. *RrmJ* deletion strains expressing the E199A or Y201A variant protein showed only slight growth defects, indicating that these two residues are not as important in the catalytic mechanism.

The growth defect of *rrmJ* deletion strains is apparent not just on McConkey plates but can also be observed in liquid LB medium (1). Therefore, we analyzed the growth rate of our mutant strains in liquid medium. *RrmJ* deletion strains expressing no RrmJ or one of the D83A, K38A, D124A, or K164A RrmJ mutants revealed a 2.5–3-fold slower growth rate than cells expressing wild type RrmJ (data not shown). RrmJ deletion strains expressing the E199A or the Y201A variant protein grew almost as well as wild type cells.

Analysis of Polysome Profiles—RrmJ deletion strains show very significantly altered polysome profiles compared with wild type strains (1, 4). In the absence of functional RrmJ, lysates prepared under dissociating salt conditions (200 mM NH_4Cl, 1 mM $MgCl_2$) accumulate a large 40 S intermediate peak at the

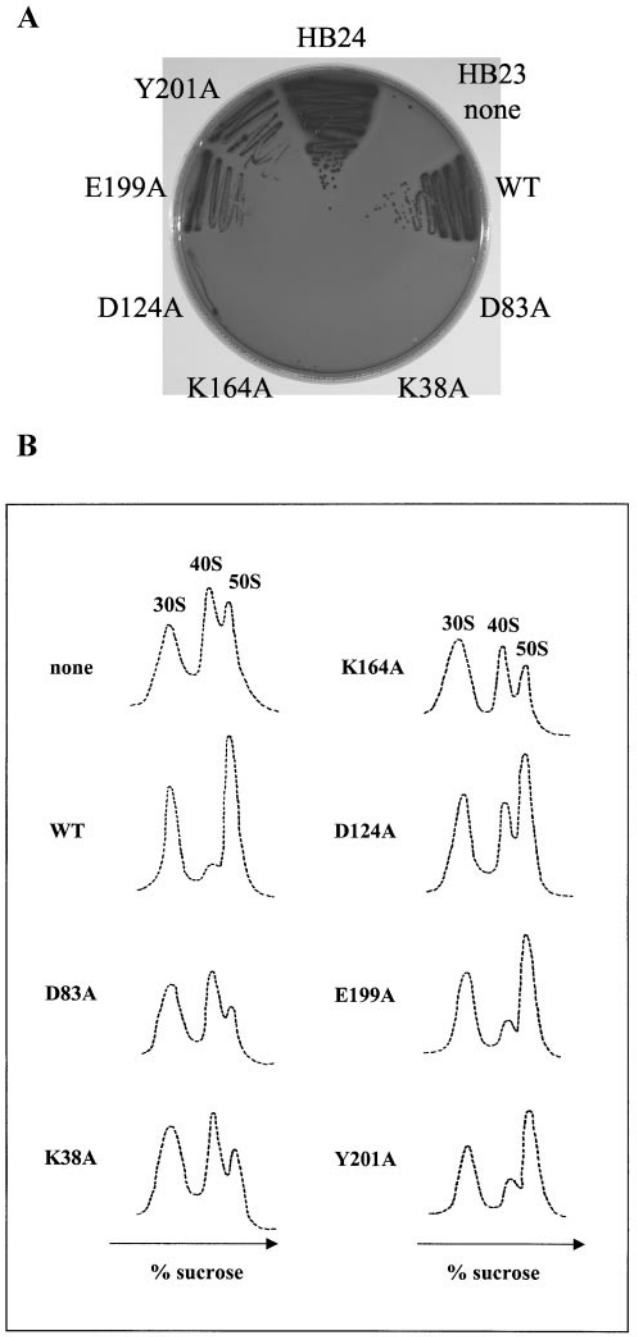

FIG. 4. **Phenotype of the active site mutants.** *A*, growth of HB24 (WT) and HB23 (*rrmJΔ567*) strains harboring either no plasmid or pHB1-derived plasmids encoding wild type *rrmJ* (WT) or the mutant *rrmJ* genes as indicated, on McConkey plates at 37 °C. *B*, polysome profiles of the *rrmJ* deletion strain HB23 expressing no plasmid or pHB1-derived plasmids encoding WT RrmJ or the active site mutants as indicated, under dissociating conditions (1 mM $MgCl_2$, 200 mM NH_4Cl) in 10–50% sucrose gradients. In the absence of functional RrmJ, 40 S ribosomal particles accumulate at the expense of intact 50 S ribosomal subunits.

expense of intact 50 S ribosomal subunits (see Ref. 1 and Fig. 4*B*). To further investigate to what extent our amino acid substitutions affect the *in vivo* function of RrmJ, we analyzed the polysome profile of *rrmJ* deletion strains expressing wild type RrmJ or our mutant RrmJ variants from a plasmid. As shown in Fig. 4*B*, the mutants D83A, K38A, and K164A exhibited a ribosome profile very similar to the profile of the *rrmJ* deletion strain. This agrees well with the growth defect seen with these mutants and suggests that ribosome destabilization is responsible for the observed growth disadvantage of *rrmJ* deletion strains.

Polysome profiles prepared from *rrmJ* deletion strains expressing the D124A variant revealed a slightly larger proportion of stable 50 S ribosomal subunits than *rrmJ*$^-$ strains that express the K38A or K164A variant. Comparison of the polysome profiles of these three mutant strains prepared under associating salt conditions, however, did not reveal any significant differences (data not shown), suggesting that the three residues Lys-38, Lys-164, and Asp-124 are equally important for the *in vivo* function of RrmJ. The ribosome profile of cells expressing the E199A and Y201A RrmJ variants, on the other hand, showed only a slight accumulation of 40 S ribosomal subunits, suggesting that mutation of these two residues does not cause a severe defect in RrmJ function.

AdoMet Binding Affinity of Purified RrmJ Mutants—To analyze the structural integrity and *in vitro* activity of our RrmJ mutants, the plasmids overexpressing the RrmJ mutants were transformed into BL21 *rrmJΔ567* strains, and the respective mutant proteins were overexpressed. All but one of the proteins were soluble and could be purified as described under "Experimental Procedures." The D124A mutant protein was present in inclusion bodies, a fact that prevented us from purifying this RrmJ variant.

Wild type RrmJ contains bound AdoMet cofactor when purified, as demonstrated by mass spectrometry (1). The amount of bound AdoMet can be quantified from the absorption ratio at 280 and 260 nm ($A_{280/260}$ ratio), because AdoMet absorbs at 260 nm. Wild type RrmJ has an $A_{280/260}$ ratio of 0.9 (1), whereas nucleotide-free proteins typically show $A_{280/260}$ ratios of 1.8–1.9. As a first measure of the structural integrity, the ability of each of the mutant proteins to retain bound AdoMet during the purification process was assessed. As predicted, the D83A mutant showed an $A_{280/260}$ ratio equivalent to that of nucleotide-free proteins ($A_{280/260}$ = 1.8), demonstrating that Asp-83 is important for AdoMet binding. All other mutant proteins, however, revealed $A_{280/260}$ ratios smaller than 1.8, indicating that various amounts of AdoMet were still associated with the proteins after the purification. To determine the approximate amount of bound AdoMet for wild type RrmJ and the mutants, an AdoMet-titration curve was established using the AdoMet-free D83A mutant (Fig. 5, *inset*). Using this standard curve, we then calculated the amounts of bound AdoMet for wild type and each mutant protein using their respective $A_{280/260}$ ratios. As shown in Fig. 5, preparations of wild type RrmJ and each of the active site mutants of RrmJ contained between 70 and 80% AdoMet. The ability of all mutants to bind and retain the cofactor AdoMet to the same extent as wild type RrmJ during the purification suggested that the introduced mutations did not cause substantial structural changes in the respective proteins that would lead to significantly altered AdoMet binding affinities.

In Vitro Activity of the RrmJ Mutants—To characterize the *in vitro* methylation activity of our mutants, we determined the specific activity of our purified RrmJ mutant proteins under conditions in which the two substrates, 50 S ribosomes and AdoMet, are present in saturating concentrations (Table II). Both lysine mutants, K38A and K164A, showed at least a 50-fold decrease in our *in vitro* methylation assays. The very small amount of methyl incorporation observed was within the limits of the background incorporation, and an increase in enzyme concentration did not cause an increase in methyl incorporation (data not shown). This showed that these two lysine residues play a very critical role in the methyltransfer reaction and corroborated our *in vivo* data that suggested that both residues are important for the overall function of RrmJ.

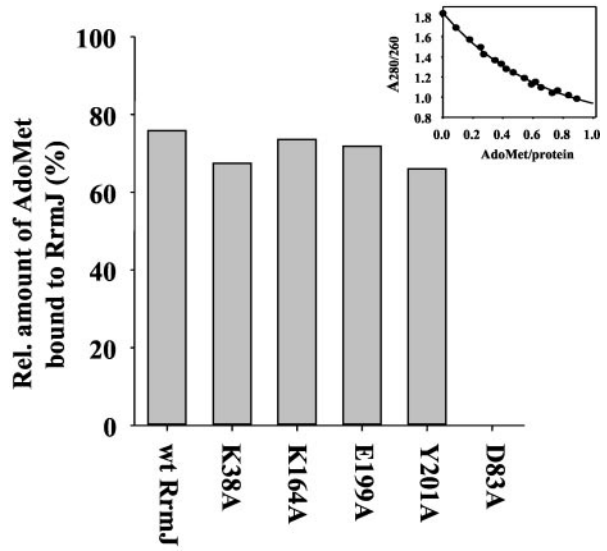

FIG. 5. **AdoMet binding of the active site mutants.** The amount of AdoMet bound to wild type RrmJ and the mutant proteins after the purification was calculated according to the AdoMet standard curve (see *inset*). All of the mutant proteins except D83A contained approximately the same amount of AdoMet after the purification process. *Inset*, AdoMet was titrated in 1 μM steps to a 23 μM solution of the AdoMet-free RrmJ mutant D83A. The absorption spectra were measured after each AdoMet addition, and the respective $A_{280/260}$ ratios were plotted against the corresponding amount of AdoMet/protein.

Substitution of Glu-199 caused a 16-fold reduction in K_{cat} without changing the K_m for 50 S ribosomal subunits. This suggested a less important role for this residue in the catalytic mechanism, an assumption that agreed well with the phenotype of *rrmJ* deletion strains expressing this E199A mutant protein. These cells showed only slightly affected polysome profiles and minor growth disadvantages on McConkey plates suggesting that the activity of this mutant protein is sufficient *in vivo* to partly rescue the *rrmJ* deletion. To ascertain that the E199A mutant protein shows sufficient *in vivo* methylation activity to account for the rescued phenotype, we analyzed the extent of 23 S rRNA modification in 50 S ribosomal subunits prepared from this mutant strain, by testing them as substrates in our *in vitro* methylation assay (data not shown). If the E199A mutant was fully active *in vivo*, most of the 50 S ribosomal subunits should be already methylated, and the *in vitro* methyl incorporation should be as low as the methyl incorporation observed with 50 S ribosomal subunits prepared from the wild type strain HB24. If the E199A mutant was inactive *in vivo*, on the other hand, the *in vitro* methylation should be as substantial as the *in vitro* methylation of 50 S ribosomal subunits prepared from the *rrmJ* deletion strain HB23. More than 60% of 50 S ribosomal subunits prepared from HB23 strains expressing the E199A mutant were methylated and no longer served as *in vitro* substrate for RrmJ. These results confirmed our *in vivo* data that revealed the presence of a substantial amount of stable 50 S ribosomal subunits and suggested a considerable methylation activity of the E199A mutant *in vivo*.

The specific activity of the Y201A mutant protein was only slightly decreased, suggesting that this residue does not take a direct part in the methyltransfer reaction. Surprisingly, the D83A mutant protein that showed no activity *in vivo* showed about 20% of wild type activity *in vitro*. This may reflect the fact that this mutant shows an increase in K_m for both substrates (AdoMet, apparent K_m = 7.0 μM; 50 S ribosomal subunit, apparent K_m = 1.4 μM) leading to a more significant decrease in catalytic activity at lower substrate concentrations.

DISCUSSION

Very little is known about the mechanism of the methyltransfer reaction in 2′-*O*-ribose methyltransferases such as VP39 and RrmJ. Based on the resemblance between VP39 and COMT, whose methyltransfer reaction has been analyzed (23), a general base-catalyzed reaction has been proposed for VP39 (20). In this model, a general base catalyzes the deprotonation of the 2′-OH group of the ribose to activate the nucleophilic oxygen, which attacks the methyl group of AdoMet in a S_N2-type reaction. In COMT, Mg^{2+} is bound to the active site and is proposed to play a crucial role in substrate binding and positioning the hydroxyl group close to the methyl group of AdoMet (9, 24). The methyltransferase activity of RrmJ has also been shown to be dependent on the presence of Mg^{2+} ions (2). This divalent cation, however, might be essential to stabilizing the 50 S ribosomal substrate rather than playing a role in the catalytic mechanism of the protein. Lowering the Mg^{2+} concentration to 1 mM causes the dissociation of the 50 S ribosomal subunits prepared from *rrmJ* deletion strains into 40 S particles, which are no longer substrates for RrmJ (1). Because the active site of RrmJ superimposes very well with the active site of the Mg-independent 2′-*O*-ribose methyltransferase VP39 (see Fig. 3*A* and Ref. 21), the methyltransferase activity of RrmJ likely does not require Mg^{2+}.

Based on the geometry of the catalytic center in RrmJ and VP39 two highly conserved lysine residues, Lys-38 (Lys-41*)* and Lys-164 (Lys-175*)* were identified as likely candidates for being involved in either deprotonating the hydroxyl group directly or in lowering the pK_a of the hydroxyl group (20). Superposition of RrmJ and VP39 and modeling of the ribose substrate of VP39 into the potential active site of RrmJ also revealed the presence of two highly conserved negatively charged residues, Asp-124 and Glu-199, in close proximity to the substrate (Fig. 3*A*). From a comparison of the methyltransferase domains of reovirus λ2 protein, VP39, and RrmJ, Bujnicki and Rychlewski (21) have proposed recently that these four conserved residues form a catalytically active K-D-K-E tetrad (21). Simultaneous superposition of all three structures revealed a perfect conservation of these four residues. In addition, alanine mutagenesis scans that were performed with VP39 suggested that some of these residues are involved in AdoMet binding and methyltransferase activity (25). These alanine scans and additional structure and sequence comparisons also suggested a possible involvement of Tyr-201, a highly conserved residue that lies underneath the putative active site of RrmJ.

We have now individually mutated these five, potentially crucial amino acids to alanine residues and analyzed the activity of the mutants both *in vivo* and *in vitro*. We demonstrated that the introduced mutations did not significantly decrease the expression level and solubility of the mutant proteins *in vivo* or the AdoMet binding affinity of the purified proteins *in vitro*, suggesting that no major structural rearrangements occurred in the mutant proteins.

Our results clearly show that lysine residues Lys-38 and Lys-164 both play critical roles in the methyltransfer reaction of RrmJ. RrmJ variants with alanine substitutions for either of these two lysine residues were unable to rescue the *rrmJ* deletion phenotype when expressed at wild type level and revealed a significant decrease in the methyltransfer activity *in vitro*. Substitution of residue Asp-124 also caused a severe phenotype and the accumulation of 40 S ribosomal subunits, indicating that the methyltransfer reaction is severely impaired. Mutations in Glu-199, however, did not reveal a clear phenotype *in vivo*, although the mutated protein showed a reduced specific activity *in vitro*. These results suggest that Glu-199 plays a more minor role in the methyltransfer reaction

TABLE II
Summary of the in vivo and in vitro characterization of the RrmJ active site mutants

Mutation	Growth 37 °C	Polysome profile	AdoMet bound	Apparent K_{cat}	Apparent K_m (50 S)
			%	min^{-1}	μM
Wild type	+++	+++	76	0.064	0.8
D83A	−	−	0	0.012	1.4[a]
K38A	−	−	68	<0.001	ND[b]
D124A	(+)	(+)	ND[c]	ND[c]	ND[c]
K164A	−	−	74	<0.001	ND
E199A	++	++	72	0.004	0.7
Y201A	++	++	66	0.012	0.5

[a] The apparent K_m for AdoMet was determined to be 7.0 μM.
[b] ND, not determined.
[c] D124A mutant aggregated upon overexpression in BL21*rrmJΔ567* cells and could not be purified. This mutant protein was soluble in the strains that were used to investigate the *in vivo* activity of the protein.

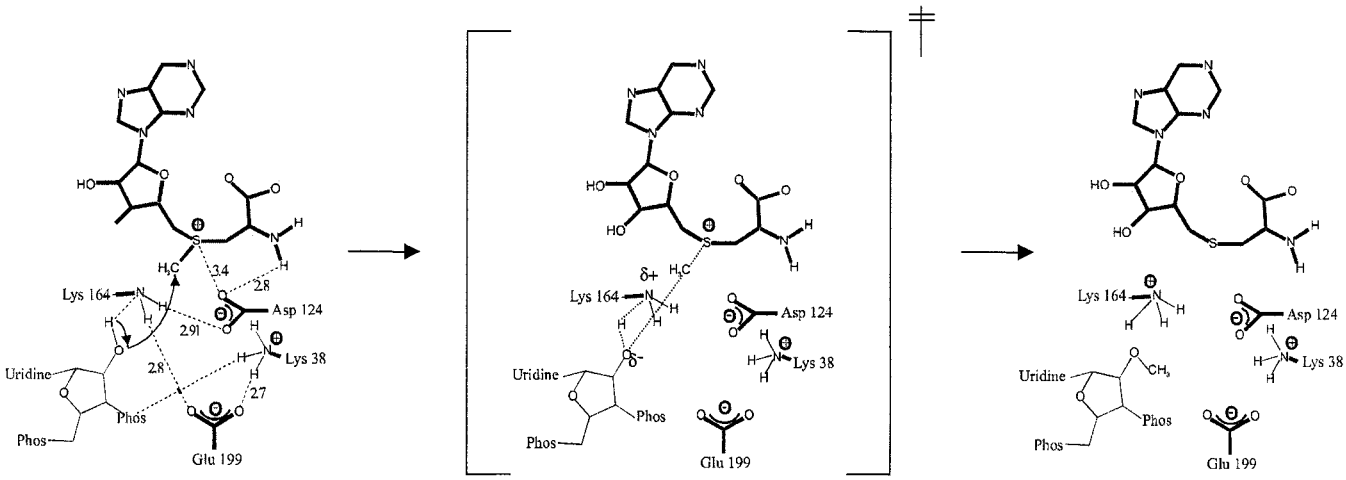

FIG. 6. **Proposed reaction mechanism of RrmJ.** After deprotonation of the target hydroxyl group, the nucleophilic attack occurs at the reactive methyl group of AdoMet in a S_N2 reaction, and the methyl group is transferred onto the 2′-OH group of the ribose.

than anticipated from the structural considerations. Tyr-201 also seems not to be directly involved in the catalytic reaction. The function of the Y201A variant of RrmJ was not significantly impaired *in vivo* or *in vitro*. We, therefore, conclude that RrmJ and VP39 function with the use of a catalytic K-D-K triad rather than a catalytic K-D-K-E tetrad as proposed previously (21).

Based on our results, structural considerations, and comparisons to the proposed mechanism of the small molecule 2′-*O*-methyltransferase COMT, we suggest the model shown in Fig. 6. In analogy to COMT (23), where Lys-144 has been proposed to act as general base, we suggest that Lys-164 acts as a general base in RrmJ. The ϵ-NH_2 of Lys-164 is oriented to directly face the target hydroxyl group of the ribose molecule and, in this model, is within hydrogen bonding distance of the 2′-hydroxyl group. This model requires that Lys-164 is in its deprotonated form and suggests, therefore, that the pK_a of this amino group is lowered. This decrease in pK_a has also been suggested for VP39 by Hodel *et al.* (18) and has been found to be the case in aldolases (26) and amidases (18). In RrmJ, the pK_a for Lys-164 may be lowered because of the proximity of the amine to the positively charged sulfur atom of AdoMet and the amine group of Lys-38. This could also explain the important catalytic role of Lys-38, the second residue in RrmJ whose substitution causes an enormous decrease in the methyltransferase activity. In addition, the surroundings of Lys-164 are dominated by non-polar amino acids like Met-125, Ala-126, Leu-143, Val-144, Val-163, Val-165, Phe-166, Val-200, and Tyr-201 that might destabilize the protonated amine group and thereby lower the pK_a of this side chain (27). The general base-activated hydroxyl group of the RNA substrate then attacks the reactive methyl group to form the S_N2-like transition state as shown in Fig. 6. Asp-124 is positioned in the crystal structure to stabilize the positive charge on the sulfur atom of AdoMet and the amino group of Lys-164. It is conceivable that a proton from protonated Lys-164 is transferred to Asp-124 during catalysis. Substitution of this central residue causes the protein to aggregate upon overexpression. Glu-199, which is positioned by hydrogen bonds with Lys-38, might play a role by positioned the ϵ-NH_2 group of Lys-164, thereby ensuring that the free electron pair of Lys-164 is located next to the target hydroxyl.

The functional analysis of our active site RrmJ mutant proteins has allowed us to propose a reaction mechanism of RrmJ. It has also enabled us to show that the lack of methyltransferase activity of RrmJ is responsible for the appearance of less stable ribosomes in *rrmJ* deletion strains. This clearly rules out the possibility that influence of RrmJ on ribosome stability is because of a second, methyltransfer-independent function of RrmJ as has been observed for the mitochondrial methyltransferase Pet56p (6). It remains to be directly demonstrated, however, whether it is the absence of the modification at position U2552 in the A-site of the ribosome that destabilizes the ribosome as seems likely or whether the potential tRNA methylation activity of RrmJ could be indirectly responsible for the ribosome defect. This tRNA methylation activity has been observed for RrmJ *in vitro* (1) and has now been demonstrated for Trm7p, the cytosolic RrmJ homologue in yeast, *in vivo* (22). In this context, it will be also very interesting to determine which functions of RrmJ require the up-regulation of this highly conserved protein under heat shock conditions.

Acknowledgments—We are very grateful to Dr. Knud Nierhaus, in whose lab the 2D gel analysis was performed. We thank Drs. Detlev Kamp and Uli Stelzl for advice and help performing the 2D gels. We are indebted to Drs. David Ballou, James Bardwell, and Carol Fierke for helpful discussions and for critically reading the manuscript.

REFERENCES

1. Bügl, H., Fauman, E. B., Staker, B. L., Zheng, F., Kushner, S. R., Saper, M. A., Bardwell, J. C., and Jakob, U. (2000) *Mol. Cell* **6,** 349–360
2. Caldas, T., Binet, E., Bouloc, P., Costa, A., Desgres, J., and Richarme, G. (2000) *J. Biol. Chem.* **275,** 16414–16419
3. Hansen, M. A., Kirpekar, F., Ritterbusch, W., and Vester, B. (2002) *RNA* **8,** 202–213
4. Caldas, T., Binet, E., Bouloc, P., and Richarme, G. (2000) *Biochem. Biophys. Res. Commun.* **271,** 714–718
5. Pintard, L., Bujnicki, J. M., Lapeyre, B., and Bonnerot, C. (2002) *EMBO J.* **21,** 1139–1147
6. Lovgren, J. M., and Wikstrom, P. M. (2001) *J Bacteriol* **183,** 6957–6960
7. Bjoerk, G. R. (1996) *E. coli and Salmonella. Cellular and Molecular Biology* (Neidhardt, F. C., ed) pp. 861–880, ASM Press, Washington, D. C.
8. Wang, H., Boisvert, D., Kim, K. K., Kim, R., and Kim, S. H. (2000) *EMBO J.* **19,** 317–323
9. Vidgren, J., Svensson, L. A., and Liljas, A. (1994) *Nature* **368,** 354–358
10. Hodel, A. E., Gershon, P. D., Shi, X., and Quiocho, F. A. (1996) *Cell* **85,** 247–256
11. Bujnicki, J. M., Blumenthal, R. M., and Rychlewski, L. (2002) *J. Mol. Microbiol. Biotechnol.* **4,** 93–99
12. Geyl, D., Bock, A., and Isono, K. (1981) *Mol. Gen. Genet.* **181,** 309–312
13. Barbosa, E., and Moss, B. (1978) *J. Biol. Chem.* **253,** 7698–7702
14. Denoya, C. D., and Dubnau, D. (1987) *J. Bacteriol.* **169,** 3857–3860
15. Hu, G., Oguro, A., Li, C., Gershon, P. D., and Quiocho, F. A. (2002) *Biochemistry* **41,** 7677–7687
16. Harms, J., Schluenzen, F., Zarivach, R., Bashan, A., Gat, S., Agmon, I., Bartels, H., Franceschi, F., and Yonath, A. (2001) *Cell* **107,** 679–688
17. Nierhaus, K. H. (1991) *Biochimie* (*Paris*) **73,** 739–755
18. Hodel A. E., Quiocho, F. A., Gershon P. D. (1999) *S-Adenosylmethionine-dependent Methyltransferases: Structures and Functions* (Cheng, X. and Blumenthal, R. M., eds), pp. 255–282, World Scientific, Riveredge, NJ
19. Schnierle, B. S., Gershon, P. D., and Moss, B. (1992) *Proc. Natl. Acad. Sci. U. S. A.* **89,** 2897–2901
20. Hodel, A. E., Gershon, P. D., and Quiocho, F. A. (1998) *Mol. Cell* **1,** 443–447
21. Bujnicki, J. M., and Rychlewski, L. (2001) *Genome Biol.* **2,** RESEARCH0038
22. Pintard, L., Lecointe, F., Bujnicki, J. M., Bonnerot, C., Grosjean, H., and Lapeyre, B. (2002) *EMBO J.* **21,** 1811–1820
23. Vidgren, J., Ovaska, M., Tenhunen, J., Tilgmann, C., Lotta, T., and Maennistoe, P. T. (1999) *S-Adenosylmethionine-dependent Methyltransferases: Structures and Functions* (Cheng, X. Blumenthal, R. M., eds) pp. 55–91, World Scientific, Riveredge, NJ
24. Jeffery, D. R., and Roth, J. A. (1987) *Biochemistry* **26,** 2955–2958
25. Schnierle, B. S., Gershon, P. D., and Moss, B. (1994) *J. Biol. Chem.* **269,** 20700–20706
26. Barbas, C. F., III, Heine, A., Zhong, G., Hoffmann, T., Gramatikova, S., Bjornestedt, R., List, B., Anderson, J., Stura, E. A., Wilson, I. A., and Lerner, R. A. (1997) *Science* **278,** 2085–2092
27. Fersht, A. (2000) *Structure and Mechanism in Protein Science, a Guide to Enzyme Catalysis and Protein Folding* (Russel, J. M., and Hadler, G. L., eds) pp. 188–189, W. H. Freeman and Company, New York
28. McRee, D. F. (1993) *Practical Protein Crystallography*, Academic Press, San Diego, CA

JOURNAL OF BACTERIOLOGY, Oct. 2004, p. 6634–6642 Vol. 186, No. 19
0021-9193/04/$08.00+0 DOI: 10.1128/JB.186.19.6634–6642.2004

Substrate Binding Analysis of the 23S rRNA Methyltransferase RrmJ

Jutta Hager,[1] Bart L. Staker,[2] and Ursula Jakob[1]*

Molecular, Cellular and Developmental Biology Department, University of Michigan, Ann Arbor, Michigan,[1] and Decode Genetics, Biostructures Group, West Bainbridge Island, Washington[2]

Received 22 April 2004/Accepted 6 July 2004

The 23S rRNA methyltransferase RrmJ (FtsJ) is responsible for the 2′-O methylation of the universally conserved U2552 in the A loop of 23S rRNA. This 23S rRNA modification appears to be critical for ribosome stability, because the absence of functional RrmJ causes the cellular accumulation of the individual ribosomal subunits at the expense of the functional 70S ribosomes. To gain insight into the mechanism of substrate recognition for RrmJ, we performed extensive site-directed mutagenesis of the residues conserved in RrmJ and characterized the mutant proteins both in vivo and in vitro. We identified a positively charged, highly conserved ridge in RrmJ that appears to play a significant role in 23S rRNA binding and methylation. We provide a structural model of how the A loop of the 23S rRNA binds to RrmJ. Based on these modeling studies and the structure of the 50S ribosome, we propose a two-step model where the A loop undocks from the tightly packed 50S ribosomal subunit, allowing RrmJ to gain access to the substrate nucleotide U2552, and where U2552 undergoes base flipping, allowing the enzyme to methylate the 2′-O position of the ribose.

Modified nucleotides have been identified in nearly every cell and organism analyzed so far (11). Of the almost 100 posttranscriptional modifications that have been characterized in ribonucleotides, about one-third are present in rRNAs (30). Of those, the majority are methylation reactions on either the base or the 2′-*O*-ribose of the respective nucleotide. Most of these modifications cluster in conserved regions of functionally important rRNA domains and have been suggested to be important for the structure and function of the ribosome (4, 12, 13).

Although the chemical nature of the individual rRNA modifications has been known for some years, most of the enzymes that are responsible for these modifications have not yet been identified. In the case of *Escherichia coli* 23S rRNA, which has at least 14 different methylated nucleotides, only 5 modifying enzymes have been identified so far. These are the three base-modifying methyltransferases, RrmA (m^1G745) (15), RumA (m^5U1939) (1), and RumB (m^5U747) (23), as well as the two unrelated 2′-*O*-ribose methyltransferases, RlmB (Gm2251) (22) and RrmJ (Um2552) (6, 7).

Our study focuses on the highly conserved RrmJ (FtsJ) protein, which is the first identified heat-inducible 2′-*O*-methyltransferase of *E. coli* (6, 7). While the deletion of most of the known 23S rRNA methyltransferases has been shown not to affect *E. coli* growth or ribosome assembly, the deletion of RrmJ has been found to affect both activities (6, 7). The *rrmJ* deletion strain, which no longer harbors the highly conserved Um2552 modification in the A loop of the ribosome, accumulates large amounts of free 30S and 50S ribosomal subunits at the expense of functional 70S ribosomes. This ribosome defect appears to be due specifically to a lack of methyltransferase activity, because the expression of active-site RrmJ mutants in the *rrmJ* deletion strain does not rescue this phenotype (16). The ribosome defect is, furthermore, thought to be the reason for the decreased translational efficiency of S30 lysates prepared from the *rrmJ* deletion strain (8) as well as for the significant growth disadvantage that is exerted by this strain (6). This finding was consistent with those of earlier studies, which demonstrated that the incorporation of 23S rRNA carrying a U2552 mutation into ribosomes affected cell growth and peptidyl transferase activity (20, 29).

RrmJ is one of the few RNA-modifying enzymes that has been shown to act very late in the maturation process of the ribosome (6, 7). Only fully assembled 50S ribosomal subunits prepared from the *rrmJ* deletion strain appear to serve as substrates for RrmJ in vitro, while naked 23S rRNA or ~40S ribosomal particles that are prepared from the *rrmJ* deletion strain are not methylated by purified RrmJ (6). This finding suggested that either the correct folding of the 23S rRNA or additional protein-protein interactions are necessary for the substrate recognition.

While *E. coli* cells have only one RrmJ homologue, eukaryotic cells usually have several. Yeast cells, for instance, have been found to harbor three RrmJ homologues: Trm7p in the cytosol (28), Mrm2p in mitochondria (26), and Spb1p in the nucleus (27). Whereas the mitochondrial and nuclear RrmJ homologues function as rRNA methyltransferases, the cytosolic Trm7p has been shown to be responsible for two 2′-*O*-ribose methylations at position 32 (Cm32) and 34 (Gm34) in the anticodon loop of certain yeast tRNAs. The ability of yeast RrmJ homologues to recognize either rRNA or tRNA corroborates reports about a possible dual substrate specificity for *E. coli* RrmJ, which has been found to methylate tRNAs in vitro in addition to 23S rRNA (6).

How methyltransferases recognize and bind their target sequences has not been well established for the majority of known enzymes. Only very few cocrystallization studies of RNA methyltransferases with their substrates have revealed how RNA is associated with the proteins. One of these proteins is the mRNA 2′-*O*-methyltransferase VP39 from vaccinia virus, whose structure closely resembles that of RrmJ, which

* Corresponding author. Mailing address: Molecular, Cellular and Developmental Biology Department, University of Michigan, Ann Arbor, MI 48109-1048. Phone: (734) 615-1286. Fax: (734) 647-0884. E-mail: ujakob@umich.edu.

TABLE 1. Strains and plasmids used in this study

Strain or plasmid	Genotype or relevant features	Source or reference
MG1655	*rph-1*	Lab collection
HB24	MG1655, *zgi*-203::Tn*10*, Tc^r	6
HB23	MG1655, *zgi*-203::Tn*10* Tc^r, *rrmJ*Δ*567*	6
HB25	HB23, pHB1	6
HB1	BL21(DE3), pHB1	6
BL21(DE3)	F$^-$ *ompT hsdS*$_B$ (r_B^- m_B^-) *gal dcm*(DE3)	Novagene
JUH47	BL21(DE3), *rrmJ*Δ567 Tc^r	16
pET11a	pBR322 derived	Novagene
pHB1	pET11a *rrmJ*	6
pJUH12	pET11a *rrmJ* K38A	16
pJUH3	pET11a *rrmJ* D20A	This study
pHB30	pET11a *rrmJ* Y22A	This study
pJUH5	pET11a *rrmJ* R32A/R34A	This study
pJUH6	pET11a *rrmJ* F37A/L39A	This study
pJUH7	pET11a *rrmJ* Q67A/Y68A	This study
pJUH20	pET11a *rrmJ* D136N	This study
pJUH22	pET11a *rrmJ* F166A	This study
pJUH23	pET11a *rrmJ* K189A	This study
pJUH10	pET11a *rrmJ* R194A	This study
pHB31	pET11a *rrmJ* S197A	This study

has been solved in complex with *S*-adenosylmethionine (AdoMet) (6). The structure of VP39 has been solved in complex with the reaction product *S*-adenosylhomocysteine and a 5′ m^{7}G-capped, single-stranded RNA hexamer (18). The modeling of the mRNA substrate analogue of VP39 into the structure of RrmJ assisted us in identifying the active site residues in RrmJ and in proposing a reaction mechanism (16).

We used extensive mutagenesis studies to analyze the putative 23S rRNA substrate binding site in RrmJ. Sequence comparisons and an analysis of the structure of RrmJ allowed us to identify a number of residues that are potentially involved in rRNA binding. We introduced these mutations into wild-type RrmJ and functionally characterized the mutant proteins in vivo and in vitro. We identified a highly conserved, positively charged ridge that appears to serve as the RNA substrate binding site of RrmJ. Furthermore, we discovered that the isolated unmodified A loop serves as the minimal methylation substrate of wild-type RrmJ in vitro. In situ modeling studies of the A-loop structure into the proposed substrate binding site of RrmJ suggested a base flipping mechanism for RrmJ, which is postulated to be important for the methylation process.

MATERIALS AND METHODS

Site-directed mutagenesis. Site-directed mutagenesis was performed according to the QuickChange protocol (Stratagene, La Jolla, Calif.). Wild-type *rrmJ* was cloned into pET11a to generate pHB1 (6), which was used as template DNA for all mutations. All introduced mutations were confirmed by DNA sequencing. Table 1 lists all plasmids and strains that were generated. For protein expression and purification, the pET11a derivatives were introduced into a BL21 strain that contained a deletion of the *rrmJ* gene (JUH47) (16). To perform phenotypical studies, the plasmids were introduced into the *rrmJ* deletion strain HB23. The expression analysis of all of the mutants was performed as previously described (16).

Purification of the RrmJ mutants. The purification of the RrmJ mutants was performed as previously described (16). The protein concentration was determined by UV absorbance by using an extinction coefficient of 1.0 for a 1 mg/ml solution at A_{280} for all mutant proteins (6).

Analytical polysome profiles. Analytical polysome profiles of the wild-type strain HB24, the *rrmJ* deletion strain HB23, and HB23 expressing the individual *rrmJ* mutant proteins under stringent and nonstringent salt conditions were performed and analyzed as previously described (6, 16).

Preparation of ribosomal subunits and methylation assay. The preparation of the 50S ribosomal subunits of the *rrmJ* deletion strain HB23 and analysis of the methyl transfer activity of wild-type RrmJ and the mutant proteins was performed as previously described (16). RrmJ (either 100 or 200 nM) in 50 mM HEPES-KOH (pH 7.5), 85 mM NH_4Cl, 3 mM $MgCl_2$, and 2 mM β-mercaptoethanol was used. For K_m measurements, the initial rate for methylation was measured in the presence of 50 μM [^{3}H]AdoMet (85.0 Ci/mmol; Amersham Biosciences) and various concentrations of 50S ribosomal subunits, ranging from 0.25 to 10 μM. At defined time points (2.5, 5, 7.5, and 10 min) after initiation of the methylation reaction at 37°C, 8-μl aliquots were taken and the [^{3}H]methyl incorporation was determined as described previously (6). The slopes of the methyl incorporation versus time were calculated. Methylation reactions with the A loop as the substrate were performed in 50 mM HEPES-KOH (pH 7.5), 50 mM NaCl, 10 mM EDTA, 1 mM dithiothreitol, 40 U of RNase inhibitor RNasin (Promega), and 0.1 mg of bovine serum albumin/ml at 37°C. RrmJ (5 μM) was incubated with 50 μM [^{3}H]AdoMet (85 Ci/mmol), and the reaction was started by the addition of 1 μM purified A loop (nucleotides 2545 to 2563 of *E. coli* 23S rRNA; kindly provided by Joseph Puglisi, Stanford University) (3). At defined time points after the methylation reaction was initiated, 8-μl aliquots were taken and supplemented with 40 μg of tRNA (Sigma) as the carrier for precipitation, and the [^{3}H]methyl incorporation was determined as described previously (6).

AdoMet titration. To determine the amount of AdoMet present in the various RrmJ mutant preparations, we used an AdoMet titration curve (16). In short, a 23 μM solution of the AdoMet-free D83A mutant RrmJ protein was prepared, and 1 μM AdoMet (ε_{257} = 15,400 M^{-1} cm^{-1}) was added per titration step (16). After each AdoMet addition, the optical density at 280 nm (OD_{280})/OD_{260} ratio of the protein-AdoMet mixture was determined. After volume corrections, these ratios were plotted against the amounts of titrated AdoMet. The OD_{280}/OD_{260} ratios of the purified RrmJ mutants were then determined, and the amounts of bound AdoMet were calculated.

RrmJ binding to the ribosome. The preparation of 50S ribosomal subunits from the wild type (HB24), the *rrmJ* deletion strain expressing no RrmJ (HB23), or the RrmJ-D136N mutant protein was performed under stringent, high-salt conditions (1 mM $MgCl_2$ and 200 mM NH_4Cl) as described previously (6). Aliquots of 2 μM 50S ribosomal subunits alone or supplemented with various concentrations of purified wild-type RrmJ were prepared. Ten microliters of each of those aliquots was loaded onto a Tris-glycine sodium dodecyl sulfate–14% polyacrylamide gel (Invitrogen), and Western blot analysis was performed with polyclonal antibodies against RrmJ.

RESULTS

Rational RrmJ mutant design. The conservation of an amino acid residue in a protein is a strong indicator of its importance in the structure and/or function of the protein. Residues that are exposed to the surface of a protein are usually highly variable unless they are involved in the catalytic mechanism of the protein, in its structural integrity, or in substrate and/or cofactor binding. To investigate the potential substrate binding site of the 23S rRNA methyltransferase RrmJ, we therefore performed extensive site-directed mutagenesis, replacing the majority of highly conserved residues in RrmJ. We spared only those residues that have been shown to be involved in AdoMet binding and/or the catalytic site of RrmJ (16) as well as those that we predicted to play a structural role in the protein fold (Fig. 1).

Of the 27 most highly conserved amino acids in RrmJ (6), 11 amino acids either directly contact the cofactor AdoMet or are active site residues (6, 16). An analysis of the crystal structure of RrmJ allowed us to predict, furthermore, that the highly conserved residues P127, F161, F182, P190, and S193 are likely to perform structural functions in the methyltransferase, either by forming the AdoMet binding pocket (e.g., P127) or by building the hydrophobic core of the α/β protein (e.g., F161 and F182). Q119 and G159 also were excluded from our mutagenesis studies, because both amino acids are located on the opposite site of the RrmJ molecule and appeared, therefore,

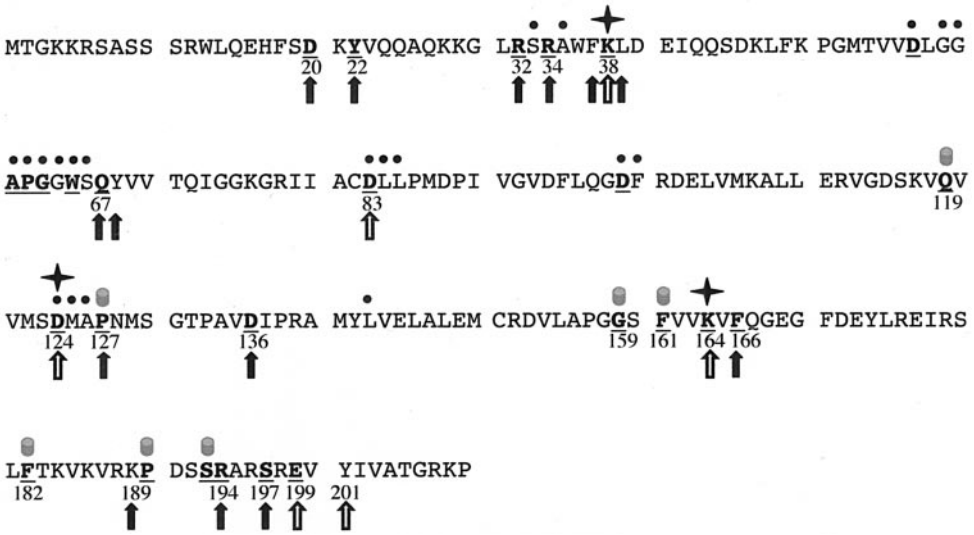

FIG. 1. Rational mutant design. The 27 most highly conserved residues in RrmJ are shown in bold and underlined letters. These amino acids have been identified as highly conserved by aligning a set of 1,112 nonredundant paralog sequences to a set of 29 likely RrmJ orthologs (6). The black dots above the RrmJ sequence indicate the residues that have been identified as involved in AdoMet binding (6). Stars mark the three amino acids that have been shown to form the catalytic triad (16). The filled cylinders above the sequence depict the amino acids which are either predicted to play a structural role in RrmJ or reside on the opposite site of the RrmJ molecule. The open arrows mark all highly conserved residues that were mutated in previous studies (16). The closed arrows depict the residues that were mutated in this study.

rather unlikely to be involved in substrate binding. These considerations left us with nine highly conserved residues (D20, Y22, R32, R34, Q67, D136, F166, R194, and S197), eight of which we replaced individually or pair-wise with alanine residues. We decided to replace D136 with an asparagine residue to maintain the size of this residue.

To expand our mutagenesis scheme, we also used a structure-based sequence alignment with the structurally most closely related 2′-*O*-methyltransferase, VP39. The structure of VP39 has been solved in complex with the mRNA substrate analogue 5′ m^7G-capped RNA hexamer (18). Studies modeling the mRNA substrate analogue onto the RrmJ structure revealed four additional, somewhat less-conserved residues in RrmJ that suggested involvement in the substrate association as well. These considerations led us to make additional alanine substitutions for the residues F37, L39, Y68, and K189 in RrmJ.

In vivo phenotype of the RrmJ mutants. To first analyze how the individual mutations affect the in vivo function of RrmJ, we transformed the plasmids encoding the respective RrmJ mutants into the *rrmJ* deletion strain HB23. We used quantitative Western blot analysis to determine the expression levels of the various mutant proteins and found that the mutant proteins were all soluble and expression levels were similar to that of a single copy of wild-type RrmJ expressed from its normal chromosomal location (data not shown). This finding excluded the possibility that any observed in vivo phenotype was due to inappropriately low or high RrmJ mutant protein levels. The wild-type-like expression levels of the RrmJ mutant proteins has been observed before and is due to their leaky expression from the uninduced pET11a vector (16).

To evaluate the in vivo function of our RrmJ mutant proteins, we first analyzed their growth phenotype in liquid Luria-Bertani medium at 37°C. As summarized in Table 2, wild-type *E. coli* strains show a doubling time of 25 min at 37°C, while the *rrmJ* deletion strain grows significantly slower, with a doubling time of more than 50 min. This severe growth defect is clearly due to a defect in the methyltransferase activity of RrmJ, because expression of the active site mutant RrmJ-K38A in the *rrmJ* deletion strain did not rescue the growth defect (Table 2). We then analyzed the growth of the individual RrmJ mutants. Three of the mutants revealed a significantly compromised in vivo activity. The doubling time for the RrmJ-F166A mutant was 40 min, the doubling time for the RrmJ-R32A/R34A mutant was 43 min, and the doubling time for the RrmJ-D136N mutant was 45 min; all of these were much longer than the doubling time determined for an *rrmJ* deletion strain expressing wild-type RrmJ, which was 25 min. Noteworthy, all other mutant strains also showed slightly longer doubling times than the wild-type strain, ranging from 32 to 38 min each. This finding suggested that the replacement of any of the conserved amino acids might impair the in vivo function of RrmJ to some extent.

Ribosome profiles of the RrmJ mutant strains. The growth defect of strains lacking functional RrmJ was proposed to be due to the absence of the highly conserved Um2552 modification in the A loop of the 23S rRNA, which causes either assembly or stability problems of the 70S ribosome and leads to an impaired translational efficiency. To investigate to what extent the growth defect of the mutant strains correlates with the ribosome profiles for these strains, we prepared lysates of the *rrmJ* mutant strains and compared the ribosome profiles under nonstringent and stringent salt conditions to the lysate of the *rrmJ* deletion strain expressing wild-type RrmJ from a plasmid (HB25). This strain accumulates slightly higher levels of 30S, 40S, and 50S ribosomal subunits than a wild-type *E. coli* strain that expresses RrmJ from its chromosomal copy (6). Because all of the RrmJ variants we used are expressed in this

TABLE 2. Summary of the in vivo and in vitro activities of RrmJ and the mutants[a]

Mutation	Doubling time at 37°C (min)	Ribosome profile for condition indicated		AdoMet/protein (%)	Apparent k_{cat} (min^{-1})	Apparent K_m (μM)	K_{cat}/K_m (μM^{-1} min^{-1})
		Associating	Dissociating				
Wild type	25	+++	+++	76	0.064	0.7 ± 0.05	0.080
rrmJ	53	(+)	(+)				
K38A[b]	58	(+)	(+)	68	<0.001		
D20A	36	+++	+++	81	0.036 ± 0.007	1.5 ± 0.4	0.024
Y22A	32	+++	++	78	0.059 ± 0.004	0.7	0.084
R32A/34A	43	+	+	72	0.017 ± 0.013	2.7 ± 0.6	0.006
F37A/L39A	38	+++	+++	ND	ND	ND	ND
Q67A/Y68A	38	+++	+++	ND	ND	ND	ND
D136N	45	+	+	71	0.034 ± 0.007	0.5 ± 0.2	0.068
F166A	40	+	+++	40 ± 4	ND	ND	ND
K189A	32	++	+++	65	0.007 ± 0.002	0.5	0.014
R194A	33	+++	++	59	0.051 ± 0.010	1.5 ± 0.4	0.034
S197A	34	+++	++	74	0.058 ± 0.004	1.4 ± 0.01	0.041

[a] The apparent k_{cat} and K_m values are the means and standard deviations of results from at least three independent experiments. The in vivo data presented for wild-type RrmJ were obtained with the *rrmJ* deletion strain HB23 expressing wild-type *rrmJ* from a pET11a plasmid (HB25). Growth of this strain is very similar to that of the corresponding wild-type *E. coli* strain (MG1655), but it accumulates slightly higher levels of 30S and 50S ribosomal subunits in lysates prepared under associating conditions and of 40S ribosomal subunits in lysates prepared under dissociating salt conditions. Western blot analysis revealed that all mutant variants were soluble and were expressed in similar amounts as the single copy of wild-type RrmJ from its normal chromosomal location in MG1655. ND, not determined; (+), +, ++, or +++, ribosome profiles are severely, moderately, slightly, or not impaired in lysates prepared under the indicated salt condition.

[b] See reference 16.

background strain, we decided to use this rescue strain, HB25, as the appropriate "wild-type" control in all of our in vivo experiments. The ribosome defect of an *rrmJ* deletion strain is revealed by the accumulation of large amounts of 30S and 50S ribosomal subunits in lysates prepared under nonstringent salt conditions (Fig. 2, left diagrams), and by the population of ~40S ribosomal particles in lysates prepared under stringent salt conditions (Fig. 2, right diagrams) (6).

We found that the degree of ribosome stabilities observed in the individual mutant strains corresponded only to a certain extent to the degree of growth of the respective mutant strains in liquid culture. The three mutant strains that showed the slowest growth in liquid Luria-Bertani medium (R32A/R34A, D136N, and F166A) indeed had the strongest ribosome defect. R32A/R34A and D136N mutant strains accumulated larger amounts of 30S and 50S ribosomal subunits than wild-type strains under nonstringent salt conditions, and had a significant amount of ~40S ribosomal particles under stringent salt conditions. The F166A mutant protein accumulated more ribosomal subunits without populating the ~40S particles. All other mutant strains, however, showed ribosome profiles that were either only slightly different from or identical to the ribosome profiles prepared from wild-type strains (Fig. 2; Table 2). This result was in contrast to the growth disadvantages that we observed in all of these strains and suggested that the growth defects observed in the *rrmJ* deletion strain might not be directly connected to defects in ribosome assembly and/or stability.

Kinetic characterization of the RrmJ mutant proteins. Biochemical characterization of the mutated RrmJ proteins was necessary to further elucidate which residues might be involved in substrate binding. We therefore decided to purify all mutant proteins, excluding only the two RrmJ variants that had substitutions for less-conserved amino acids (F37A/L39A and Q67A/Y68A) and showed ribosome profiles that were indistinguishable from wild-type ribosome profiles (Table 2). All other mutant proteins were expressed as soluble proteins to near wild-type protein levels in the transformed *rrmJ* deletion strain, indicating that the mutations did not significantly alter the stability of the proteins. To obtain additional evidence that the respective mutations did not cause a major change in the conformation of the mutant proteins, we determined the amount of AdoMet that remained associated with each of the eight mutant RrmJ proteins after their purification (16). Wild-type RrmJ appears to have a very high affinity for its cofactor, because AdoMet is still bound to more than 70% of the protein after its purification. As shown in Table 2, at least 59% and up to 81% of AdoMet was associated with all but one of the RrmJ mutant proteins after their purification, confirming that the overall structural integrity of the mutant proteins very likely has been maintained. Only the RrmJ-F166A mutant protein, which showed one of the most severe growth and ribosome defects when expressed in the *rrmJ* deletion strain in vivo, was associated with significantly less AdoMet after purification. This result suggested a decrease in AdoMet binding affinity and/or the presence of a certain amount of an inactive yet stably folded RrmJ mutant species in our preparation that is no longer able to bind AdoMet. We therefore decided to not use this mutant protein for our further in vitro studies.

To test the enzymatic activities of the various RrmJ mutant proteins in vitro, we investigated their ability to methylate 50S ribosomal subunits prepared from the *rrmJ* deletion strain (HB23). By using a 100 nM concentration of enzyme and keeping both substrates, AdoMet, and 50S ribosomal subunits in large excess, we determined the apparent k_{cat} values for each of the purified mutant proteins at 37°C. As shown in Fig. 3 and summarized in Table 2, four of the mutant proteins revealed at least a 50% decrease in their k_{cat} values, with the RrmJ variants harboring a mutation in R32/R34 and K189 showing the most significant decrease in enzymatic activity. Mutations in D20 and D136 also led to slight decrease in k_{cat} values, while mutations in Y22, R194 and S197 did not dra-

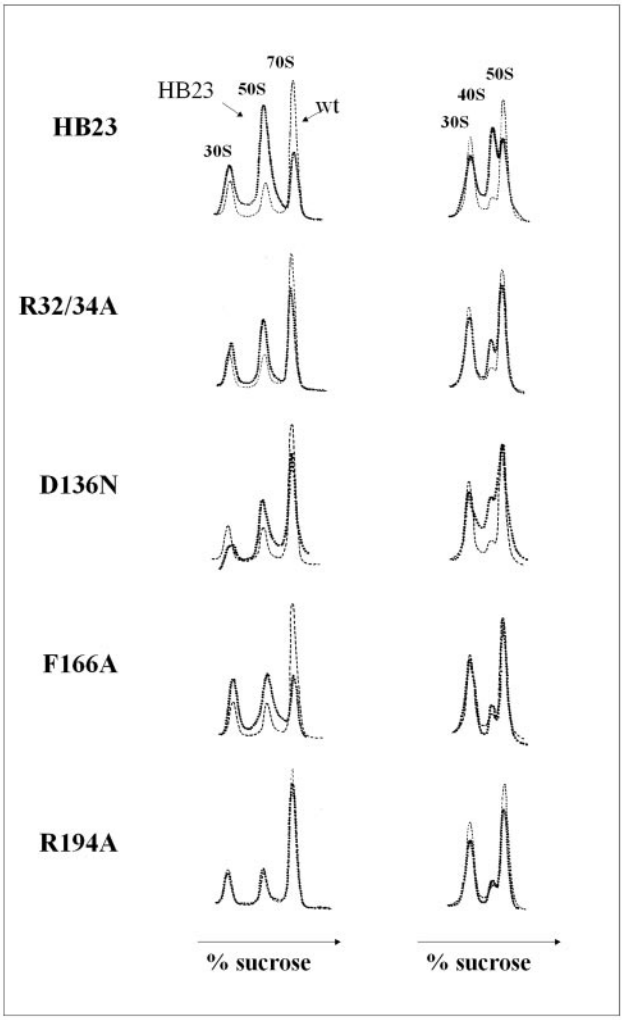

FIG. 2. In vivo activity of the RrmJ mutants. Polysome profiles of *rrmJ* deletion strain HB23 expressing no RrmJ or expressing wild-type RrmJ or the mutant proteins from a plasmid to wild-type protein levels. The ribosome profiles were analyzed under either associating, nonstringent salt conditions (10 mM $MgCl_2$, 100 mM NH_4Cl) (left panel) or dissociating, stringent salt conditions (1 mM $MgCl_2$, 200 mM NH_4Cl) (right panel). The ribosome profiles of lysates prepared from the individual strains (dark broken lines) are compared to the polysome profile of an *rrmJ* deletion strain expressing wild-type (wt) RrmJ (light broken lines).

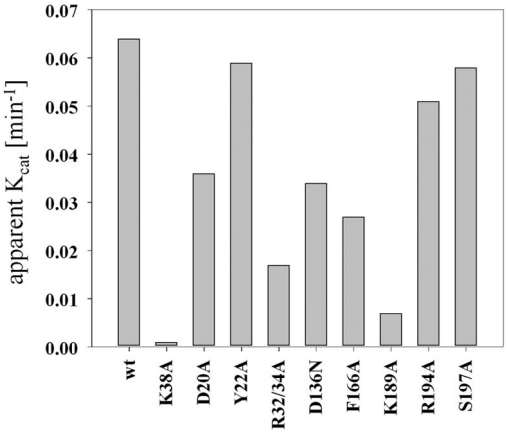

FIG. 3. In vitro activity of the various RrmJ mutants. A 100 nM concentration of purified enzyme was incubated with 50 μM [^{3}H]AdoMet (200 μC/ml) in methylation buffer (50 mM HEPES-KOH [pH 7.5], 85 mM NH_4Cl, 3 mM $MgCl_2$, 2 mM β-mercaptoethanol, 40 U of RNasin) at 37°C. The methylation reaction was started by the addition of either 5 μM or 8 μM 50S subunits prepared from the *rrmJ* deletion strain HB23. At defined time points, aliquots were taken and the [^{3}H]methyl incorporation was determined as described previously. wt, wild type.

matically alter the turnover numbers of RrmJ under the conditions tested.

Next, we determined the apparent K_m values of 50S ribosomal subunits for each of the purified RrmJ mutants. For these experiments, we kept the AdoMet concentration at 50 μM and varied the concentration of 50S ribosomal subunits from 0.2 to 10 μM. As shown in Table 2, an increased apparent K_m value for 50S ribosomal subunits was found for four of our RrmJ variants. These RrmJ mutants harbored substitutions for the surface-exposed amino acids D20, R32/R34, R194, or S197, implicating these amino acids as potentially involved in the binding of the 23S rRNA. The observed changes in apparent K_m values for 50S subunit binding in RrmJ mutant proteins were very similar to the changes in K_d and K_m values that have been determined for substrate binding mutants of the 23S rRNA dimethyltransferase ErmC′ (24). For ErmC′ mutant proteins, K_d and K_m values increased about 1.6- to 5-fold. This finding indicated that RNA binding is a highly cooperative, multivalent process, in which the mutation of single amino acids in the substrate binding site might not alter the substrate binding affinity as dramatically as do amino acid substitutions in the substrate binding site of other non-nucleic acid binding proteins.

In vitro enzymatic activity and in vivo ribosome profile: a good but not absolute correlation. A comparison of the in vitro and in vivo activities of RrmJ and the mutants indicated a good but not absolute correlation between changes in k_{cat} and K_m values of the purified RrmJ variants and alterations in the ribosome profiles of the corresponding mutant strains. The two most obvious outliers in this correlation were the RrmJ-K189A and the RrmJ-D136N mutant proteins. The RrmJ-K189A mutant strain revealed no apparent ribosome defect in vivo and no significant change in K_m for 23S rRNA but had an almost 10-fold decrease in apparent k_{cat} value (Table 2). This result could be explained by the possibility that analysis of the ribosome profiles under steady-state conditions might not be sufficiently sensitive to detect these changes in the catalytic activity of RrmJ. The RrmJ-D136N mutant protein, on the other hand, showed a very severe growth disadvantage and ribosome defect in vivo but had wild-type k_{cat} and K_m values in vitro. To investigate whether the D136N mutant protein was indeed inactive in vivo, we analyzed the methylation status of 23S rRNA prepared from RrmJ-D136N expressing mutant strains. Our rationale was that if the D136N mutant protein was inactive in vivo, the 50S ribosomal subunits would be unmethylated and would serve as in vitro substrates for wild-type RrmJ much like 50S ribosomal subunits prepared from the *rrmJ* deletion strain. If, on the other hand, the D136N mutant protein was active in vivo, the ribosomal subunits would be methylated and,

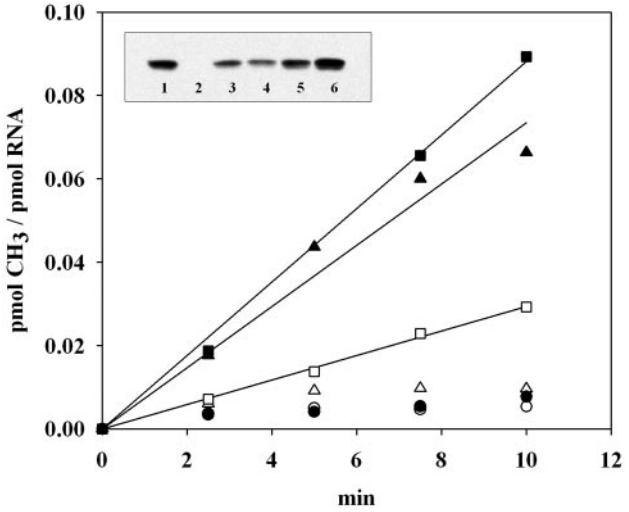

FIG. 4. RrmJ is associated with 50S ribosomal subunits in vivo. Methyl incorporation into 2 μM 50S ribosomal subunits prepared from wild-type strain HB24 (circles), *rrmJ* deletion strain HB23 (triangles), or *rrmJ* deletion strain HB23 expressing the D136N mutant protein (squares), either in the absence (open symbols) or in the presence (closed symbols) of 300 nM purified wild-type RrmJ. At defined time points, aliquots were taken and the [^{3}H]methyl incorporation was determined as described previously. Inset: RrmJ is bound to 50S ribosomal subunits. Analysis of the RrmJ content in 2 μM 50S ribosomal subunits prepared from the wild-type strain (HB24) (lane 1), the *rrmJ* deletion strain (HB23) (lane 2), or the *rrmJ* deletion strain expressing the D136N mutant from a plasmid (lane 3). To evaluate how much RrmJ is bound to the ribosomal subunits, 50S ribosomal subunits prepared from the *rrmJ* deletion strain (HB23) were supplemented with 50 nM (lane 4), 100 nM (lane 5), or 200 nM (lane 6) concentrations of purified RrmJ. Aliquots of the ribosomal subunits were loaded onto a sodium dodecyl sulfate–14% polyacrylamide gel, and Western blot analysis was performed with antibodies against RrmJ.

like 50S ribosomal subunits prepared from wild-type strains, would no longer serve as in vitro substrates (Fig. 4). We prepared 50S ribosomal subunits from the *rrmJ* deletion strain expressing the RrmJ-D136N mutant protein and tested the ability of wild-type RrmJ to methylate these ribosomal subunits in vitro. As shown in Fig. 4, 50S ribosomal subunits prepared from the *rrmJ* deletion strain expressing the D136N mutant showed the same incorporation of methyl groups upon incubation at 37°C as subunits prepared from the strain that lacked RrmJ altogether (Fig. 4). This result clearly showed that the D136N mutant is indeed unable to methylate 23S rRNA of 50S ribosomal subunits in vivo, which agreed well with the observed ribosome defect of the D136N-expressing *rrmJ* deletion strain.

RrmJ binds to 50S ribosomal subunits in vivo. Interestingly, the analysis of the methyl incorporation into ribosomal subunits of D136N mutant cells was dependent only in part on the presence of exogenous wild-type RrmJ. Incubation of the D136N-50S ribosomal subunits at 37°C in the presence of [^{3}H]AdoMet but in the absence of purified RrmJ led to a substantial methylation of the 23S rRNA (Fig. 4). This finding was in contrast to that for the 50S ribosomal subunits prepared from the *rrmJ* deletion strain, whose methylation was absolutely dependent on the presence of exogenous RrmJ (Fig. 4), and to the results obtained with 50S ribosomal subunits prepared from the wild-type strain, which did not show any methyl incorporation independent of the presence of purified RrmJ (Fig. 4). These results suggested that a methyltransferase activity was present in the 50S ribosomal subunits prepared from the *rrmJ* deletion strain expressing the RrmJ-D136N protein, which only became active under the chosen in vitro methylation conditions.

The purified D136N mutant protein showed near wild-type activity in vitro when tested on unmethylated 50S ribosomal subunits prepared from the *rrmJ* deletion strain. This finding, together with the observation that the yeast RrmJ homologue Mrm2p cofractionates with mitochondrial 21S rRNA, led us to investigate whether the observed methyltransferase activity was indeed the RrmJ-D136N mutant protein bound to its 50S ribosomal subunits, which might become active under our chosen in vitro conditions. As shown in the inset to Fig. 4, Western blot analyses of 50S ribosomal subunits from the *rrmJ* wild-type strain and the *rrmJ* deletion strain expressing the D136N mutant protein showed that *E. coli* RrmJ stays associated with the 50S ribosomal subunit during their preparation under stringent, high-salt conditions (1 mM $MgCl_2$, 200 mM NH_4Cl). No RrmJ was detected in the 30S subunits or the intact 70S ribosomes (data not shown). The amount of bound D136N mutant protein, in combination with the observed slightly lower in vitro activity of the purified D136N mutant (Fig. 3), explained very well the methylation activity that we observed with isolated 50S ribosomal subunits prepared from the D136N-expressing *rrmJ* deletion strain. This finding suggested that there might be a lack of efficient substrate release of D136N from 50S subunits in vivo, which could cause the apparent inactivity of the D136N mutant protein in vivo but might be less apparent under our chosen in vitro conditions.

Modeling of the A-loop structure onto the surface of RrmJ. U2552, the methylation target of RrmJ, is one of the five residues that constitute the A loop in the peptidyltransferase center of the ribosome. Both the crystal structure (2) and the solution structure (nucleotides 2548 to 2560) (3) of the A loop have been solved. To model the solution structure of the A loop into RrmJ, the A loop was initially positioned manually by using the crystal structure of the mRNA 2′-*O*-methyltransferase VP39 from vaccinia virus bound with the reaction product *S*-adenosylhomocysteine and 5′ m^{7}G-capped single-stranded RNA hexamer as a guide (18). The RNA was positioned by first overlaying the ribose and phosphate atoms of the reactive nucleotides into the active site of RrmJ (Fig. 5A). This positioning gave close agreements between the individual atom positions in the active site between U2552 of the A-loop RNA model and the 5′ m^{7}G-capped RNA of VP39. However, the rest of the A loop clashed with protein residues. Most noteworthy, the double-helical stalk of the A loop clashed severely with the protruded helix 4 of RrmJ (Fig. 5A).

To accommodate the A loop, we then kept the phosphodiesters of the reactive U2552 in position and rotated the A loop by approximately 85 degrees. This rotation prevented all clashes between the A loop and RrmJ protein (Fig. 5A). The phosphodiesters of the double helix now fit snugly into a deep cleft of RrmJ. Importantly, RNA-protein interactions involved exactly those residues (R34, R194, and S197) in RrmJ that when mutated to alanine residues exerted an increased K_m for 23S rRNA binding (Fig. 5C). This finding suggested that these

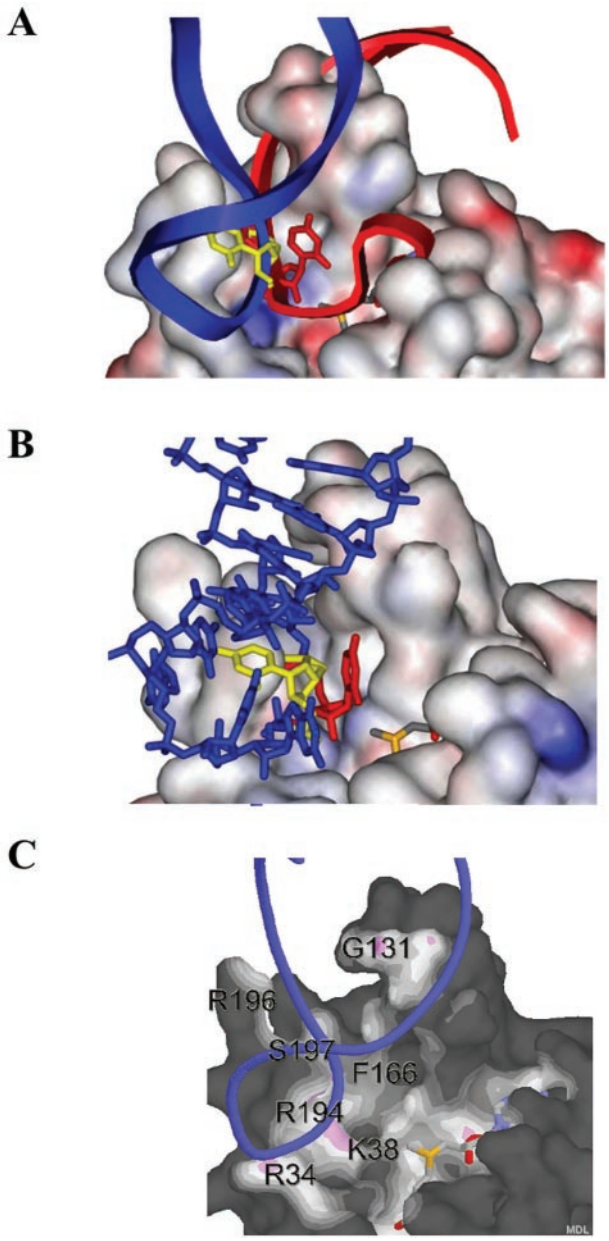

FIG. 5. Modeling of the A loop onto the surface of RrmJ. (A) In situ modeling of the A-loop structure (nucleotides 2548 to 2560) as solved by NMR (3) onto the surface of RrmJ. Modeling is based on overlaying the U2552 reactive nucleotide into the active site of RrmJ with the 5′ m^7G-capped reactive nucleotide in the VP39 structure. Without turning the A loop, the double helical stalk of the A loop clashes severely with the extended α4 helix of RrmJ (red model). To avoid this clashing, the A loop is turned by 85 degrees (blue model). Now, phosphodiesters occupy the same location in the model of RrmJ as do phosphodiesters of the 5′ m^7G-capped RNA hexamer in the VP39 structure. (B) Base flipping of U2552. The model shows U2552 in the closed position (yellow), where the 2′ hydroxyl group of the ribose is not accessible to the methyl donor AdoMet, and in the flipped configuration (red), where the 2′ hydroxyl group is in the optimal position to be methylated. (C) Solvent-accessible surface of RrmJ colored by distance to ligand atoms from U2552-flipped A-loop RNA (blue ribbon) and AdoMet (shown as stick model). The surface is colored by distance from nearby atoms. Dark areas are too far away from any atoms outside the surface to be bonded. White or light areas are close enough for hydrophobic van der Waals interactions. Pink areas are close enough for hydrogen bonds. The figure was made with Protein Explorer (25).

amino acids are indeed involved in the binding and positioning of 23S rRNA in RrmJ. In this model, the phosphodiesters now occupy the same location as the phosphodiesters of the 5′ m^7G-capped RNA hexamer in the VP39 structure. Additionally, the minor groove of the A-loop RNA is now positioned to sit nicely atop helix 4 of RrmJ, rather than clashing with the protein.

Interestingly, however, once the A loop was turned to fit into the protein, the 2′-hydroxyl group of U2552 was no longer accessible to the active site of RrmJ (Fig. 5B). These observations suggested a base-flipping mechanism for U2552 methylation in which the A-loop RNA first binds into the RrmJ binding site and then undergoes a base-flipping rotation of U2552 by 85 degrees, thereby placing the 2′-hydroxyl in position for the methylation.

The base-flipped model of the A-loop RNA was constructed and positioned into the putative binding site of RrmJ (Fig. 5B). Both base-flipped U2552 and unflipped models were then energy-minimized by positional and simulated annealing by using the CNX program (5). During these refinements, the protein atoms were allowed to adjust to the RNA model. Only two residues were found to move slightly. The side chains of R194 and R196, both located on the surface of RrmJ, are required to change conformation in order for the A-loop RNA model to position optimally into the substrate binding cleft. These residues are then closely positioned next to the phosphate backbone of the model A loop.

Very similar results were obtained when we modeled the crystal structure of the A loop into RrmJ, because the major differences between the A-loop conformations in the crystal structure and in the solution structure involve parts of the A loop that do not contact RrmJ. The phosphate backbone of the A loop, however, which makes most of the contacts with RrmJ, is not significantly different in the two structures.

The unmodified A loop: the minimal substrate for RrmJ. Modeling studies revealed that the A loop can be modeled into the substrate binding site we identified. This finding suggested that the A loop might serve as an in vitro substrate for RrmJ. We therefore performed in vitro methylation assays using the same unmodified A loop that was used in the nuclear magnetic resonance (NMR) (3) and our modeling studies (Fig. 5). The Um2552-methylated A loop was used as the control (3). As shown in Fig. 6, we observed a significant RrmJ-mediated methyl incorporation into the nonmodified A loop (Fig. 6). The methylated A loop, on the other hand, did not serve as an in vitro substrate for purified RrmJ (Fig. 6), strongly suggesting that the methylation of the A loop by RrmJ was indeed a specific process. Because the methyl incorporation into the A loop was slow compared to the methyl incorporation into 50S ribosomal subunits, we wanted to exclude the possibility that the observed A-loop methylation is due to small amounts of a different methyltransferase that might contaminate our wild-type RrmJ preparation. We therefore tested the active site mutant RrmJ-K38A, and found that this mutant protein was completely unable to methylate the unmodified A loop in vitro (data not shown). Together, these results show that RrmJ can specifically recognize, bind, and methylate the A loop when it adopts its solution structure. The slow methyl incorporation, however, might be due to missing contact sites that are present in the 50S ribosomal subunit.

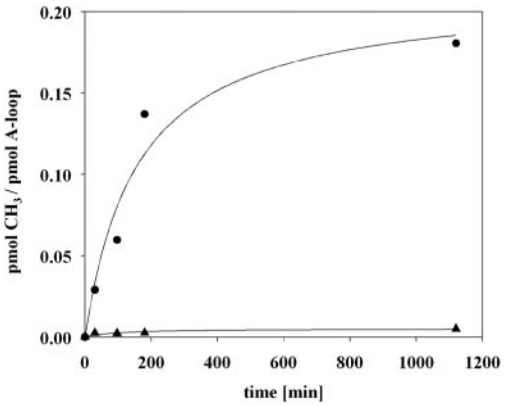

FIG. 6. Nonmethylated, isolated A loop: a minimal substrate for RrmJ in vitro. A 5 μM concentration of wild-type RrmJ was incubated with a 1 μM concentration of nonmodified (circles) or methylated (triangles) A loop (nucleotides 2545 to 2563) and 50 μM [^{3}H]AdoMet (200 μCi/ml) in methylation buffer (50 mM HEPES-KOH [pH 7.5], 50 mM NaCl, 10 mM EDTA, 1 mM dithiothreitol, 40 U of RNasin, and 0.1 mg of bovine serum albumin/ml) at 37°C. Aliquots were taken at defined time points, and the [^{3}H]methyl incorporation was measured as described previously.

An analysis of the ribosome structure suggested that RrmJ is unable to access the A loop unless it is looped out of the ribosome. Such reversible undocking of the A loop has been proposed before and was suggested to occur as a regular step in tRNA selection and accommodation (3). Our findings confirm these considerations and suggest that the A loop adopts its solution structure when looped out of the ribosome, where it can be methylated by RrmJ. This provides an excellent explanation of how RrmJ is able to methylate a buried 23S rRNA residue so late in the maturation process of the ribosome.

DISCUSSION

In this study, we have used structure predictions, structural modeling approaches, and structure-based sequence alignments to identify highly conserved, surface-exposed residues that could be involved in the binding of the 2′-*O*-methyltransferase RrmJ to its substrate 23S rRNA. We mutated the residues identified, and after careful in vivo and in vitro analysis we are now proposing that a positively charged ridge built by the highly conserved arginines 32, 34, and 194 plays an important role in the coordination of the rRNA sugar phosphate backbone. In addition to this ridge, the highly conserved serine 197 appears to contribute to the binding of the RNA substrate. Moreover, based on the overall high similarity between the structures of VP39 and RrmJ, we also cannot exclude the possibility that the N terminus of RrmJ might be involved in the substrate coordination. An analysis of the crystal structure of VP39 revealed that the N terminus of VP39 lies like a lid on top of the RNA binding region, thereby retaining the RNA substrate in its correct position (19). This finding implies that a certain amount of flexibility of the N terminus is necessary in order to bind and release the substrate, which is in accord with the findings that the N terminus of RrmJ is not rigid enough to crystallize in the empty state of the enzyme (6).

Both the crystal and solution structures of the 19-residue A loop were then modeled into RrmJ. In neither case was it possible to position the 2′-hydroxyl of U2552 into the active site of RrmJ without significant clashes with the surrounding protein. However, for both the crystal and NMR structures, which differ mainly in those parts of the RNA that do not contact the protein, it was possible to model the A loop into RrmJ by overlaying the U2552 nucleotide in the active site with the 5′ m^{7}G-capped reactive nucleotide in the VP39 structure and then simply turning the whole A loop into a cleft in the surface of RrmJ. This turning positioned the phosphodiesters into the same position as the phosphodiesters of the mRNA hexamer substrate in VP39. The residues that are in closest contact with the A-loop structure in our model were found to be the active site residue K38, and the surface residues Arg34, G131, F166, R194, and S197. Except for the less-conserved G131, all amino acids are highly conserved and have been found to alter the catalytic activity of the enzyme (K38), the apparent AdoMet affinity (F166), or the apparent K_m for substrate binding (R34, R194, and S197) when mutated. The finding that the A-loop modeling positions exactly those surface exposed amino acids closest to the A loop that have been found to cause increased K_m values for 23S rRNA when mutated in RrmJ strongly suggested that we have indeed identified the 23S rRNA binding site in RrmJ. This model now positions the ribose of the target U2552 next to the active site Lys164 and to the reactive methyl group of AdoMet. The suggested substrate binding site in RrmJ, which is very similar to the known substrate binding site of VP39, also resembles other predicted RNA binding sites in methyltransferases. Mutagenesis studies and structural predictions of ErmC′, the 23S rRNA dimethyltransferase from *Bacillus subtilis*, for instance, suggested a positively charged patch consisting of three arginine residues and one threonine residue, which positions the 23S rRNA right next to the catalytic site of the protein (24). Moreover, the recently solved crystal structure of a putative RNA methyltransferase from *Mycobacterium tuberculosis*, Rv2118c, displays a groove lined with positively charged residues which is wide enough to fit the RNA (14).

The methylation target of RrmJ, U2552, is one of five highly conserved A-loop residues that form part of the peptidyltransferase center in the ribosome. The residues of the A loop are thought to play a role in tRNA selection and accommodation. In the context of the ribosome, U2552 is positioned on the bottom of a deep cleft and, although it is solvent accessible, it appears not to be accessible to the 23-kDa protein RrmJ. This finding raised the intriguing question about the mechanism of substrate recognition and binding by RrmJ. It was suggested that docking of the A loop might be a reversible process and that undocking is required for tRNA binding (14). Our findings that the A loop, when it adopts its solution structure, can be modeled into the substrate binding site of RrmJ and, even more importantly, can be recognized by RrmJ as a substrate in vitro support this hypothesis. This reversible undocking of the A loop from the 50S ribosome could explain how RrmJ can gain access to the A-loop structure and can methylate U2552 so late in the maturation process of the ribosome assembly. It could, furthermore, represent the rate-limiting step, which was suggested to be the reason for the low turnover rates that have been observed for RrmJ in vitro (14).

Modeling studies of the A loop into the putative substrate

binding site of RrmJ showed us that a base flipping of U2552 is likely to be required for the methylation reaction. A base flip would conserve both the active site orientation of the methylated U2552 and the phosphodiester contacts, as well as prevent a clash with the extended α4 helix, which is uniquely longer in RrmJ and VP39 than in structurally related catechol *O*-methyltransferases (14). Base flipping was first discovered when a DNA cytosine 5-methyltransferase was cocrystallized with its DNA substrate (21). Since then, base flipping has been shown or suggested for many other DNA-modifying enzymes. Now there are several indications that base flipping is a mechanism that can occur in RNA, as well (10). Base flipping of RNA has recently been shown to be induced by the binding of initiation factor IF1 to the 30S ribosomal subunit. Here, the binding of IF1 causes the bases A1492 and A1493 of the 16S rRNA to flip out of helix 44. This flipping buries the bases in specific pockets of initiation factor 1 (9). Furthermore, tRNA- and rRNA-modifying enzymes, which make modifications within base-paired regions, have been suggested to induce base flipping as well. The recently solved structure of the tRNA pseudouridine synthase TruB, in complex with its tRNA substrate, revealed that the target base U55 flips out completely, thereby disrupting the U55-G18 base pair and, with that, the tertiary structure of the tRNA (17). This action could give misfolded tRNAs the chance to correct their tertiary structure. The target nucleotide U2552 of RrmJ forms an unusual pyrimidine-pyrimidine base pair with C2556, which gives the A loop its compact loop structure (3). A base flip would also disrupt this base pair and, possibly, the A-loop structure. Our discovery that the A loop can be used as a minimal substrate in vitro now allows us to perform crystallization experiments with RrmJ substrate complexes, which should give us more insight into the methylation events and more evidence that RrmJ is indeed the first known rRNA methyltransferase that induces base flipping.

ACKNOWLEDGMENTS

We thank Hans Bügl for initiating this project. We thank Scott Blanchard and Joseph Puglisi for providing us with purified A loops. We thank James Bardwell for critically reading the manuscript.

National Institutes of Health grant GM065318 and a Burroughs Wellcome Fund Career Award to U.J. supported this work.

REFERENCES

1. **Agarwalla, S., J. T. Kealey, D. V. Santi, and R. M. Stroud.** 2002. Characterization of the 23S rRNA m^5U1939 methyltransferase from *Escherichia coli*. J. Biol. Chem. **277:**8835–8840.
2. **Ban, N., P. Nissen, J. Hansen, P. B. Moore, and T. A. Steitz.** 2000. The complete atomic structure of the large ribosomal subunit at 2.4 Å resolution. Science **289:**905–920.
3. **Blanchard, S. C., and J. D. Puglisi.** 2001. Solution structure of the A loop of 23S ribosomal RNA. Proc. Natl. Acad. Sci. USA **98:**3720–3725.
4. **Brimacombe, R., P. Mitchell, M. Osswald, K. Stade, and D. Bochkariov.** 1993. Clustering of modified nucleotides at the functional center of bacterial ribosomal RNA. FASEB J. **7:**161–167.
5. **Brunger, A. T., P. D. Adams, G. M. Clore, W. L. DeLano, P. Gros, R. W. Grosse-Kunstleve, J. S. Jiang, J. Kuszewski, M. Nilges, N. S. Pannu, R. J. Read, L. M. Rice, T. Simonson, and G. L. Warren.** 1998. Crystallography & NMR system: a new software suite for macromolecular structure determination. Acta Crystallogr. Sect. D **54:**905–921.
6. **Bügl, H., E. B. Fauman, B. L. Staker, F. Zheng, S. R. Kushner, M. A. Saper, J. C. Bardwell, and U. Jakob.** 2000. RNA methylation under heat shock control. Mol. Cell **6:**349–360.
7. **Caldas, T., E. Binet, P. Bouloc, A. Costa, J. Desgres, and G. Richarme.** 2000. The FtsJ/RrmJ heat shock protein of Escherichia coli is a 23 S ribosomal RNA methyltransferase. J. Biol. Chem. **275:**16414–16419.
8. **Caldas, T., E. Binet, P. Bouloc, and G. Richarme.** 2000. Translational defects of *Escherichia coli* mutants deficient in the Um_{2552} 23S ribosomal RNA methyltransferase RrmJ/FTSJ. Biochem. Biophys. Res. Commun. **271:**714–718.
9. **Carter, A. P., W. M. Clemons, Jr., D. E. Brodersen, R. J. Morgan-Warren, T. Hartsch, B. T. Wimberly, and V. Ramakrishnan.** 2001. Crystal structure of an initiation factor bound to the 30S ribosomal subunit. Science **291:**498–501.
10. **Cheng, X., and R. M. Blumenthal.** 2002. Cytosines do it, thymines do it, even pseudouridines do it—base flipping by an enzyme that acts on RNA. Structure **10:**127–129.
11. **Curran, J. F.** 1998. Modified nucleotides in translation, p. 493–516. *In* H. Grosjean and R. Benne (ed.), Modification and editing of RNA. ASM Press, Washington, D.C.
12. **Green, R., and H. F. Noller.** 1996. In vitro complementation analysis localizes 23S rRNA posttranscriptional modifications that are required for Escherichia coli 50S ribosomal subunit assembly and function. RNA **2:**1011–1021.
13. **Grosjean, H., G. Bjork, and B. E. H. Maben.** 1995. Nucleotide modification and base conversion of RNA: summary and outlook. Biochimie **77:**3–6.
14. **Gupta, A., P. H. Kumar, T. K. Dineshkumar, U. Varshney, and H. S. Subramanya.** 2001. Crystal structure of Rv2118c: an AdoMet-dependent methyltransferase from Mycobacterium tuberculosis H37Rv. J. Mol. Biol. **312:**381–391.
15. **Gustafsson, C., and B. C. Persson.** 1998. Identification of the *rrmA* gene encoding the 23S rRNA m^1G745 methyltransferase in *Escherichia coli* and characterization of an m^1G745-deficient mutant. J. Bacteriol. **180:**359–365.
16. **Hager, J., Staker, B. L., Bügl, H., and Jakob, U.** 2002. Active site in RrmJ, a heat shock induced methyltransferase. J. Biol. Chem. **277:**41978–41986.
17. **Hoang, C., and A. R. Ferre-D'Amare.** 2001. Cocrystal structure of a tRNA Psi55 pseudouridine synthase: nucleotide flipping by an RNA-modifying enzyme. Cell **107:**929–939.
18. **Hodel, A. E., P. D. Gershon, and F. A. Quiocho.** 1998. Structural basis for sequence-nonspecific recognition of 5′-capped mRNA by a cap-modifying enzyme. Mol. Cell **1:**443–447.
19. **Hodel, A. E., P. D. Gershon, X. Shi, and F. A. Quiocho.** 1996. The 1.85 A structure of vaccinia protein VP39: a bifunctional enzyme that participates in the modification of both mRNA ends. Cell **85:**247–256.
20. **Kim, D. F., and R. Green.** 1999. Base-pairing between 23S rRNA and tRNA in the ribosomal A site. Mol. Cell **4:**859–864.
21. **Klimasauskas, S., S. Kumar, R. J. Roberts, and X. Cheng.** 1994. HhaI methyltransferase flips its target base out of the DNA helix. Cell **76:**357–369.
22. **Lövgren, J. M., and P. M. Wikström.** 2001. The *rlmB* gene is essential for formation of Gm2251 in 23S rRNA but not for ribosome maturation in *Escherichia coli*. J. Bacteriol. **183:**6957–6960.
23. **Madsen, C. T., J. Mengel-Jorgensen, F. Kirpekar, and S. Douthwaite.** 2003. Identifying the methyltransferases for m^5U747 and m^5U1939 in 23S rRNA using MALDI mass spectrometry. Nucleic Acids Res. **31:**4738–4746.
24. **Maravic, G., J. M. Bujnicki, M. Feder, S. Pongor, and M. Flogel.** 2003. Alanine-scanning mutagenesis of the predicted rRNA-binding domain of ErmC′ redefines the substrate-binding site and suggests a model for protein-RNA interactions. Nucleic Acids Res. **31:**4941–4949.
25. **Martz, E.** 2002. Protein Explorer: easy yet powerful macromolecular visualization. Trends Biochem. Sci. **27:**107–109.
26. **Pintard, L., J. M. Bujnicki, B. Lapeyre, and C. Bonnerot.** 2002. MRM2 encodes a novel yeast mitochondrial 21S rRNA methyltransferase. EMBO J. **21:**1139–1147.
27. **Pintard, L., D. Kressler, and B. Lapeyre.** 2000. Spb1p is a yeast nucleolar protein associated with Nop1p and Nop58p that is able to bind *S*-adenosyl-L-methionine in vitro. Mol. Cell. Biol. **20:**1370–1381.
28. **Pintard, L., F. Lecointe, J. M. Bujnicki, C. Bonnerot, H. Grosjean, and B. Lapeyre.** 2002. Trm7p catalyses the formation of two 2′-*O*-methylriboses in yeast tRNA anticodon loop. EMBO J. **21:**1811–1820.
29. **Porse, B. T., and R. A. Garrett.** 1995. Mapping important nucleotides in the peptidyl transferase centre of 23 S rRNA using a random mutagenesis approach. J. Mol. Biol. **249:**1–10.
30. **Rozenski, J., P. F. Crain, and J. A. McCloskey.** 1999. The RNA Modification Database: 1999 update. Nucleic Acids Res. **27:**196–197.